JÉSSICA DUARTE DA SILVA

ISOLATION AND CHARACTERIZATION OF LYTIC BACTERIOPHAGES FOR THE COMPOSITION OF A PHAGE COCKTAIL CAPABLE OF REDUCING BACTERIAL BIOFILMS IN OIL-RELATED ENVIRONMENTS

Thesis submitted to the Agricultural Microbiology Graduate Program of the Universidade Federal de Viçosa in partial fulfillment of the requirements for the degree of *Doctor Scientiae*.

Adviser: Sérgio Oliveira de Paula

VIÇOSA - MINAS GERAIS
2023

Ficha catalográfica elaborada pela Biblioteca Central da Universidade Federal de Viçosa - Campus Viçosa

T
S586i
2023

Silva, Jéssica Duarte da, 1994-
Isolation and characterization of lytic bacteriophages for the composition of a phage cocktail capable of reducing bacterial biofilms in oil-related environments / Jéssica Duarte da Silva. – Viçosa, MG, 2023.
1 tese eletrônica (109 f.): il. (algumas color.).

Texto em inglês.
Orientador: Sérgio Oliveira de Paula.
Tese (doutorado) - Universidade Federal de Viçosa, Departamento de Microbiologia, 2023.
Inclui bibliografia.
DOI: https://doi.org/10.47328/ufvbbt.2023.557
Modo de acesso: World Wide Web.

1. Bacteriófagos. 2. Petróleo. 3. Bactérias redutoras de sulfato. 4. Biofilmes bacterianos. 5. Microbiologia industrial. I. Paula, Sérgio Oliveira de, 1976-. II. Universidade Federal de Viçosa. Departamento de Microbiologia. Programa de Pós-Graduação em Microbiologia Agrícola. III. Título.

CDD 22. ed. 579.26

Bibliotecário(a) responsável: Bruna Silva CRB-6/2552

JÉSSICA DUARTE DA SILVA

ISOLATION AND CHARACTERIZATION OF LYTIC BACTERIOPHAGES FOR THE COMPOSITION OF A PHAGE COCKTAIL CAPABLE OF REDUCING BACTERIAL BIOFILMS IN OIL-RELATED ENVIRONMENTS

Thesis submitted to the Agricultural Microbiology Graduate Program of the Universidade Federal de Viçosa in partial fulfillment of the requirements for the degree of *Doctor Scientiae*.

APPROVED: July 06, 2023.

Assent:

Documento assinado digitalmente
gov.br
JESSICA DUARTE DA SILVA
Data: 18/09/2023 16:16:38-0300
Verifique em https://validar.iti.gov.br

Jéssica Duarte da Silva
Author

Documento assinado digitalmente
gov.br
SERGIO OLIVEIRA DE PAULA
Data: 18/09/2023 16:24:31-0300
Verifique em https://validar.iti.gov.br

Sérgio Oliveira de Paula
Adviser

ACKNOWLEDGMENTS

How sad it must be to go through this life alone. I always had little but excellent company. I thank my mother Rejane for being my biggest supporter. In everything. I would like to thank my father, Gerson, for his kind and constant presence. To my brother Jefferson, for being my love reference. You three are the foundation of my life, and if I'm here, it's because of you. I also thank Jhonny, who, in addition to being a partner, was also my statistician, scientific consultant, grammar checker, and point of calm in the midst of life's inconsistencies. I would like to thank my friends, whom I will not mention for fear of forgetting someone, but who were my family during these years away from home. For all the parties together, the conversations, the smiles, the hugs. Viçosa wouldn’t have any charm if it weren't for you. I thank all my teachers and professors, especially Professor Sérgio and Roberto, who for so many years guided, taught, and showed me the scientific path. I thank Professor Rob for promptly welcoming me into his lab, Jeroen for always explaining complex methodologies with a smile, and all the other researchers who made Leuven a dream come true for me. Thanks to the Brazilian public education system, which allowed me access to free quality education from kindergarten to graduate school, to the Federal University of Viçosa, for the opportunity to carry out my graduate and postgraduate courses. To Petrobrás, for the project funding and for granting my scholarship. And most important, thanks to God for writing such a beautiful story for me. This study was financed in part by the Coordenação de Aperfeiçoamento de Pessoal de Nível Superior – Brasil (CAPES) – Finance Code 001

ABSTRACT

SILVA, Jéssica Duarte, D.Sc., Universidade Federal de Viçosa, July, 2023. **Isolation and characterization of lytic bacteriophages for the composition of a phage cocktail capable of reducing bacterial biofilms in oil-related environments**. Adviser: Sérgio Oliveira de Paula.

Phages are viruses that infect bacteria and since their discovery in the early 20th century, they have been used to control bacterial growth. This work was divided into three chapters. The first genomically and biologically characterizes the *Enterobacter* phage vB_EclM-UFV01, presenting general characteristics of its genus, the Karamviruses. Chapter 2, examines the capacity of a phage cocktail (composed by enterobacteria-isolated phages) to reduce the biofilm of sulfate-reducing bacteria. The formulation of the cocktail, named Petro01, was performed by selecting phages from the collection of the Laboratory of Molecular Immunovirology at UFV and ended up being composed of three phages of the *Tequatrovirus* genus (briefly characterized genomically in this chapter) and one of the *Karamvirus* genus (described in Chapter 1). The stability of Petro01 under conditions similar to those found in petroleum-related environments, its shelf life at high storage temperatures, the supernatant composition (LB enriched with conservative compounds), as well as the propagation capacity of the phages that make up the cocktail in bench and a 12 L bioreactor, was also evaluated. Petro01 showed significant biotechnological potential and positive capacity for the composition of a phage-based product. Chapter 3 moves away from the environmental application of bacteriophages and characterizes, biologically and genomically, the Proteus mirabilis phages BigMira UFV01 and MidiMira UFV02, providing an overview of the common features of their genus, the Acadeviruses. It also presents the genomic evaluation of 10 strains of *P. mirabilis*, isolated in clinical environments, focusing on the LPS locus and the antimicrobial resistance profile. All phages described in this study have good potential as antibacterial agents.

Keywords: Bacteriophages. Industrial microbiology. Sulfate-reducing bacteria. Bioproducing.

RESUMO

SILVA, Jéssica Duarte da, D.Sc., Universidade Federal de Viçosa, julho de 2023. **Isolamento e caracterização de bacteriófagos líticos para a composição de um coquetel fágico capaz de diminuir biofilmes bacterianos em ambientes relacionados à petróleo.** Orientador: Sérgio Oliveira de Paula

Fagos são vírus que infectam bactérias e desde a sua descoberta, no início do século XX, têm sido utilizados para controlar o crescimento bacteriano. Este trabalho foi dividido em três capítulos. O primeiro caracteriza genômica e biologicamente o fago de *Enterobacter* vB_EclM-UFV01, apresentando as características gerais do seu gênero, os *Karamvirus*. O capítulo 2, testa a efetividade de um coquetel de fagos isolados contra enterobactérias quanto à sua capacidade de diminuir o biofilme de bactérias redutoras de sulfato. A formulação do coquetel, nomeado Petro01, foi feita selecionando fagos à partir do acervo do Laboratório de Imunovirologia Molecular da UFV e terminou sendo composto por três fagos do gênero *Tequatrovirus* (brevemente caracterizados genômicamente nesse capítulo) e um do gênero *Karamvirus* (descrito no capítulo 1). A estabilidade do Petro01 em condições semelhantes às encontradas em ambientes relacionados ao petróleo, seu tempo de prateleira em temperaturas elevadas de estocagem, a composição do sobrenadante (LB enriquecido com compostos conservadores), assim como a capacidade de propagação dos fagos que compõem o coquetel em bancada e em biorreator de 12 L, também foi avaliada. Petro01 apresentou significativo potencial biotecnológico e positiva capacidade para a composição de um produto *phage-based*. O capítulo 3 se afasta um pouco da aplicação ambiental dos bacteriófagos e caracteriza, biológica e genômicamente, os fagos de *Proteus mirabilis* BigMira UFV01 e MidiMira UFV02, fornecendo uma visão geral sobre as características comuns do seu gênero, os *Acadevirus*. É apresentado ainda a avaliação genômica de 10 cepas de *P. mirabilis*, isoladas em ambientes hospitalares, no que diz respeito ao locus LPS e ao perfil de resistência antimicrobiana. Todos os fagos descritos neste estudo apresentam um bom potencial como agentes antibacterianos.

Palavras-chave: Bacteriófagos. Microbiologia industrial. Bactérias redutoras de sulfato. Bioprodução.

SUMMARY

General Introduction

Bacteriophages, also called phages, are viruses that infect bacteria. Independently described by Frederick Twort in 1915 and Felix d'Herelle in 1917, they are considered the most abundant entities on the planet, with an estimative of approximately 10^{31} particles in the biosphere [1,2]. In a pre-antibiotic era, d'Herelle rapidly recognized the relevance of his discovery. Although a better understanding of phages' particularities and their infection mechanisms has been gradually elucidated over the years, in 1919 d'Herelle had already isolated specific phages against several pathogenic bacteria, including *Salmonella typhi, Escherichia coli, Pasteurella multocida, Vibrio cholerae, Yersinia pestis, Pseudomonas aeruginosa,* and *Neisseria meningitis* [3,4]. During the 20th century, the foundations of what we now call phage therapy were established. Several patients had bacterial infections treated with phage cocktails in Europe, the USA, and even Brazil [5,6]. However, in 1934 the Journal of the American Medical Association (JAMA) published a warning about the use of phage cocktails, and in 1941 the same journal categorically advised against their use, citing the lack of scientific evidence and large inconsistencies in the results when compared to a drug recently discovered, the penicillin [4,7]. Thus, the use of phages as agents controlling bacterial growth was mostly replaced by their use as biological models. Only in a few countries, such as Georgia, France, Russia, Poland, and Belgium, studies involving phage therapy continued to be developed, and phage cocktails were used to treat patients with therapeutic failure [6].

Phage therapy could have remained dormant, if it hadn't been for a growing need in the scientific community: methodologies to fight against multi-drug resistant bacteria [8–10]. Since the discovery of penicillin, more than 1 million tons of antibiotics have been used worldwide [8,9]. The evolutive pressure of all this use was quickly observed, with the more and more common emergence of antimicrobial-resistant (AMR) strains [6,11]. In 2017, the World Health Organization released a global priority pathogens list of AMR bacteria, which englobes the ESKAPE organisms (*Enterococcus faecium, Staphylococcus aureus, Klebsiella pneumoniae, Acinetobacter baumannii, Pseudomonas aeruginosa, Enterobacter species, and Escherichia coli*) and other difficult-to-treat and prevalent bacterial strains [6,12,13]. Thus, microbial resistance to antibiotics was already a major source of worry before being exacerbated by the COVID-19 pandemic and reached crisis proportions [11,14]. According to the latest CDC and PAHO reports, the use of antibiotics in SARS-CoV-2 patients during the COVID-19 pandemic had an average of 94-100% and has absurdly exceeded the incidence of

secondary infections and coinfections (10-15%), suggesting an inappropriate and excessive prescribing. This led to an increase of 15% in gram-negative multidrug-resistant strains still in 2020, the first year of the pandemic [15,16].

However, despite the undeniable relevance of phages against AMR, much still needs to be done in terms of regulatory legislation and high-quality clinical trials before it can be widely used. Important scientific initiatives, such as PHAGOBURN and PhageForce have been developed in this direction, along with the commitment of organizations such as the Belgium Society of Viruses of Microbes, Society For Bacteriophage Research and Therapy, Phage UK, and Phage Australia are committed to promoting a dialogue between important governance bodies and researchers so that advances in this regard can be made [17–19]. On the other hand, the application of bacteriophages to control bacterial damage in fields such as animal health, agri-food, and biocontrol is being developed more easily and with excellent results [20]. For instance, phages are not only being used to kill individual pathogenic cells but also to decrease bacterial biofilms that can grow in one infinity of clinical and industrial apparatus [20–22].

Biofilms are complex bacterial communities, composed of multi-species bacterial cells, immersed by a self-produced matrix of extracellular polymeric substances (EPS), such as exopolysaccharides, extracellular deoxyribonucleic acids (eDNA), and proteins, usually adhered to a surface [23–25]. A biofilm typically begins with a planktonic bacterial cell that binds reversibly to a surface. Then, attachment substances are synthesized, the binding becomes irreversible, and the EPS is produced. The cell proliferation and the establishment of intercellular connections led to a tangled complex of cells and exopolysaccharides, with a 3D structure. In fact, this arrangement becomes so dense, that some peripheric cells need to be detached, to allow the entrance of water and nutrients. The maintenance of a biofilm is a complex process, based on the control of gene expression exercised by the bacterial quorum-sensing and the constant production of sugars, outer membrane vesicles, and other biofilm-forming components [23,24,26]. This process is highly energy-consuming for a cell, yet these costs are evolutionarily explained. When a biofilm is mature, the external layer is so thick and sticky, that protects the community above by physically avoiding biotic and abiotic stressors, such as biocides and antibiotics, as well as predators, like phages [23,24,26,27].

As in a normal predator-prey dynamic, phages also have different mechanisms to circumvent the biofilm barrier, and one of the most studied are the Virion-Associated Exopolysaccharide Degrading Enzymes, also known as depolymerases [23]. Depolymerases

can be divided into two categories: lyases and hydrolases. Hydrolases cleave a covalent bond by using a water molecule. Lyases can break the bonds between carbon with another atom, in a process other than hydrolysis and oxidation [28,29]. Depolymerases target the sugars of the cell wall, such as capsule and LPS, and can be used not only to disrupt biofilms but also to release bacterial receptors that can be covered and allow the infection to begin. This enzyme is common in structural components of phage virions, such as tail fibers and whiskers [23,28,30]. Enzymes used to create holes in the bacterial cell wall during the infection process, such as endolysins and virion-associated peptidoglycan hydrolases (VAPGHs) also can act into biofilm components when released from the host [30–32]. Phages also can interfere with bacterial quorum-sensing by producing quorum-quenching molecules, disturbing the bacterial communication system, as well as phages also produce DNases that can participate in biofilm disruption. Finally, an important fact to be considered is the presence of an abundant number of hypothetical proteins in the phage's genomes, even in compact ones. The search for conserved domains and the increase of annotation tools have been helping in the attribution of the function of some genes, but other remains completely unknown [23]. Visnapuu *et al.*, 2022 hypothesize that, because of the higher metabolic manipulation that phages possess over their hosts, they can disrupt the biofilms from inside, changing the intracellular communication and disturbing the maintenance of this structure [23].

Sulfate Reducing Bacteria (SRB) are a polyphyletic group of anaerobic organisms, with representatives from both the Archaea and Bacteria domains, which include more than 80 bacterial genera [33–35]. Microorganisms of this group are capable of using sulfate as a final electron acceptor during respiration, having hydrogen sulfide (H_2S) as the main product of this metabolism. SRB can be found in diverse anoxygenic environments, including ruminant's gastrointestinal tract, soil, and marine [33,36]. Hence, SRB play an important role in the sulfur cycle and are key species in the maintenance of anaerobic microbial communities, mainly due to their ability to cycle sulfate in H_2S [33,36]. Secondary recovery is a method used by the oil industry in which seawater is injected into wells that have lost their natural pressure, to improve oil extraction efficiency. This mixture is called "production water" and is held on the platform until being processed. The atmosphere in the storage tanks quickly becomes anoxic and sulfur-rich, providing perfect circumstances for the establishment of sulfate-reducing species [37]. The growth of these organisms in oil-related environments is undesirable and causes numerous damages since H_2S is a gas neurotoxic, flammable, and

corrosive. These organisms also increase the concentration of sulfur compounds in the oil in a process called “souring”, which lowers its market price [38,39]. Furthermore, SRB and their biofilms are the primary cause of biogenic corrosion in oil-related environments, resulting in annual expenditures that run into trillions of dollars. The biofilms frequently cause localized “pitting” corrosions that are impossible to anticipate and difficult to avoid, leading to perforations and even oil spills [40–42]. Currently, the use of biocides is the most common option in an attempt to control the growth of SRB. The most used are “Tetrakis-hydroxymethyl Phosphonium Sulfate” (THPS) and 50% glutaraldehyde. Both are biocides considered safe for the environment. However, because of the high operating costs (with recurring biweekly and even weekly dosages), as well as evidence of microbial resistance to these compounds, new efficient solutions for controlling the growth of these organisms are important and of great interest to the industry [25,40–43].

Traditionally, phage-based methodologies aiming for bacterial growth control relied on the isolation of phages against specific bacterial strains [44,45]. In this work, we suggested an indirect approach, mainly focused on avoiding the development of SRB biofilms and unravel the use of phages as biocontrol agents in the oil industry, focusing on an environment-industrial application. This way was chosen based on different reasons. First of all, microbial communities changed drastically according to diverse factors such as geographic location, temperature, chemical composition, pressure, light availability and pH [46,47]. Environments associated with the oil industry are extremely diverse, as well as the microbial communities present there, despite the functional core preservation provided by metabolic redundancy. Taking into account the more than 80 SRB genera, in addition to the complex cultivation of anaerobic bacteria, isolating specific phages for this group becomes a nearly impossible task. Thus, the action of phage-based products in highly complex contexts may be more successful when using enzymes present in phages that infect easily cultivated bacteria to control undesired bacterial effects, by disrupting the bacterial biofilms by the action of phage enzymes and exposing bacterial cells to the action of different antimicrobial agents or reaching bacteria that are not necessarily the focus of the problem, but that are keystone species of certain communities [48,49].

Another of the main limitations of using bacteriophages in environmental systems is the need for large amounts of viral particles. As a result, a large-scale production strategy is required, which includes an in-depth investigation of the composition of the culture medium, production parameters, previous preparation stages, downstream steps, storage conditions,

transport, and so on. Although some studies have already been published in this field [50–53], the production of new phage particles will always be dependent on other organism machinery, in such a complex and biased process that is almost individual for each case. In addition, cocktails of phages are normally used in complex environments (to reduce the possibility of the appearance of resistant mutants), and the production would not only be standardized for one phage but for several [18].

The selection of phages to compose a cocktail is not a simple process, since some properties need to be identified for a phage to be considered suitable, such as a broad host range, being strictly lytic, being easily propagated, having the genome sequenced, having absence of pathogenic genes, be sufficiently stable over long periods of storage and application; and be amendable to scale up for commercial production [54]. One of the goals of this study was to isolate and characterize new phages and evaluate their potential as biocontrol agents. This is a continuous process, once if a newly isolated phage has a better profile than those currently in the cocktail, it can be replaced and the formulations increased. Because of this, genomic analysis was performed, and the biotechnological potential and safety of the phages used in this study were deeply investigated. We also evaluated the phage's stability in unusual conditions, once our cocktail was designed to be used in oil facilities, an environment with very particular characteristics. The large-scale production efficiency was the last procedure evaluated in this work.

Hence, this work aimed to explore the vast potential of bacteriophages, proposing and evaluating their application in different contexts. First, the utilization of phages in the still little explored, but with a massive potential for future applications, oil-related environments. This approach can bring important perspectives for increasing or even replacing the methods currently used to control the growth and the impact of unwanted bacterial genera and their biofilms. The use of phage cocktails aiming the non-developmentof biofilms due to the presence of phage enzymes is also an innovative approach. Secondly, was present a well-designed study that unraveled the use of phages to control a highly pathogenic strain of Proteus mirabilis. Thus, this work contribute to expand and strengthen the use of phages and phage-based products in important fields

Bibliography

1. Comeau, A.M.; Hatfull, G.F.; Krisch, H.M.; Lindell, D.; Mann, N.H.; Prangishvili, D. Exploring the prokaryotic virosphere. *Res. Microbiol.* **2008**, *159*, 306–313, doi:10.1016/j.resmic.2008.05.001.

2. Keen, E.C. Phage therapy : concept to cure. *Front. Microbiol.* **2012**, *3*, 238, doi:10.3389/fmicb.2012.00238.

3. Fruciano, E.; Bourne, S. Phage as an antimicrobial agent: d'Herelle's heretical theories and their role in the decline of phage prophylaxis in the West. *Can. J. Infect. Dis. Med. Microbiol.* **2007**, *18*, 19–26.

4. Lin, D.M.; Koskella, B.; Lin, H.C. Phage therapy: An alternative to antibiotics in the age of multi-drug resistance. *World J. Gastrointest. Pharmacol. Ther.* **2017**, *8*, 162, doi:10.4292/wjgpt.v8.i3.162.

5. Almeida, G.M. de F.; Sundberg, L.R. The forgotten tale of Brazilian phage therapy. *Lancet Infect. Dis.* **2020**, *20*, e90–e101, doi:10.1016/S1473-3099(20)30060-8.

6. Brives, C.; Pourraz, J. Phage therapy as a potential solution in the fight against AMR: obstacles and possible futures. *Palgrave Commun.* **2020**, *6*, 1–11, doi:10.1057/s41599-020-0478-4.

7. Cahan, E. As Superbugs Flourish, Bacteriophage Therapy Recaptures Researchers' Interest. *J. Am. Med. Assoc.* **2023**, *329*.

8. Ventola, C.L. The Antibiotic Resistance Crisis. *P&T* **2015**, *40*, 278–283, doi:10.5796/electrochemistry.82.749.

9. Andersson, D.I.; Hughes, D. Antibiotic resistance and its cost: Is it possible to reverse resistance? *Nat. Rev. Microbiol.* **2010**, *8*, 260–271, doi:10.1038/nrmicro2319.

10. Brives, C.; Pourraz, J. Phage therapy as a potential solution in the fight against AMR: obstacles and possible futures. *Palgrave Commun.* **2020**, *6*, 1–11, doi:10.1057/s41599-020-0478-4.

11. Pérez de la Lastra, J.M.; Anand, U.; González-Acosta, S.; López, M.R.; Dey, A.; Bontempi, E.; Morales delaNuez, A. Antimicrobial Resistance in the COVID-19 Landscape: Is There an Opportunity for Anti-Infective Antibodies and Antimicrobial Peptides? *Front. Immunol.* **2022**, *13*, 1–13, doi:10.3389/fimmu.2022.921483.

12. Luong, T.; Salabarria, A.C.; Roach, D.R. Phage Therapy in the Resistance Era: Where Do We Stand and Where Are We Going? *Clin. Ther.* **2020**, *42*, 1659–1680, doi:10.1016/j.clinthera.2020.07.014.

13. Denissen, J.; Reyneke, B.; Waso-Reyneke, M.; Havenga, B.; Barnard, T.; Khan, S.; Khan, W. Prevalence of ESKAPE pathogens in the environment: Antibiotic resistance status, community-acquired infection and risk to human health. *Int. J. Hyg. Environ. Health* **2022**, *244*, 114006, doi:10.1016/j.ijheh.2022.114006.

14. Coșeriu, R.L.; Vintilă, C.; Mare, A.D.; Ciurea, C.N.; Togănel, R.O.; Cighir, A.; Simion, A.; Man, A. Epidemiology, Evolution of Antimicrobial Profile and Genomic Fingerprints of Pseudomonas aeruginosa before and during COVID-19: Transition from Resistance to Susceptibility. *Life* **2022**, *12*, doi:10.3390/life12122049.

15. CDC Covid-19: US. Impact on Antimicrobial Resistance, Special Report 2022. *U.S. Dep. Heal. Hum. Serv. CDC* **2022**.

16. Pan American Health Organization Antimicrobial Resistance , Fueled By the Covid-19 Pandemic. **2022**, 1–14.

17. Verbeken, G.; Pirnay, J.P. European regulatory aspects of phage therapy: magistral phage preparations. *Curr. Opin. Virol.* **2022**, *52*, 24–29, doi:10.1016/j.coviro.2021.11.005.

18. Jault, P.; Leclerc, T.; Jennes, S.; Pirnay, J.P.; Que, Y.A.; Resch, G.; Rousseau, A.F.; Ravat, F.; Carsin, H.; Le Floch, R.; et al. Efficacy and tolerability of a cocktail of bacteriophages to treat burn wounds infected by Pseudomonas aeruginosa (PhagoBurn): a randomised, controlled, double-blind phase 1/2 trial. *Lancet Infect. Dis.* **2019**, *19*, 35–45, doi:10.1016/S1473-3099(18)30482-1.

19. Onsea, J.; Uyttebroek, S.; Chen, B.; Wagemans, J.; Lood, C.; Van Gerven, L.; Spriet, I.; Devolder, D.; Debaveye, Y.; Depypere, M.; et al. Bacteriophage therapy for difficult-to-treat infections: The implementation of a multidisciplinary phage task force (the phageforce study protocol). *Viruses* **2021**, *13*, doi:10.3390/v13081543.

20. Gambino, M.; Brøndsted, L. Looking into the future of phage-based control of zoonotic pathogens in food and animal production. *Curr. Opin. Biotechnol.* **2021**, *68*, 96–103, doi:10.1016/j.copbio.2020.10.003.

21. Kumar, C.G.; Anand, S.K. Significance of microbial biofilms in food industry : a review. *Int. J. Food Microbiol.* **1998**, *42*, 9–27.

22. Harper, D.R.; Parracho, H.M.R.T.; Walker, J.; Sharp, R.; Hughes, G.; Werthé, M. Bacteriophages and Biofilms. **2014**, 270–284, doi:10.3390/antibiotics3030270.

23. Visnapuu, A.; Der Gucht, M.; Wagemans, J.; Lavigne, R. Deconstructing the Phage–Bacterial Biofilm Interaction as a Basis to Establish New Antibiofilm Strategies. *Viruses* **2022**, *14*, doi:10.3390/v14051057.

24. Flemming, H.C.; Wingender, J.; Szewzyk, U.; Steinberg, P.; Rice, S.A.; Kjelleberg, S. Biofilms: An emergent form of bacterial life. *Nat. Rev. Microbiol.* **2016**, *14*, 563–575, doi:10.1038/nrmicro.2016.94.

25. Costerton, J.W.; Cheng, K.J.; Geesey, G.G.; Ladd, T.I.; Nickel, J.C.; Dasgupta, M.; Marrie, T.J. Bacterial biofilms in nature and disease. *Annu. Rev. Microbiol.* **1987**, *41*, 435–464.

26. López, D.; Vlamakis, H.; Kolter, R. Biofilms. *Cold spings* **2010**, 1–12.

27. Pires, D.P.; Oliveira, H.; Melo, L.D.R.; Sillankorva, S.; Azeredo, J. Bacteriophage-encoded depolymerases : their diversity and biotechnological applications. *Appl. Microbiol. Biotechnol.* **2016**, *100*, 2141–2151, doi:10.1007/s00253-015-7247-0.

28. Shymialevich, D.; Wójcicki, M.; Wardaszka, A.; Świder, O.; Sokołowska, B.; Błażejak, S. Application of Lytic Bacteriophages and Their Enzymes to Reduce Saprophytic Bacteria Isolated from Minimally Processed Plant-Based Food Products-In Vitro Studies. *Viruses* **2022**, *15*, doi:10.3390/v15010009.

29. Oliveira, H.; Drulis-Kawa, Z.; Azeredo, J. Exploiting phage-derived carbohydrate depolymerases for combating infectious diseases. *Trends Microbiol.* **2022**, *30*, 707–709, doi:10.1016/j.tim.2022.05.002.

30. Fernandes, S.; São-José, C. Enzymes and mechanisms employed by tailed bacteriophages to breach the bacterial cell barriers. *Viruses* **2018**, *10*, 1–22, doi:10.3390/v10080396.

31. Rodríguez-Rubio, L.; Martínez, B.; Donovan, D.M.; Rodríguez, A.; García, P. Bacteriophage virion-associated peptidoglycan hydrolases: Potential new enzybiotics. *Crit. Rev. Microbiol.* **2013**, *39*, 427–434, doi:10.3109/1040841X.2012.723675.

32. Carlos, S. Engineering of Phage-Derived Lytic Enzymes : Improving Their Potential as Antimicrobials. **2018**, doi:10.3390/antibiotics7020029.

33. Rabus, R.; Venceslau, S.S.; Wöhlbrand, L.; Voordouw, G.; Wall, J.D.; Pereira, I.A.C. A Post-Genomic View of the Ecophysiology, Catabolism and Biotechnological Relevance of Sulphate-Reducing Prokaryotes. *Adv. Microb. Physiol.* **2015**, *66*, 55–321, doi:10.1016/bs.ampbs.2015.05.002.

34. Song, J.; Hwang, J.; Kang, I.; Cho, J.C. A sulfate-reducing bacterial genus, Desulfosediminicola gen. nov., comprising two novel species cultivated from tidal-flat sediments. *Sci. Rep.* **2021**, *11*, 1–13, doi:10.1038/s41598-021-99469-5.

35. Waite, D.W.; Chuvochina, M.; Pelikan, C.; Parks, D.H.; Yilmaz, P.; Wagner, M.; Loy, A.; Naganuma, T.; Nakai, R.; Whitman, W.B.; et al. Proposal to reclassify the proteobacterial classes deltaproteobacteria and oligoflexia, and the phylum thermodesulfobacteria into four phyla reflecting major functional capabilities. *Int. J. Syst. Evol. Microbiol.* **2020**, *70*, 5972–6016, doi:10.1099/ijsem.0.004213.

36. Barton, L.L.; Fauque, G.D. Biochemistry, Physiology and Biotechnology of Sulfate-Reducing Bacteria. In *Advances in Applied Microbiology*; Elsevier Inc.: Amsterdam, The Netherlands, 2009; Vol. 68, pp. 41–98 ISBN 9780123748034.

37. Gieg, L.M.; Jack, T.R.; Foght, J.M. Biological souring and mitigation in oil reservoirs. *Appl. Microbiol. Biotechnol.* **2011**, *92*, 263–282, doi:10.1007/s00253-011-3542-6.

38. Reiffenstein, R.J.; Hulbert, W.C.; Roth, S.H. Toxicology of hydrogen sulfide. *Annu. Rev. Pharmacol. Toxicol.* **1992**, *32*, 109–134, doi:10.1146/annurev.pa.32.040192.000545.

39. Tang, K.; Baskaran, V.; Nemati, M. Bacteria of the sulphur cycle: An overview of microbiology, biokinetics and their role in petroleum and mining industries. *Biochem. Eng. J.* **2009**, *44*, 73–94, doi:10.1016/j.bej.2008.12.011.

40. Fraise, A.P. Susceptibility of antibiotic-resistant cocci to biocides. *J. Appl. Micriobiology Symp. Suppl.* **2002**, *92*, 158–162.

41. Okoro, C.C. The Biocidal Efficacy of Tetrakis-hydroxymethyl Phosphonium Sulfate (THPS) Based Biocides on Oil Pipeline PigRuns Liquid Biofilms The Biocidal Efficacy of Tetrakis-hydroxymethyl Phosphonium Sulfate (THPS) Based Biocides on Oil Pipeline PigRuns Liquid . **2015**, *6466*, doi:10.1080/10916466.2015.1062781.

42. Gu, D.X.Y.L.T. A synergistic D -tyrosine and tetrakis hydroxymethyl phosphonium sulfate biocide combination for the mitigation of an SRB biofilm. **2012**, 3067–3074, doi:10.1007/s11274-012-1116-0.

43. Stewart, P.S.; Costerton, J.W. Antibiotic resistance of bacteria in biofilms. *Lancet* **2001**, *358*, 135–138.

44. Mattila, S.; Ruotsalainen, P.; Jalasvuori, M. On-Demand Isolation of Bacteriophages Against Drug- Resistant Bacteria for Personalized Phage Therapy Bacteria Strains and Culturing. *Front. Microbiol.* **2015**, *6*, 1–7, doi:10.3389/fmicb.2015.01271.

45. Hyman, P. Phages for phage therapy: Isolation, characterization, and host range breadth. *Pharmaceuticals* **2019**, *12*, doi:10.3390/ph12010035.

46. Schlechter, R.O.; Miebach, M.; Remus-Emsermann, M.N.P. Driving factors of epiphytic bacterial communities: A review. *J. Adv. Res.* **2019**, *19*, 57–65, doi:10.1016/j.jare.2019.03.003.

47. Nemergut, D.R.; Schmidt, S.K.; Fukami, T.; O'Neill, S.P.; Bilinski, T.M.; Stanish, L.F.; Knelman, J.E.; Darcy, J.L.; Lynch, R.C.; Wickey, P.; et al. Patterns and Processes of Microbial Community Assembly. *Microbiol. Mol. Biol. Rev.* **2013**, *77*, 342–356, doi:10.1128/mmbr.00051-12.

48. Berry, D.; Widder, S. Deciphering microbial interactions and detecting keystone species with co-occurrence networks. *Front. Microbiol.* **2014**, *5*, 1–14, doi:10.3389/fmicb.2014.00219.

49. Tudela, H.; Claus, S.P.; Saleh, M. Next Generation Microbiome Research: Identification of Keystone Species in the Metabolic Regulation of Host-Gut Microbiota Interplay. *Front. Cell Dev. Biol.* **2021**, *9*, doi:10.3389/fcell.2021.719072.

50. Silva, J.; Dias, R.; Junior, I.; Silva, M.; Carmo, A.; Sousa, M.; Silva, C.; Paula, S. De A Rapid Method for Performing a Multivariate Optimization of Phage Production Using the RCCD Approach. *Pathogens* **2021**, *10*, 1–19, doi:https://doi.org/10.3390/pathogens 10091100.

51. Agboluaje, M.; Sauvageau, D. Bacteriophage Production in Bioreactors. In *Bacteriophage Therapy: From Lab to Clinical Practice*; Azeredo, J., Sillankorva, S.,

Eds.; Human Press: Totowa, NJ, USA, 2018; Vol. 1693, pp. 173–193 ISBN 9781493973958.

52. Mancuso, F.; Shi, J.; Malik, D.J. High throughput manufacturing of bacteriophages using continuous stirred tank bioreactors connected in series to ensure optimum host bacteria physiology for phage production. *Viruses* **2018**, *10*, 537, doi:10.3390/v10100537.

53. Bonilla, N.; Barr, J.J. Phage on tap: A quick and efficient protocol for the preparation of bacteriophage laboratory stocks. *Methods Mol. Biol.* **2018**, *1838*, 37–46, doi:10.1007/978-1-4939-8682-8_4.

54. Goodridge, L.D.; Bisha, B. Phage-based biocontrol strategies to reduce foodborne pathogens in foods. *Bacteriophage* **2011**, *1*, 130–137, doi:10.4161/bact.1.3.17629.

Chapter 1: Isolation and characterization of the *Karamvirus* member vB_EclM-UFV01, an *Enterobacter cloacae* infecting phage.

Jéssica Duarte da Silva[1], Adriele Jéssica do Carmo[1], Roberto Sousa Dias[1], Pedro Marcus P. Vidigal[2], Bruna Almeida Leão Ayupe[1], José Júnior Ferreira Soares[1,] Mariana Pyramides Napoleão, Marcella Silva Vieira[1], Paloma Cavalcante Cunha[1], Isabela Silva Paes[1], Sérgio Oliveira de Paula.

[1] Laboratório de Imunovirologia. Universidade Federal de Viçosa. Viçosa. Minas Gerais.

[2] Núcleo de Análise de Biomoléculas, Universidade Federal de Viçosa, Vila Gianetti. Viçosa. Minas Gerais

Abstract

Bacteriophages are viruses that infect bacteria. Since their discovery, in the early 20th century, these viruses have been used to kill pathogenic bacteria, in a method known as phage therapy. Several enterobacteria are known as opportunistic pathogens, among them, *Enterobacter cloacae* is one of the most well-known and source of concern. This work aimed to characterize the phage vB_EclM-UFV01, isolated from the bacterial strain *Enterobacter cloacae* ATCC 13047, and evaluate its potential as a phage therapy agent. Biological and genomic features of this phage were investigated, such as host range, one-step growth curve, and presence of putative depolymerase-like domains, as well as their tertiary structure prediction. Our findings were compared to those available for the other members of the *Karamvirus*, highlighting the common characteristics of the genus. *Enterobacter* phage vB_EclM-UFV01 has a myovirus morphology, a latent period of 15 minutes, and an estimated burst size of 55 p.p/i.c. Its dsDNA genome, with 174,517 bp, 286 ORFs, 14 tRNAs, and 2 predicted genes with depolymerase domains. The genome still possesses 60 predicted promoters and 13 terminator regions. This phage also can decrease the biofilm formation of *Proteus vulgaris* and *Escherichia coli* isolates. Such results indicate that vB_EclM-UFV01 is an excellent candidate to be used in phage therapy cocktails.

Key-words: Bacteriophage. Phage-therapy. ESKAPE.

1. Introduction

The ESKAPE acronym comprises the antimicrobial-resistant pathogens *Enterococcus faecium, Staphylococcus aureus, Klebsiella pneumoniae, Acinetobacter baumannii, Pseudomonas aeruginosa,* and *Enterobacter spp* [1,2]. The species of the ESKAPE group are well known for their role as causative agents of nosocomial infections and the increasing number of strains containing multidrug resistance and virulence genes [1,3,4]. The World Health Organization (WHO) defined carbapenem-resistant *A. baumannii* and *P. aeruginosa* as well as extended-spectrum β-lactamase (ESBL) or carbapenem-resistant *K. pneumoniae* and *Enterobacter spp.* as critical priorities for public health monitoring and research effort on the development antimicrobial strategies [1,3,5–7]. *Enterobacter cloacae*, along with *E. asburiae, E. hormaechei, E. kobei, E. ludwigii,* and *E. nimipressuralis,* forms the "*Enterobacter cloacae complex" (ECC)* [8,9]. These organisms are frequently associated with urinary tract and skin infections, gastroenteritis, endocarditis, and pneumonia, playing a significant role as opportunistic pathogens, especially in clinical settings. Data from 2012 indicate that the ECC is responsible for 5% of hospital-acquired sepsis, 5% of nosocomial pneumonia cases, 4% of nosocomial urinary tract infections, and 10% of postsurgical peritonitis in the United States [8]. These statistics are not surprising given the intrinsic resistance of *E. cloacae* to antibiotics such as ampicillin, amoxicillin/clavulonate, cephamycins, and first and second-generation cephalosporins. More recently, carbapenem and colistin-resistant strains have also been isolated [9–11]. Consequently, ECC ranked as the second most common carbapenem-resistant Enterobacteriaceae in the United States in 2019, just behind *Klebsiella pneumonia*e [10].

Bacteriophages, also called phages, are viruses that infect bacteria. After their discovery - at the beginning of the 20th century - Félix d'Herelle explored the lytic potential of these viruses, using them to combat bacterial diseases and developing the so-called "phage therapy" [12–14]. Although phage cocktails had been effective in treating patients with infections caused by important pathogens such as *Salmonella typhi, Escherichia coli, Vibrio cholerae,* and *Yersinia pestis*, the cure did not occur in all cases. These inconsistencies, together with the discovery of penicillin in 1928, put an end to the rising use of phage therapy over the world, which quickly became obsolete [12,13,15]. However, the emergence of numerous multi-drug resistant bacterial strains, stimulated mainly by the overuse of antibiotics over all these years, made phage therapy once again considered an effective alternative in the treatment of bacterial diseases [16,17]. Advances in scientific understanding of the kinetics of viral infection, phage enzymes, and the particularities of phage-host

relationships were essential to explain why phage therapy was so unstable early in its development and enable the utilization of this methodology in a much more efficient and safe way nowadays [18–21]. Studies evaluating the potential of phage cocktails to control ESKAPE infections have increased since phage therapy was reintroduced as a viable treatment option for difficult-to-treat infections [4–7]. Phage-encoded enzymes, such as endolysins and polysaccharide depolymerase are also been investigated to decrease the biofilm formation of these bacteria [22–24]. Fortunately, both approaches have demonstrated promising results [25].

Thus, the isolation of specific bacteriophages against bacteria of the *ECC* is an interesting alternative for the strengthening of methodologies that are effective in treating infections caused by this organism, especially multi-drug resistant strains. This work aims to characterize a phage capable of infecting the bacterium *E. cloacae* ATCC 13047 and to evaluate its potential as a bioremediation agent for bacterial growth, focusing on phage therapy.

2. Materials and Methods

2.1. Phage isolation

Enterobacter phage vB_EclM-UFV01 (shortly called ENT01) was isolated from a sample taken from the São Bartolomeu River in Viçosa, Minas Gerais, Brazil (geographical coordinates: latitude -20.743191; longitude -42.881961), following the protocol adapted from Van Twest and Kropinski, 2009 [26]. Briefly, the environmental sample was centrifuged at 8000 g for 15 minutes. The supernatant was recovered and filtered through 0.45 μm and 0.22 μm filters. Isolation host *E. cloacae* ATCC13047 was grown to an exponential growth phase and added to the mixture (100 μL), followed by overnight incubation at 37 °C while shaking (100 rpm). After the incubation, a double agar overlay assay was performed [27]. The lysis plates resulting from this process, or lysis that showed distinct morphology, were picked from the agar and propagated independently in the LB medium containing the host. This process was repeated at least five times.

2.2. Biological features

2.2.1. Transmission electron microscopy (TEM).

The transmission electron microscopy (TEM) was performed using a concentrated phage suspension. 10 μl of this supernatant was added to Formvar® coated grids. After 5

minutes, the surplus liquid was collected with absorbent paper, and the sample was counterstained for 30 seconds with 3% uranyl acetate. Until the visualization, the grid was maintained in a desiccator. The visualization of viral particles was performed on a Zeiss EM 109 transmission electron microscope using 250,000x 80 kv HV magnification

2.2.2. Host range

The host range screening of the *Enterobacter* phage vB_EclM-UFV01 was done both by spot and killing assays. Briefly, the bacterial strains tested as potential hosts (Table 1) were incubated overnight in LB medium, without agitation, at 37°C. An aliquot of 700 µL of the grown strains was mixed with 5 mL of LB top agar (0.7%) and poured into a petri dish containing LB bottom agar (1.5%). After solidification, 10 µL of the phage ENT01 supernatant, (10^8 PFU/mL), was dropped onto the plate. The presence of an inhibition halo in the bacterial layer at the site where the phage suspension was present indicated the ability of the phage to use that isolate as a host [28]. The phage-killing curves were made by consecutive OD_{600} absorbance measurements (every 15 minutes). Briefly, 10 µL of the phage supernatant (final concentration of 10^8 PFU/mL) was added to 190 µL of freshly grown bacterial host strains (OD_{600} of 0.1) in a 96-well plate. The experiment was conducted in triplicate. The bacterial growth curves (with and without phages) were compared to identify differences between the growth curves.

2.2.3. One-step growth curve

The one-step growth curve was performed to determine the latency time and the burst size of the phage ENT01, adapting the protocol of Manohar (2019)[29]. Briefly, 100µL of phage (10^9 PFU/mL) was added to 10mL of bacterial culture of *Enterobacter cloacae* ATCC 13047 grown in liquid LB medium until the beginning of the logarithmic phase (OD_{600} of 0.3, and MOI of 0.01). The resulting mixture was incubated for 10 minutes, then centrifuged at 8000 g for 20 minutes. The supernatant was discarded and the pellet was resuspended in 10 mL of liquid LB medium. An aliquot of 100µL was collected and plated by the double layer method every five minutes, while the mixture was incubated with gentle agitation at 37 °C. The experiment was performed in triplicate.

2.2.4. Biofilm inhibition

The ability to inhibit the biofilm formation of strains that ENT01 is not able to infect was tested using the protocol of Knezevic and Petrovic, 2008 [30], with few modifications. In

96-well plates, biofilm-forming bacteria (that do not compose the vB_EclM-UFV01 host range) were incubated at 37 °C for 24 hours. After this, the supernatant was discarded, the wells washed with 0.9% saline solution and left at 55 °C until be completely dry. 250 µL of methanol was added to the wells and discarded after 15 minutes. After further incubation at 55 °C and complete evaporation of methanol, 250 µL of 0.1% crystal violet solution was added to the wells. After 30 minutes, the solution was discarded, the wells were washed with 0.9% saline solution and after drying, an alcohol/acetone 4:1 solution was used to dissolve the violet crystals that adhered to the biofilm formed. The absorbance of this mixture was read at the wavelength of 590 nm.

2.3. Viral genome extraction

The phage genome extraction was performed using the phenol-chloroform protocol (Sambrook and Russel, 2001). Briefly, into 500 µL of ENT01 supernatant was added proteinase K (final concentration of 50 µg/mL) and SDS (final concentration of 0.5% (w/v)). The mixture was incubated for one hour at 56 °C. Then, 500 µL of phenol pH 8.0 was added to the mixture, which was subsequently centrifugated at 8000 g, for 5 minutes. The aqueous phase was collected and transferred to a new tube. An equal volume of a 1:1 chloroform/phenol solution was added to the tube. After further centrifugation, the aqueous phase was recovered and an equal volume of chloroform was added. The mixture was centrifuged and the aqueous phase was transferred to a new tube. Ethanol in a 2:1 ratio was added and the solution was stored at -20°C for 12 hours. Finally, the tube was centrifuged at 15,000 xg for 20 minutes, the ethanol was discarded and, after evaporating completely, the pellet was resuspended in 20 µL of ultrapure water.

2.4. Genome sequencing, assembly and annotation

ENT01 genome was sequenced by the company MR DNA (Shallowater, TX, USA), using the Illumina NovaSeq technology. The reads quality was evaluated by FASTQC version 0.1.16 (https://github.com/s-andrews/FastQC) and the remaining adapters were taken by the TrimGalore tool, version 0.0.6 (https://github.com /FelixKrueger/TrimGalore). Trimmomatic, version 0.39 [31] was used to trim and filter the reads by size and quality, according to the parameters HEADCROP:40 CROP:100 SLIDINGWINDOW:4:20 MINLEN:100. SPAdes Genome Assembler [32], version 3.14.1, was used for the *ab initio* assembly, using odd k-mers between 21 and 99. Bbmap (https://anaconda.org/bioconda/bbmap) assessed the quality of the generated contigs. For the second stage of genome assembly, necessary once the

SPAdes failed to merge all the contigs belonging to the vB_EclM-UFV01 into a single one, the bwa software (Burrows-Wheeler Aligner) [33] was used to complete the assembly using *Enterobacter* phage PG7 as reference genome, guiding the position of the genes. The coding DNA sequences (CDS) were annotated using RAST (Rapid Annotation using Subsystem Technology) platform (https://rast.nmpdr.org) [34].

2.5. Genomic and phylogenetic analysis

To identify the similarity of ENT01 with the NCBI (National Center for Biotechnology Information) database (https://blast.ncbi.nlm.nih.gov/Blast) a comparative megablast was performed. All the fourteen genomes belonging to the genus *Karamvirus* available on NCBI were used to create a proteomic tree on The Viral Proteomic Tree server (Viptree) [35]. The *Enterobacteria* phage T4 was used as an outgroup, and the *Citrobacter* phage Ckp1, which belongs to a related genus, was used to confirm ENT01's correct taxonomic clade. Viptree was also used to create the alignment among these genomes. The ones that were not already opened in rIIA lysis inhibition protein were re-opened using QIAGEN CLC Genomics Workbench 21.0. The same phages were used by VIRIDIC to calculate the pairwise intergenomic distances/similarities and to obtain the phylogenetic correlation between them. The search for depolymerase-like enzymes was performed using Phage Depolymerase Finder [36] (Galaxy Version 0.1.0) from the Galaxy Docker Build platform (https://galaxy.bio.di.uminho.pt/). The genomic map was generated by Clinker [37], followed by a manual edition. The proteins predicted as putative depolymerases were then submitted on HMMER - Sensitive sequence searching based on profile HMMs [38], and HHPRED on the MPI bioinformatics toolkit (https://toolkit.tuebingen.mpg.de/) [39] for the confirmation of the enzymatic domains. Phage promoters were predicted by MEME (Multiple Em for Motif Elicitation) (https://meme-suite.org/meme/tools/meme) [40], followed by manual checking. tRNAscan_SE [41] was used to search for tRNAs and ARNold-finding terminators for the identification of Rho-independent terminators [42]. The AlphaFold2 [43] pipeline, version 1.3.0, was used to predict the tertiary structure of the proteins, using the default settings.

3. Results

3.1. Biological features

The transmission electron microscopy (TEM) showed that phage vB_EclM-UFV01 (ENT01) has a typical Myovirus morphology (Figure 1), with an icosahedral capsid and a contractile tail of approximately 170 nm in length.

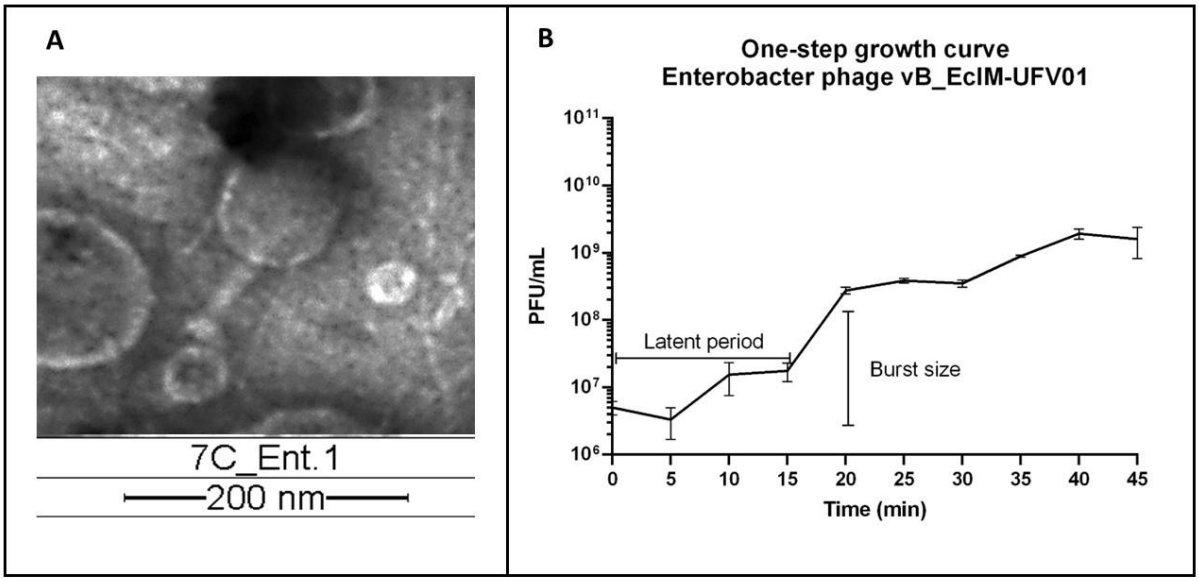

The One-Step growth curve shows that phage ENT01 has a latent period of approximately 15 minutes and an estimated burst size of 55 phage particles per infected cell (p.p/i.c).

The 19 strains tested in the host range assay belong to 12 different genera from five bacterial families. As summarized in Table 1, ENT01 was only able to infect its isolation host strain (*E. cloacae* ATCC 13047).

Tabela 1: Bacterial strains used on Enterobacter phage vB_EclM-UFV01 host range determination.

Bacterial family	Bacterial strain	Result
Enterobacteriaceae	*Klebsiella pneumoniae* MCS	Negative
Enterobacteriaceae	*Klebsiella pneumoniae* HPM	Negative
Enterobacteriaceae	*Klebsiella oxytoca* ATCC 13182	Negative
Enterobacteriaceae	*Salmonella enterica* ATCC 13076	Negative
Enterobacteriaceae	*Citrobacter freundii* ATCC 8090	Negative
Enterobacteriaceae	*Cronobacter sakazakii* ATCC 29004	Negative
Enterobacteriaceae	*Enterobacter cloacae* ATCC 13047	Positive
Enterobacteriaceae	*Shigella flexneri LIVM 3*	Negative
Enterobacteriaceae	*Escherichia coli 30*	Negative
Enterobacteriaceae	*Escherichia coli 11C*	Negative
Enterobacteriaceae	*Escherichia coli SAN 1*	Negative
Enterobacteriaceae	*Escherichia coli SAN 3*	Negative
Enterobacteriaceae	*Escherichia coli K12*	Negative
Yersiniaceae	*Serratia marcenscens* MIND01	Negative
Enterococcaceae	*Enterococcus faecalis* ATCC 29212	Negative
Morganellaceae	*Morganella morganii* MCS	Negative
Morganellaceae	*Proteus vulgaris* LIVM 1	Negative
Morganellaceae	*Proteus mirabilis* MCS	Negative
Streptococcaceae	*Streptococcus agalactiae* LIVM 2	Negative

The biofilm inhibition assay was performed with all the bacterial strains that present a negative result in the host range test (Table 1). The results can be observed in the figure 2. Six of the eighteen strains did not produce enough biofilm to guarantee a good colorimetric quantification (Abs 590 nm >0,1) and are not represented in the figure. Although in ten of the twelve strains no significant alterations in the biofilm were found between the treatments, in two of them it was possible to observe significant decreases (Student's t-test, p-value < 0.05): *P. vulgaris* LIVM 1 and *E. coli SAN 3*.

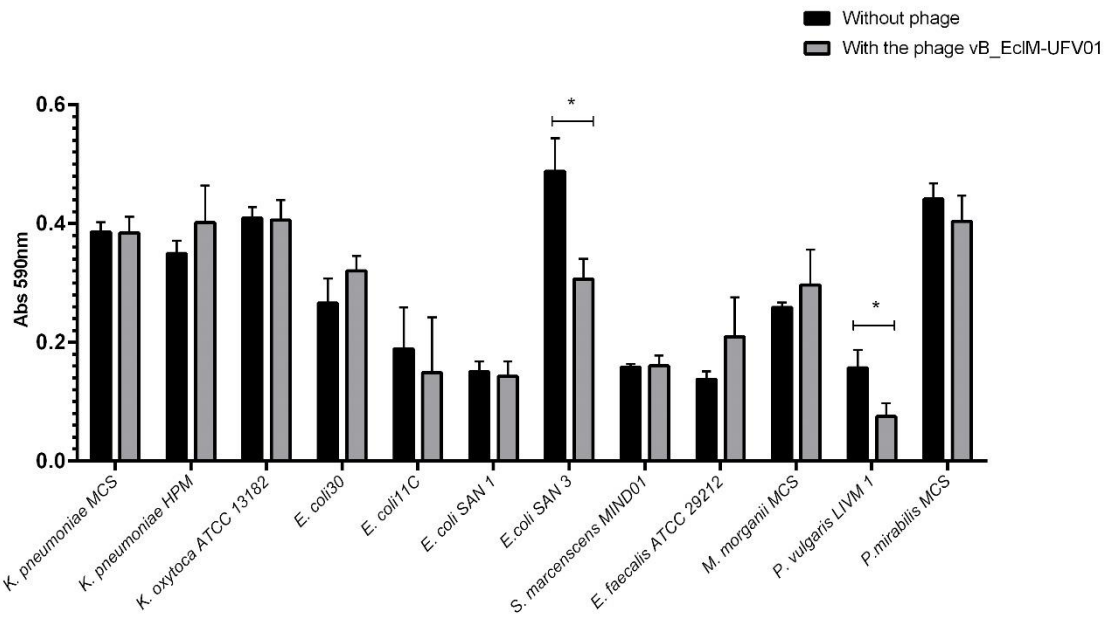

Figure 2: Violet Crystal quantification of the biofilm produced by different bacterial strains in the presence (gray columns) and absence (black columns) of the Enterobacter phage vB_EclM-UFV01.

3.2. Genomic features

ENT01 has a linear double-stranded DNA genome, with 174,517 base pairs (bp) and 287 open reading frames (ORFs). None of the predicted ORFs encode for lysogeny-associated proteins or virulence genes. Hence ENT 01 can be classified as a virulent phage.

A search for related phages using BLASTn showed that ENT01 present more than 95% of identity with the *Enterobacter* phages vB-EclM_KMB17 (OL849997), vB_VIPECLUMC02 (OQ721913), vB_VIPECLOM01 (OQ721912), PG7 (NC_023561), fGh-Ecl04 (ON212267), fGh-Ecl01 (ON212265) and more than 90% with Entb_43 (ON585039), myPSH1140 (NC_055739), vB-EclM_KMB19 (OL828290), CC31 (NC_014662) and vB-EclM_KMB20 (OL828291). Phages isolated from other bacterial genera also presented more than 90% similarity with ENT01, such as *Klebsiella* phage vB_KaeM_KaAlpha (MN013084) and *Cronobacter* phage Pet-CM3-4 (NC_055726). All these phages are members of the genus *Karamvirus* (subfamily *Tevenvirinae*, family *Straboviridae*). VIRIDIC was used to calculate the intergenomic distance between the Karamvirus and phage ENT01 (Figure 3A). The *Tequatrovirus* T4 (NC_000866.4) and *Citrobacter* phage CkP1 (MW239124) were also used in this analysis, as the *Karamvirus* has previously been classified as T4-like phages and CkP1 is the most similar phage belonging to a different genus to ENT01.

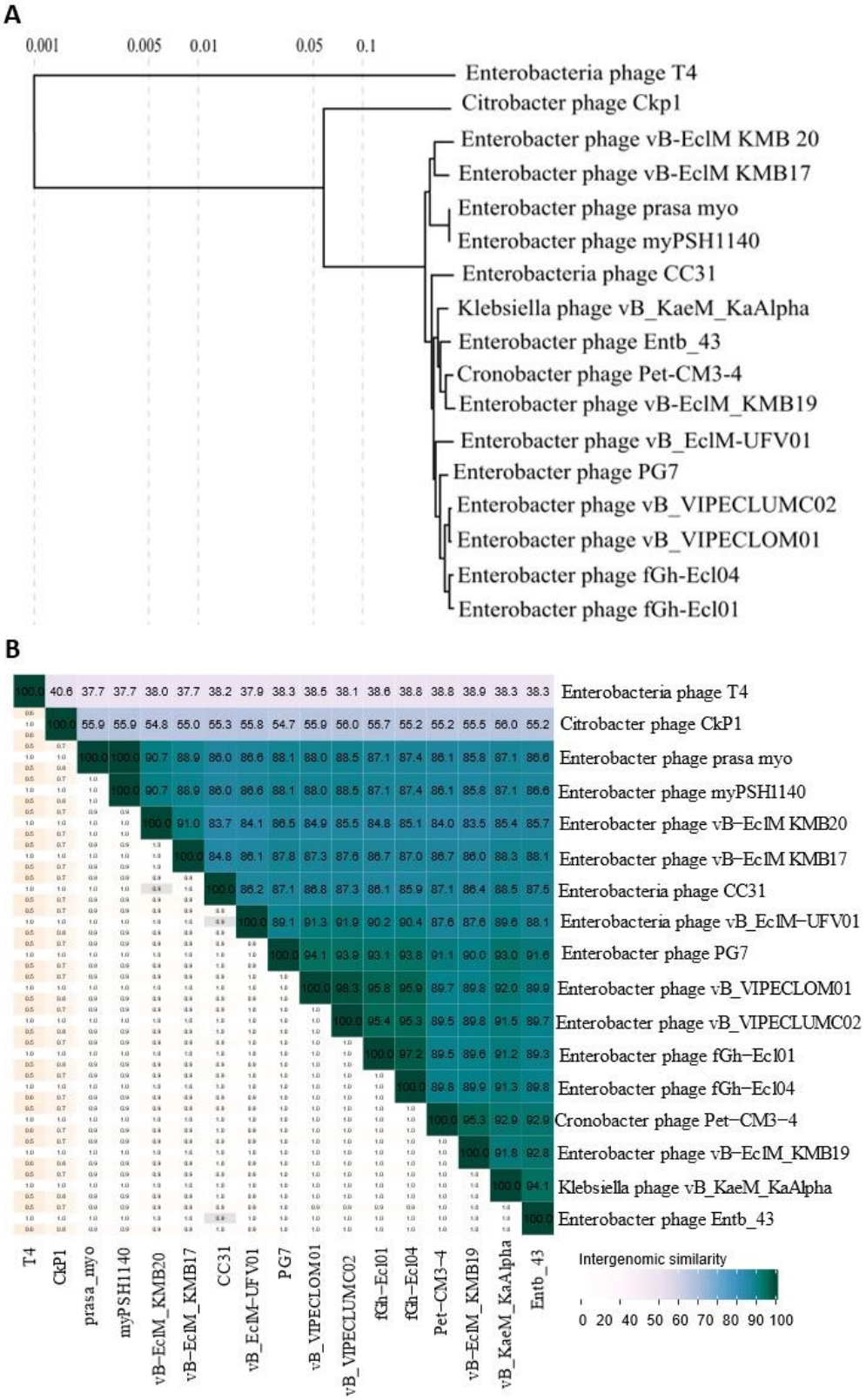

Figure 3: Karamviruses phylogeny. **A.** Phylogenetic tree created with all the genomes of members of the genus *Karamvirus* available in NCBI. *Citrobacter* phage CkP1 was used as a related phage but from a different genus. The phage *Tequeatrovirus* T4 (NC_000866.4) was used as an outgroup. **B.** VIRIDIC heatmap showing the intergenomic distance among the related phages. Phages with more than 95%

similarity belong to the same species and with more than 70% to the same genus. *Citrobacter* phage CkP1 and phage *Tequeatrovirus* T4 (NC_000866.4) were also used as comparison parameters with the karamviruses.

VIRIDIC results demonstrate that phage ENT01 shares more than 70% of its DNA with the members of the genus *Karamvirus*, indicating that they are from the same genus but different species. The results of phylogenetic and VIRIDIC analysis matched with the ones obtained from BLASTn and reinforced that the *Enterobacter* phages vB_VIPECLUMC02, vB_VIPECLOM01, PG7, fGh-Ecl04, and fGh-Ecl01 are the most similar to ENT01.

Table 2 summarizes some features of the *Karamvirus* genus members. G+C content is the most conserved aspect, and in a general way, the genome length and number of tRNAs are also similar. Except for *Enterobacteria* phage CC31, all of the other genomes are larger than 170kb and contain more than 10 tRNAs, being *Asp*, *Met*, *His*, *Ser*, *Trp*, *Gly*, *Pro*, *Phe*, *Arg*, *Cys*, *Leu*, and *Thr* common to all them.

Table 2: *Karamvirus* phages features. tRNAs marked with * were calculated manually for this work. Phage T4 was used as a comparison parameter.

Phage	Length (bp)	ORFs	tRNA	G+C (%)	Burst size	Host range
Enterobacter phage fGh-Ecl01	171663	288	19	39,8	-	-
Enterobacter phage fGh-Ecl04	172419	288	19	39,8	-	-
Enterobacter phage PG7	173276	294	19	39,8	-	-
Enterobacter phage vB_VIPECLOM01	171903	306	18	39,8	-	-
Enterobacter phage vB_VIPECLUMC02	172129	305	18	39,8	-	-
Enterobacter phage prasa_myo	172614	307	19	39,9	-	-
Klebsiella phage vB_KaeM_KaAlpha	172334	318	18	39,8	-	-
Enterobacteria phage CC31	165540	279	8	39,9	-	
Enterobacter phage Entb_43	174681	314	19	39,7	-	8/20
Enterobacter phage myPSH1140	172614	240	19*	39,9	135	22/26
Enterobacter phage vB-EclM_KMB17	172607	275	14*	39,8	53	8/38
Enterobacter phage vB-EclM_KMB19	172697	278	19*	39,8	17	16/38
Enterobacter phage vB-EclM_KMB20	174418	276	19*	39,7	42	14/38
Cronobacter phage Pet-CM3-4	171975	284	18	39,8	61	36/38
Enterobacter phage vB_EclM-UFV01	174517	286	14	39,7	55	1/19
Enterobacteria phage T4	168903	276	8	35,3	-	-

The genome map of ENT01 is shown in Figure 4. From the 286 predicted ORFs, 87 (30.4 %) encode genes related to DNA metabolism, 52 (18.2 %) to structural functions, 9 (3.2 %) to lysis and packaging, and 138 (48.4%) are annotated as hypothetical proteins. The

genome still possesses 60 putative promoters (Figure 5) and 13 Rho-independent terminators. The genomic organization resembles those found on T4 phage-like phages.

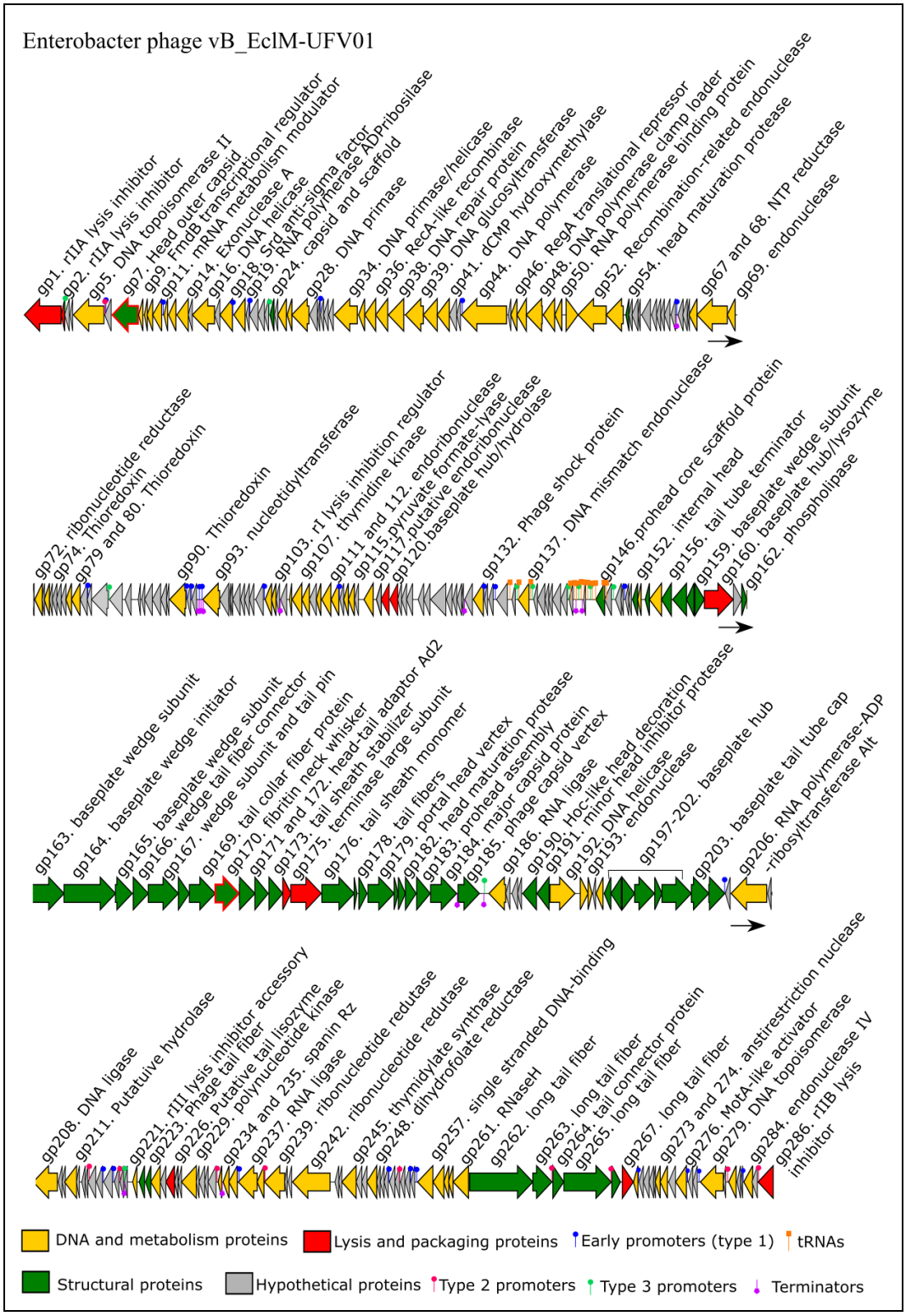

Figure 4: Genomic map of *Enterobacter* phage vB_EclM-UFV01. Each arrow represents an ORF, colored according to their encoded protein function: yellow – proteins associated with DNA and metabolism; green – structural proteins; red – lysis and package proteins; gray – hypothetical proteins. The colored pins illustrate the predicted promoters. The Rho-independent terminators are represented by purple pins.

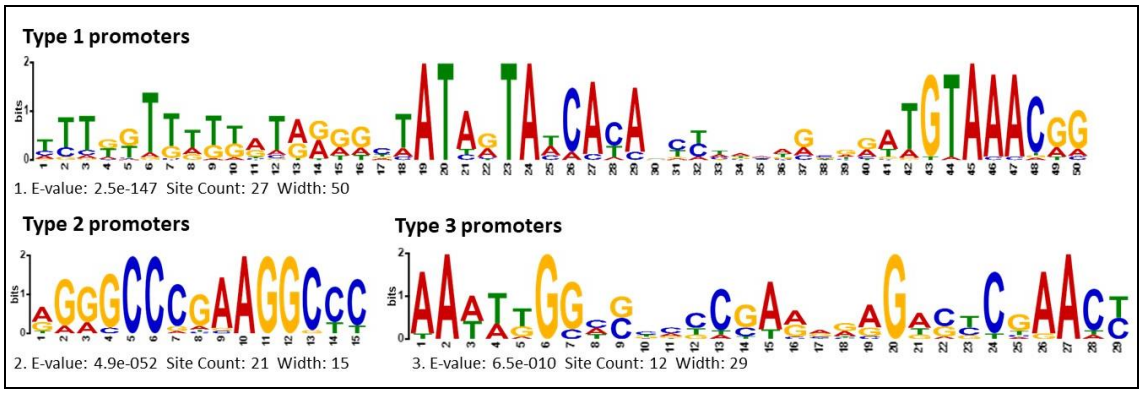

Figure 5: The three types of promoters predicted into the ENT01 genome.

A search for proteins with putative depolymerase domains (DPO) revealed that all the *Karamvirus* genomes contain at least two ORFs with this function. In the case of Ent01, they are annotated as a Head outer capsid protein (gp 7) and the Fibritin neck whisker (gp 170). Table 3 summarizes the location and the structural function of genes containing depolymerase domains present in karamviruses genomes. The prediction made with the Tequatrovirus T4 did not present positive results.

Table 3: Open reading frames (ORFs) containing depolymerase domains in the members of the genus K*aramvirus.*

Phage name	Accession number	DPO ORF	Function
Cronobacter phage Pet-CM3-4	NC_055726	gp 6 gp 161 gp 163	Head decoration Tail collar fiber protein Fibritin neck whisker
Enterobacter phage vB_VIPECLUMC02	OQ721913	gp 7 gp 192	Head decoration Fibritin neck whisker
Enterobacter phage vB_VIPECLOM01	OQ721912	gp 7 gp 194	Head decoration Fibritin neck whisker
Enterobacter phage vB-EclM_KMB17	OL849997	gp 6 gp 166	Capsid and scaffold Fibritin protein
Enterobacter phage vB-EclM_KMB20	OL828291	gp 7 gp 163	Capsid and scaffold protein Fibritin protein
Enterobacter phage Entb_43	ON585039	gp 10 gp 180	Hydrolase family protein Neck protein fibritin
Enterobacter phage fGh-Ecl01	ON212265	gp 8 gp 175	Head outer capsid protein Fibritin neck whisker protein
Enterobacter phage fGh-Ecl04	ON212267	gp 8 gp 176	Head outer capsid protein Fibritin neck whisker protein
Enterobacter phage myPSH1140	NC_055739	gp 9 gp 146	Head decoration Fibritin neck whisker
Enterobacter phage PG7	KJ101592	gp 6 gp 178	Head outer capsid protein Fibritin
Enterobacter phage vB-EclM_KMB19	OL828290	gp 7 gp 165	Capsid and scaffold protein Fibritin protein
Enterobacteria phage CC31	NC_014662	gp 7 gp 164	Head decoration Fibritin neck whisker
Enterobacter phage vB_EclM-UFV01	ON454249	gp 7 gp 170	Head outer capsid protein Fibritin neck whisker
Klebsiella phage vB_KaeM_KaAlpha	MN013084	gp 11 gp 203	Putative head outer capsid protein Putative fibritin neck whisker
Enterobacter phage prasa_myo	MN617835	gp 9 gp 196	hypothetical protein head completion

The distribution of the genes containing depolymerase-domains throw the *Karamvirus* members, together with their genomic architecture can be found in Figure 6. The DPO genes are contoured in red and can be found in the same region in all the genomes. The *Cronobacter* phage Pet-CM3-4 was the only case where three DPOs, instead of two, were predicted. The alignment was also able to illustrate the similar genomic organization although the low identity level between the karamviruses and the *Tequatrovirus* T4.

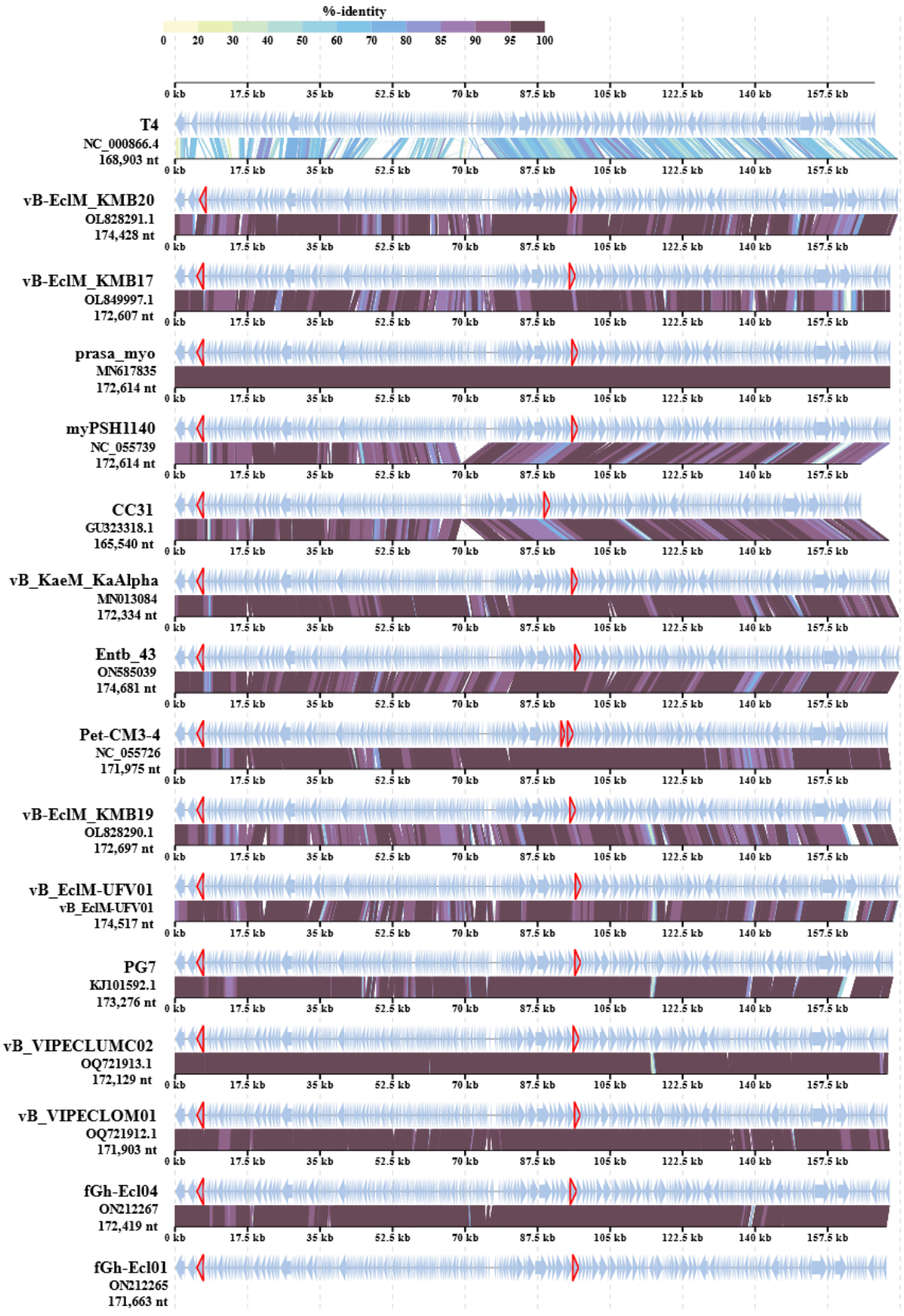
%-identity
0 20 30 40 50 60 70 80 85 90 95 100
0 kb 17.5 kb 35 kb 52.5 kb 70 kb 87.5 kb 105 kb 122.5 kb 140 kb 157.5 kb
T4
NC_000866.4
168,903 nt
vB-EclM_KMB20
OL828291.1
174,428 nt
vB-EclM_KMB17
OL849997.1
172,607 nt
prasa_myo
MN617835
172,614 nt
myPSH1140
NC_055739
172,614 nt
CC31
GU323318.1
165,540 nt
vB_KaeM_KaAlpha
MN013084
172,334 nt
Entb_43
ON585039
174,681 nt
Pet-CM3-4
NC_055726
171,975 nt
vB-EclM_KMB19
OL828290.1
172,697 nt
vB_EclM-UFV01
vB_EclM-UFV01
174,517 nt
PG7
KJ101592.1
173,276 nt
vB_VIPECLUMC02
OQ721913.1
172,129 nt
vB_VIPECLOM01
OQ721912.1
171,903 nt
fGh-Ecl04
ON212267
172,419 nt
fGh-Ecl01
ON212265
171,663 nt

Figure 6: Alignment of phage genomes that compose the genus *Acadevirus*. The genomes were opened in the gene encoding for rIIA lysis inhibition. The ORFs contoured in red have predicted depolymerase domains.

The prediction of the tertiary structure of the genes containing depolymerase domains is shown in Figure 7.

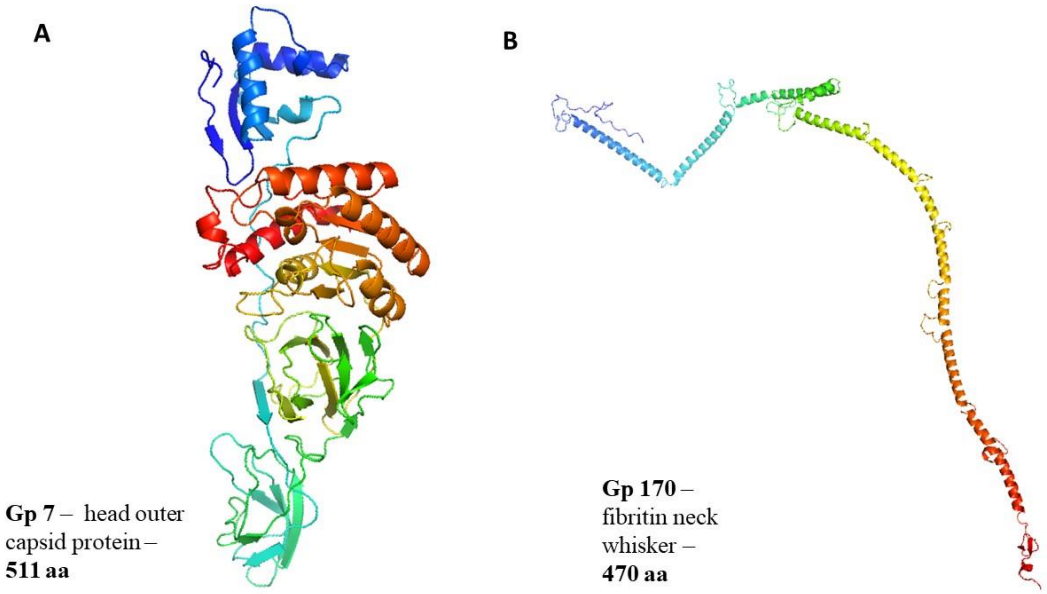

Figure 7: Head outer capsid (gp 7) and fibritin neck whisker (gp 170) tertiary structure prediction.

The tertiary prediction showed good quality results, and the structural architecture is similar to those described for related proteins.

4. Discussion

On the World Health Organization (WHO) list of priority organisms for research and development of new antibiotics, carbapenem-resistant *Enterobacteriaceae* with extended-spectrum β-lactamases (ESBL) have critical priority. *Enterobacter cloacae*, along with *E. asburiae*, *E. hormaechei*, *E. kobei*, *E. ludwigii*, and *E. nimipressuralis*, forms the "Enterobacter cloacae complex" (ECC) [8,9]. Although ECC members are widely found in terrestrial and aquatic environments, these organisms are opportunistic pathogens, frequently associated with nosocomial infections [8,44]. ECC are naturally resistant to several antibiotics, such as ampicillin, amoxicillin, cephalosporins, and cefoxitins, but gradually newly isolated strains have been presenting resistance to extended-spectrum β-lactamases and carbapenems [8,10,44]. The use of bacteriophages to treat bacterial infections is not new, but its appeal has resurfaced in the last decade [12,46,47]. Phage therapy is once again being explored as a treatment option for bacterial infections, but this time it has the benefit of more

than 100 years of research and the establishment of facilities specializing in this type of approach, such as the Eliava Institute (Georgia – USA) and the “Center for Innovative Phage Applications and Therapeutics” at the School of Medicine at the University of San Diego, California.

The *Enterobacter* phage vB_EclM-UFV01 (ENT01) was isolated from samples taken from the São Bartolomeu River in Viçosa, Minas Gerais, Brazil. TEM revealed that ENT01 presents a myovirus morphology, and comparative genomics allowed its classification as a member of the genus *Karamvirus*. This genus was created in 2019, as a result of the effort of the Bacterial Viruses Subcommittee of the International Committee on Taxonomy of Viruses to implement a binomial system of nomenclature for bacterial viruses and to abolish the paraphyletic morphological families *Podoviridae*, *Siphoviridae*, and *Myoviridae* as well as the order *Caudovirales* and create new phylogenetically related taxa [48,49]. The *Karamvirus* members were previously classified as T4-like phages, and because of this, the *Tequatrovirus* T4 was used as reference in part of the analyses of this study. Table 2 contains a comparison of important biological features of Ent01 and other karamviruses, despite the fact that some data are available in the literature. For instance, the burst size was not calculated for all karamviruses, but for those that were, the number of phage particles per infected cell (p.p./i.c) ranged from 17 to 135, and the latency time from 11 to 20 minutes. Ent01 has a burst size of 55 p.p./i.c., and a latency time of 15 minutes (figure 1), both of which are within the range described for the other genus members. Although the variation between the burst sizes of the karamviruses is fairly substantial (the difference between the largest burst and the smallest burst is nearly ten times) this is a property that does not have a universal calculation. In fact, small variations in the protocol or the calculation of the one-step growth curve can cause significant differences in the final result [50–52].

The host range is also a feature only available in the literature for six members of the *Karamvirus* genus. *Enterobacter* phage Entb_43 was able to infect 40% of the tested bacterial strains, all of them belonging to *E. cloacae* complex (ECC) [53]. *Enterobacter* phage myPSH1140 was also tested against ECC hosts, and was able to infect 15 (100%) *E. cloacae,* 3 (75%) *E. hormaechei*, 2 (50%) *E. asburiae and* 2 (67%) *E. aerogenes* strains [29]. *Cronobacter* phage Pet-CM3-4, *Enterobacter* phage vB-EclM_KMB17, *Enterobacter* phage vB-EclM_KMB19, and *Enterobacter* phage vB-EclM_KMB20 were characterized in the same paper [54], and the host range was tested against 15 *Cronobacter* spp and 22 *Enterobacter* spp. Pet-CM3-4 showed a massive host range, being able to infect all the

Cronobacter and 95% of the *Enterobacter* strains. The phages KMB17, KMB19, and KMB20, on the other hand, were able to infect respectively 21.26%, 43.24%, and 37.83% of the host's panel. It is crucial to note that, although Ent01 had the most limited host range of the genus, no other ECC complex species or *E. cloacae* isolates, besides the isolation host, was tested in its host range panel. This fact undermines the idea that Ent01 is more specific in its infection than other members of its genus, given that only a new round of tests, this time using bacterial isolates closer to the isolation host, could confirm this claim. Also, based on what was found for the other karamviruses, the bacterial genus *Cronobacter* seems to permit the karamviruses infection and propagation, but again, no isolates of this genus were tested against Ent01. Interestingly, phages vB_VIPECLUMC02 and vB_VIPECLOM01, which share respectively 91,3 and 91,9 of intergenic similarity with Ent01, were isolated from the same host, the bacterial strain *Enterobacter cloacae* ATCC 13047.

Enterobacter phage vB_EclM-UFV01 possesses a 174,517 bp dsDNA genome, with a G+C content of 39,7% which encodes 286 ORFs and 14 tRNAs. The genomic map of ENT01 is shown in Figure 4. The 60 predicted promoter and 13 predicted terminators are also present in the map. The combination of MEME (Figure 5) and Sapphire results led to strong reliability in the location of the early promoters position, although the middle and late promoters predicted by MEME also showed strong e-value scores. Table 2 summarizes some genomic properties of the karamviruses phages. The average genome size for the genus is 172.205 bp (± 2.109 bp), average G+C content is 39,8 (± 0,06), average number of ORFs is 289 (± 20), and average number of tRNAs is 19 (± 0,4). The genome size, the G+C content, and the number of ORFs are features that showed relatively low variability among the members of the genus *Karamvirus.* Based on the karamviruses alignment (Figure 6), is possible to observe that *Enterobacter* phage CC31 has a deletion in the 70 kb area, the same regions where the tRNAs are encoded and are rich in small hypothetical proteins. This deletion may explain why this phage is the *Karamvirus* member with the most distinguishing traits, since it has the shortest size and the fewest ORFs, in addition to encoding fewer tRNAs than the others.

Figure 6 also illustrates the location of genes predicted as having putative depolymerase domains (DPOs) across the karamviruses members. Table 3 presents the name and the ORF number of the predicted DPOs. Although there exists a difference of nearly 40 genes among the location of the fibritin neck whisker along the evaluated genomes, probably given by annotation artifacts, the DPO genes look well conserved, being present in all the

karamviruses genomes. The *Cronobacter* phage Pet-CM3-4 is the only one that, besides the two common DPOs, possesses a third, located in the gp 161 and which encodes a tail collar fiber protein. It is also worth noting that the same analysis was performed on Tequatrovirus T4 and no DPO was found. Another interesting finding is that depolymerase domains are usually present in structures related to host receptor recognition, such as tail or phage tail fibers. In the case of karamviruses members, these domains are present in a head outer capsid protein (gp 7) and fibritin neck whisker (gp 170). Head outer capsid proteins (*hoc*) are dispensable for phage head morphogenesis and infection, and have only a minor effect on capsid stability [55]. On the other hand, fibritin neck whiskers (also known as whisker antigen control, *wac*) are structures more related to phage tail remodeling and contraction during the infection process and are also considered a nonessential gene [56]. Both proteins are highly antigenic and curiously have a small or inexistent hole with peptidoglycan interactions [55,56]. But is the presence of depolymerase domains that may explain why, as shown in Table 1 and Figure 2, even though ENT01 is not able to infect *P. vulgaris* LIVM1 and *E. coli* SAN 3, its presence is sufficient to decrease the biofilm of these bacteria [57,58]. The presence of other phage enzymes, such as lysozymes, also present in ENT01 genomes (gp 119, gp 120, and gp160), can also help in this process [59].

Although some genomic features of the Karamvirus can resemble those found in the Tequatrovirus (Figure 6), such as the genomic architecture, the lack of its RNA polymerase, the use of genes such as *alt* (RNA polymerase-ADP-ribosyltransferase) to lead the connection of RNApol from the host to the initial promoters, and *motA* to drive the intermediate promoters, the programs that calculate indices of genetic similarities show that these similarities present, in reality, a low similarity index. The effort of the ICTV to reorganize families and viral genera in a binomial system based on calculations of intergenomic distances brings to light differences and particularities present in the new genera that were not previously unknown.

5. Conclusions

Our findings showed that *Enterobacter* phage vB_EclM-UFV01 is a member of the genus Karamvirus. Its genomics and biological features were similar to those found in other karamviruses, and although these phages had been previously classified as T4-like phages, some important differences were highlighted. vB_EclM-UFV01 also does not present any lysogeny or pathogenicity genes. Two putative depolymerase domains were found in genes usually not related to peptidoglycan interactions, the head outer capsid (gp 7) and the fibritin's

neck whisker (gp 170). These domains are highly preserved among the karamviruses members. The presence of this phage was also able to decrease the biofilm of the not infecting strains *P. vulgaris* LIVM1 and *E. coli* SAN 3. These positive results indicate that *Enterobacter* phage vB_EclM-UFV01 is a good candidate for bacterial growth control.

6. Bibliography

1. De Oliveira, D.M.P.; Forde, B.M.; Kidd, T.J.; Harris, P.N.A.; Schembri, M.A.; Beatson, S.A.; Paterson, D.L.; Walker, M.J. Antimicrobial resistance in ESKAPE pathogens. *Clin. Microbiol. Rev.* **2020**, *33*, doi:10.1128/CMR.00181-19.
2. Denissen, J.; Reyneke, B.; Waso-Reyneke, M.; Havenga, B.; Barnard, T.; Khan, S.; Khan, W. Prevalence of ESKAPE pathogens in the environment: Antibiotic resistance status, community-acquired infection and risk to human health. *Int. J. Hyg. Environ. Health* **2022**, *244*, 114006, doi:10.1016/j.ijheh.2022.114006.
3. Mulani, M.S.; Kamble, E.E.; Kumkar, S.N.; Tawre, M.S.; Pardesi, K.R. Emerging strategies to combat ESKAPE pathogens in the era of antimicrobial resistance: A review. *Front. Microbiol.* **2019**, *10*, doi:10.3389/fmicb.2019.00539.
4. Ragupathi, N.K.D.; Muthuirulandi Sethuvel, D.P.; Gopikrishnan, M.; Dwarakanathan, H.T.; Murugan, D.; Biswas, I.; Bakthavachalam, Y.D.; Murugesan, M.; George Priya Doss, C.; Monk, P.N.; et al. Phage-based therapy against biofilm producers in gram-negative ESKAPE pathogens. *Microb. Pathog.* **2023**, *178*, 106064, doi:10.1016/j.micpath.2023.106064.
5. Gontijo, M.T.P.; Vidigal, P.M.P.; Lopez, M.E.S.; Brocchi, M. Bacteriophages that infect Gram-negative bacteria as source of signal-arrest-release motif lysins. *Res. Microbiol.* **2021**, *172*, 103794, doi:10.1016/j.resmic.2020.103794.
6. Luong, T.; Salabarria, A.C.; Roach, D.R. Phage Therapy in the Resistance Era: Where Do We Stand and Where Are We Going? *Clin. Ther.* **2020**, *42*, 1659–1680, doi:10.1016/j.clinthera.2020.07.014.
7. Patil, A.; Banerji, R.; Kanojiya, P.; Koratkar, S.; Saroj, S. Bacteriophages for ESKAPE: role in pathogenicity and measures of control. *Expert Rev. Anti. Infect. Ther.* **2021**, *19*, 845–865, doi:10.1080/14787210.2021.1858800.
8. Mezzatesta, M.L.; Gona, F.; Stefani, S. Enterobacter cloacae complex: clinical impact and emerging antibiotic resistance. *Futur. Microbiol.* **2012**, *7*, 887–902.
9. Liu, S.; Fang, R.; Zhang, Y.; Chen, L.; Huang, N.; Yu, K.; Zhou, C.; Cao, J.; Zhou, T. Characterization of resistance mechanisms of Enterobacter cloacae Complex co-resistant to carbapenem and colistin. *BMC Microbiol.* **2021**, *21*, 1–10, doi:10.1186/s12866-021-02250-x.
10. Annavajhala, M.K.; Gomez-Simmonds, A.; Uhlemann, A.C. Multidrug-resistant Enterobacter cloacae complex emerging as a global, diversifying threat. *Front.*

Microbiol. **2019**, *10*, 1–8, doi:10.3389/fmicb.2019.00044.

11. Jin, C.; Zhang, J.; Wang, Q.; Chen, H.; Wang, X.; Zhang, Y.; Wang, H. Molecular characterization of carbapenem-resistant enterobacter cloacae in 11 Chinese cities. *Front. Microbiol.* **2018**, *9*, 1–8, doi:10.3389/fmicb.2018.01597.

12. Keen, E.C. Phage therapy : concept to cure. *Front. Microbiol.* **2012**, *3*, 238, doi:10.3389/fmicb.2012.00238.

13. Skurnik, M.; Strauch, E. Phage therapy : Facts and fiction. **2006**, *296*, 5–14, doi:10.1016/j.ijmm.2005.09.002.

14. Nobrega, F.L.; Costa, A.R.; Kluskens, L.D.; Azeredo, J. Revisiting phage therapy: New applications for old resources. *Trends Microbiol.* **2015**, *23*, 185–191, doi:10.1016/j.tim.2015.01.006.

15. Fruciano, E.; Bourne, S. Phage as an antimicrobial agent: d'Herelle's heretical theories and their role in the decline of phage prophylaxis in the West. *Can. J. Infect. Dis. Med. Microbiol.* **2007**, *18*, 19–26.

16. Andersson, D.I.; Hughes, D. Antibiotic resistance and its cost: Is it possible to reverse resistance? *Nat. Rev. Microbiol.* **2010**, *8*, 260–271, doi:10.1038/nrmicro2319.

17. Ventola, C.L. The Antibiotic Resistance Crisis. *P&T* **2015**, *40*, 278–283, doi:10.5796/electrochemistry.82.749.

18. Chan, B.K.; Abedon, S.T. Bacteriophages and their Enzymes in Biofilm Control. *Curr. Pharm. Des.* **2015**, *21*, 85–99.

19. Chan, B.K.; Abedon, S.T.; Loc-carrillo, C. Phage cocktails and the future of phage therapy. *Futur. Med.* **2013**, *8*, 769–783.

20. Mattila, S.; Ruotsalainen, P.; Jalasvuori, M. On-Demand Isolation of Bacteriophages Against Drug- Resistant Bacteria for Personalized Phage Therapy Bacteria Strains and Culturing. *Front. Microbiol.* **2015**, *6*, 1–7, doi:10.3389/fmicb.2015.01271.

21. Pires, D.P.; Costa, A.R.; Pinto, G.; Meneses, L.; Azeredo, J. Current challenges and future opportunities of phage therapy. *FEMS Microbiol. Rev.* **2020**, *44*, 684–700, doi:10.1093/femsre/fuaa017.

22. Oliveira, H.; São-José, C.; Azeredo, J. Phage-derived peptidoglycan degrading enzymes: Challenges and future prospects for in vivo therapy. *Viruses* **2018**, *10*, doi:10.3390/v10060292.

23. Fischetti, V.A. Development of phage lysins as novel therapeutics: A historical perspective. *Viruses* **2018**, *10*, doi:10.3390/v10060310.

24. Olsen, N.M.C.; Thiran, E.; Hasler, T.; Vanzieleghem, T.; Belibasakis, G.N.; Mahillon, J.; Loessner, M.J.; Schmelcher, M. Synergistic removal of static and dynamic staphylococcus aureus biofilms by combined treatment with a bacteriophage endolysin and a polysaccharide depolymerase. *Viruses* **2018**, *10*, 1–17, doi:10.3390/v10080438.

25. Abdelkader, K.; Gerstmans, H.; Saafan, A.; Dishisha, T.; Briers, Y. The preclinical and clinical progress of bacteriophages and their lytic enzymes: The parts are easier than the whole. *Viruses* **2019**, *11*, 1–16, doi:10.3390/v11020096.

26. Twest, R.; Kropinski, A.M. *Bacteriophages: Methods and Protocols, Volume 1*; Clokie, M.R.J., Kropinski, A.M., Eds.; 2009; ISBN 9781588296825.

27. Adams, M.H. *Bacteriophages*; Interscience publisher INC: New york, 1959;

28. Beck, N.K.; Callahan, K.; Nappier, S.P.; Kim, H.; Sobsey, M.D.; Meschke, J.S. Development of a spot-titer culture assay for quantifying bacteria and viral indicators. *J. Rapid Methods Autom. Microbiol.* **2009**, *17*, 455–464, doi:10.1111/j.1745-4581.2009.00182.x.

29. Manohar, P.; Tamhankar, A.J.; Lundborg, C.S.; Nachimuthu, R. Therapeutic characterization and efficacy of bacteriophage cocktails infecting Escherichia coli, klebsiella pneumoniae, and enterobacter species. *Front. Microbiol.* **2019**, *10*, 1–12, doi:10.3389/fmicb.2019.00574.

30. Knezevic, P.; Petrovic, O. A colorimetric microtiter plate method for assessment of phage effect on Pseudomonas aeruginosa biofilm. *J. Microbiol. Methods* **2008**, *74*, 114–118, doi:10.1016/j.mimet.2008.03.005.

31. Bolger, A.M.; Lohse, M.; Usadel, B. Trimmomatic : a flexible trimmer for Illumina sequence data. *Bioinformatics* **2014**, *30*, 2114–2120, doi:10.1093/bioinformatics/btu170.

32. Prjibelski, A.; Antipov, D.; Meleshko, D.; Lapidus, A.; Korobeynikov, A. Using SPAdes De Novo Assembler. *Curr. Protoc. Bioinforma.* **2020**, *70*, 1–29, doi:10.1002/cpbi.102.

33. Li, H.; Durbin, R. Fast and accurate short read alignment with Burrows – Wheeler transform. *Bioinformatics* **2009**, *25*, 1754–1760, doi:10.1093/bioinformatics/btp324.

34. Aziz, R.K.; Bartels, D.; Best, A.; DeJongh, M.; Disz, T.; Edwards, R.A.; Formsma, K.; Gerdes, S.; Glass, E.M.; Kubal, M.; et al. The RAST Server: Rapid annotations using subsystems technology. *BMC Genomics* **2008**, *9*, 1–15, doi:10.1186/1471-2164-9-75.

35. Nishimura, Y.; Yoshida, T.; Kuronishi, M.; Uehara, H.; Ogata, H.; Goto, S. ViPTree: The viral proteomic tree server. *Bioinformatics* **2017**, *33*, 2379–2380, doi:10.1093/bioinformatics/btx157.

36. Vieira, M.F.; Duarte, J.; Domingues, R.; Oliveira, H.; Dias, O. PhageDPO: Phage Depolymerase Finder. *bioRxiv* **2023**, 2023.02.24.529883.

37. Gilchrist, C.L.M.; Chooi, Y.H. Clinker & clustermap.js: Automatic generation of gene cluster comparison figures. *Bioinformatics* **2021**, *37*, 2473–2475, doi:10.1093/bioinformatics/btab007.

38. Finn, R.D.; Clements, J.; Eddy, S.R. HMMER web server: Interactive sequence

similarity searching. *Nucleic Acids Res.* **2011**, *39*, 29–37, doi:10.1093/nar/gkr367.

39. Alva, V.; Nam, S.Z.; Soding, J.; Lupas, A.N. The MPI bioinformatics Toolkit as an integrative platform for advanced protein sequence and structure analysis. *Nucleic Acids Res.* **2016**, *44*, W410–W415, doi:10.1093/nar/gkw348.

40. Bailey, T.L.; Johnson, J.; Grant, C.E.; Noble, W.S. The MEME Suite. *Nucleic Acids Res.* **2015**, *43*, W39–W49, doi:10.1093/nar/gkv416.

41. Chan, P.P.; Lowe, T.M. tRNAscan-SE: Searching for tRNA genes in genomic sequences. *Methods Mol. Biol.* **2019**, *1962*, 1–14, doi:10.1007/978-1-4939-9173-0.

42. Naville, M.; Ghuillot-Gaudeffroy, A.; Marchais, A.; Gautheret, D. ARNold: A web tool for the prediction of rho-independent transcription terminators. *RNA Biol.* **2011**, *8*, 11–13, doi:10.4161/rna.8.1.13346.

43. Jumper, J.; Evans, R.; Pritzel, A.; Green, T.; Figurnov, M.; Ronneberger, O.; Tunyasuvunakool, K.; Bates, R.; Žídek, A.; Potapenko, A.; et al. Highly accurate protein structure prediction with AlphaFold. *Nature* **2021**, *596*, 583–589, doi:10.1038/s41586-021-03819-2.

44. Davin-Regli, A.; Pagès, J.M. Enterobacter aerogenes and Enterobacter cloacae; Versatile bacterial pathogens confronting antibiotic treatment. *Front. Microbiol.* **2015**, *6*, 1–10, doi:10.3389/fmicb.2015.00392.

45. Stewart, P.S.; Costerton, J.W. Antibiotic resistance of bacteria in biofilms. *Lancet* **2001**, *358*, 135–138.

46. Gordillo Altamirano, F.L.; Barr, J.J. Phage therapy in the postantibiotic era. *Clin. Microbiol. Rev.* **2019**, *32*, doi:10.1128/CMR.00066-18.

47. Pires, D.P.; Melo, L.D.R.; Boas, D.V.; Sillankorva, S. ScienceDirect Phage therapy as an alternative or complementary strategy to prevent and control biofilm-related infections. *Curr. Opin. Microbiol. 39*, 48–56, doi:10.1016/j.mib.2017.09.004.

48. Adriaenssens, E.M.; Sullivan, M.B.; Knezevic, P.; van Zyl, L.J.; Sarkar, B.L.; Dutilh, B.E.; Alfenas-Zerbini, P.; Łobocka, M.; Tong, Y.; Brister, J.R.; et al. Taxonomy of prokaryotic viruses: 2018-2019 update from the ICTV Bacterial and Archaeal Viruses Subcommittee. *Arch. Virol.* **2020**, *165*, 1253–1260, doi:10.1007/s00705-020-04577-8.

49. Turner, D.; Shkoporov, A.N.; Lood, C.; Millard, A.D.; Dutilh, B.E.; Alfenas-Zerbini, P.; van Zyl, L.J.; Aziz, R.K.; Oksanen, H.M.; Poranen, M.M.; et al. Abolishment of morphology-based taxa and change to binomial species names: 2022 taxonomy update of the ICTV bacterial viruses subcommittee. *Arch. Virol.* **2023**, *168*, 1–9, doi:10.1007/s00705-022-05694-2.

50. Liao, Y.-T.; Zhang, Y.; Salvador, A.; Harden, L.A.; Wu, V.C.H. Characterization of a T4-like Bacteriophage vB_EcoM-Sa45lw as a Potential Biocontrol Agent for Shiga Toxin-Producing Escherichia coli O45 Contaminated on Mung Bean Seeds. *Microbiol. Spectr.* **2022**, *10*, doi:10.1128/spectrum.02220-21.

51. Peters, D.L.; Davis, C.M.; Harris, G.; Zhou, H.; Rather, P.N.; Hrapovic, S.; Lam, E.; Dennis, J.J.; Chen, W. Characterization of Virulent T4-Like Acinetobacter baumannii Bacteriophages DLP1 and DLP2. *Viruses* **2023**, *15*, 739, doi:10.3390/v15030739.

52. Jończyk, E.; Kłak, M.; Międzybrodzki, R.; Górski, A. The influence of external factors on bacteriophages-review. *Folia Microbiol. (Praha).* **2011**, *56*, 191–200, doi:10.1007/s12223-011-0039-8.

53. Cieślik, M.; Harhala, M.; Orwat, F.; Dąbrowska, K.; Górski, A.; Jończyk-Matysiak, E. Two Newly Isolated Enterobacter-Specific Bacteriophages: Biological Properties and Stability Studies. *Viruses* **2022**, *14*, doi:10.3390/v14071518.

54. Andrezal, M.; Oravcova, L.; Kadličekova, V.; Ozaee, E.; Elnwrani, S.; Bugala, J.; Markuskova, B.; Kajsik, M.; Drahovska, H. Characterization and the host specificity of Pet-CM3–4, a new phage infecting Cronobacter and Enterobacter strains. *Virus Res.* **2023**, *324*, doi:10.1016/j.virusres.2022.199025.

55. Fokine, A.; Chipman, P.R.; Leiman, P.G.; Mesyanzhinov, V. V.; Rao, V.B.; Rossmann, M.G. Molecular architecture of the prolate head of bacteriophage T4. *Proc. Natl. Acad. Sci. U. S. A.* **2004**, *101*, 6003–6008, doi:10.1073/pnas.0400444101.

56. Hu, B.; Margolin, W.; Molineux, I.J.; Liu, J. Structural remodeling of bacteriophage T4 and host membranes during infection initiation. **2015**, doi:10.1073/pnas.1501064112.

57. Fernandes, S.; São-José, C. Enzymes and mechanisms employed by tailed bacteriophages to breach the bacterial cell barriers. *Viruses* **2018**, *10*, 1–22, doi:10.3390/v10080396.

58. Shymialevich, D.; Wójcicki, M.; Wardaszka, A.; Świder, O.; Sokołowska, B.; Błażejak, S. Application of Lytic Bacteriophages and Their Enzymes to Reduce Saprophytic Bacteria Isolated from Minimally Processed Plant-Based Food Products-In Vitro Studies. *Viruses* **2022**, *15*, doi:10.3390/v15010009.

59. Visnapuu, A.; Der Gucht, M.; Wagemans, J.; Lavigne, R. Deconstructing the Phage–Bacterial Biofilm Interaction as a Basis to Establish New Antibiofilm Strategies. *Viruses* **2022**, *14*, doi:10.3390/v14051057.

Chapter 2: Characterization, formulation, and large-scale production of a phage cocktail able to reduce sulfate-reducing bacteria biofilms.

Jéssica Duarte da Silva[1], Roberto Sousa Dias[1], Adriele Jéssica do Carmo[1], Paloma Cavalcante Cunha[1], Bruna Almeida Ayupe[1], Marcella Silva Vieira[1], Isabela Silva Paes[1], José Júnior Ferreira Soares, Sérgio Oliveira de Paula[1].

[1] Laboratory of Molecular Immunovirology, Federal University of Viçosa, Viçosa, Brazil.

Abstract

Phages are viruses that infect bacteria and since their discovery, at the beginning of the 20th century, have been used to control bacterial growth. This work aimed to formulate a cocktail of enterobacterial-infecting phages, that are able to decrease the biofilm of sulfate-reducing bacteria and to evaluate their stability in conditions similar to those found in oil-related environments. Three *Tequatrovirus* (*Escherichia* phages vB_EcoM-UFV09, vB_EcoM-UFV10, and vB_EcoM-UFV13) and one *Karamvirus* (*Enterobacter* phage vB_EclM-UFV01) were selected to compose the cocktail Petro01. The phage's genomes tested negative for pathogenic or lysogeny genes, and nine genes were predicted as phage-encode depolymerases. The long-term stability at unusual storage temperatures (30 and 37 °C), and supernatant composition (high-salinity, high-chlorine, and LB enriched with conservative compounds), showed promising results, as well as the propagation yielding of the phage's cocktail in bench ad in a 12 L bioreactor. These encouraging findings highlight the significant biotechnological potential of Petro01, and its ability to withstand environmental challenges in oil facilities and potentially reduce sulfate-reducing bacteria biofilms.

Keywords: Bacteriophages. Large-scale production. Depolymerases. Karamvirus. Tequatroviruses.

1. Introduction

Bacteriophages, also called phages, are viruses that infect bacteria. Since their discovery – which happened independently at the beginning of the 20th century by Frederick Twort and Felix d'Herelle – they are considered the most abundant entities on the planet, with an estimative of approximately 10^{31} particles in the biosphere [1,2]. Since their discovery, the phage's potential to treat bacterial infections was quickly recognized and exploited [3] and phage cocktails were used mainly in Eastern Europe and India to successfully treat diseases such as cholera, typhoid, and dysentery, in a method known as phage therapy [2–5]. Unfortunately, despite the commercialization of phage-based products, the inconsistent success in the patient's treatments, the lack of knowledge of viral mechanisms, incorrect

cocktail formulation, and the discovery of penicillin, culminated in the almost complete discontinuance of phage therapy [2]. Although phages such as λ and T4 have become model organisms [6,7], phage therapy could have remained dormant, if it hadn't been for a growing need in the scientific community: methodologies to fight against multi-drug resistant bacteria [8–10]. Besides much still needs to be done in terms of regulatory legislation and high-quality clinical trials [11–13], the application of bacteriophages to control bacterial damage in fields such as animal health, agri-food, and biocontrol is being developed more easily and with excellent results [14]. Hence, phages are not only being used to kill individual pathogenic cells but also to decrease bacterial biofilms that can grow in one infinity of clinical and industrial apparatus [14–16].

Biofilms are complex bacterial communities, composed of multi-species bacterial cells, immersed by a self-produced matrix of extracellular polymeric substances (EPS), such as exopolysaccharides, extracellular deoxyribonucleic acids (eDNA), and proteins, usually adhered to a surface [17–19]. They can be particularly problematic in industrial and healthcare settings [18,20,21] once biofilms can clog cannulas, hoses, and pipelines, as well as contribute to the corrosion of metallic materials. This arrangement also makes the cells under the exopolysaccharide matrix much more resistant to the action of antimicrobial agents [15]. As in a normal predator-prey dynamic, phages also have different mechanisms to circumvent the biofilm barrier, such as the depolymerases, which have a direct action on EPS degradation and can be divided into lyases and hydrolases [17,22,23]. Besides the enzymatic action, the ability of phages to disrupt bacterial biofilms as an entire particle is also considerably important, once they can remain stable and in environments where purified enzymes are easily inactivated [22,24]. Hence, due to the nonspecific action of phage tail enzymes, it is possible to isolate a phage from an easy-to-cultivate host and use it to combat the biofilm of another bacterial group, with more complex features, such as slow growth rates and difficult cultivation properties. This strategy makes the production process cheaper and circumvents laws that do not allow the use of viral products or organisms genetically modified in specific contexts [24–27].

Sulfate Reducing Bacteria (SRB) is a polyphyletic group of anaerobic microorganisms found in diverse environments such as the gastrointestinal tract of ruminants, soil, and marine habitats. The capacity to use sulfate as a final electron acceptor during respiration, producing hydrogen sulfide (H^2S) as a product of this metabolism is the feature that grouped bacteria from different phyla and more than 80 genera into this group [28–30]. SRB play an important

role in the sulfur cycle and are key species in the maintenance of anaerobic microbial communities, mainly due to their conversion of sulfate in H_2S [28,31]. In the oil industry, secondary recovery involves the injection of seawater into oil wells to enhance the extraction, resulting in the formation of anoxic and sulfur-rich conditions that favor the development of SRB species [32]. The growth of these organisms in oil-related environments is undesirable and causes numerous damages since H_2S is a gas neurotoxic, flammable, and corrosive. These organisms also increase the concentration of sulfur compounds in the oil in a process called “souring”, which lowers its market price [32–35]. Furthermore, SRB and their biofilms are the primary cause of biogenic corrosion in oil-related environments, resulting in annual expenditures that run into trillions of dollars. The biofilms frequently cause localized “pitting” corrosions that are impossible to anticipate and difficult to avoid, leading to perforations and even oil spills [32–35]. Biocides like "Tetrakis-hydroxymethyl Phosphonium Sulfate" (THPS) and glutaraldehyde are commonly used to control SRB growth but face challenges such as high costs and microbial resistance. Therefore, finding new effective solutions to manage SRB growth is crucial for the industry. [19,36–39].

The use of bacteriophages can be an interesting alternative solution to this problem, even using an indirect approach, mainly focused on avoiding the development of SRB biofilms. Environments associated with the oil industry are extremely diverse, as well as their microbial communities. Taking into account the more than 80 SRB genera, in addition to the complex cultivation of anaerobic bacteria, isolating specific phages for this group becomes a nearly impossible task. Thus, the action of phage-based products in highly complex contexts may be more successful when using enzymes present in phages that infect easily cultivated bacteria to control undesirable bacterial effects, by disrupting bacterial biofilms by the action of phage enzymes and displaying the bacterial cells to the action of antimicrobial agents or by interacting with bacteria that are not necessarily the focus of the problem, but that are keystone species of certain communities [26,40–44]. One of the most significant drawbacks of using bacteriophages for bacterial control in environmental systems is the need for larger volumes of virus particles, which are typically not obtained on a laboratory scale. Studies and approaches focused on optimizing large-scale manufacturing and making it economically feasible are crucial and in high demand to improve phage production [45–47].

The aim of this work is the elaboration of a phage cocktail, containing phages isolated from *Enterobacteriaceae* hosts, but that can reduce SRB biofilms. We also evaluated the

cocktail stability in oil-related conditions, the addition of conservative substances to increase their shelf-life as well and the large-scale parameter for production in bioreactors.

2. Material and Methods

2.1. Phage cocktail formulation

The phages used in this study are part of the collection of the Laboratory of Molecular Immunovirology (Federal University of Viçosa, Viçosa, Brazil) and were isolated from different bacterial hosts. Ten phages were evaluated: *Escherichia coli* phages vB_EcoM-UFV09 (UFV09), vB_EcoM-UFV13 (UFV13) [48], Eco1504, Eco05, Eco09, and vB_EcoM-UFV10 (UFV10); *Citrobacter freundii* phages Cit01 and Cit02, *Enterobacter cloacae* phage vB_EclM-UFV01 (ENT01) and *Serratia marcescens* phage vB_SmaP-UFV01 [49]. The following criteria were used to choose the phages that would compose the cocktail: 1) be exclusively lytic; 2) decrease the biofilm of non-host bacteria; 3) have good propagation capacity; 4) preferably be able to infect more than one host; 5) have strong thermal and pH stability.

2.1.1. Host range

The phage's host range was performed by spot test assay [50]. The bacterial strains (Table 2) belong to the collection of the Laboratory of Molecular Immunovirology (LIVM). Briefly, the bacterial strains were incubated overnight, without agitation, in Luria Bertani broth. 700 µl of grown bacteria was mixed with 5 ml LB top agar (0.7%) and poured into a petri dish containing bottom LB agar (1.5%). After complete solidification, 5 µL of each phage suspension was dropped onto the bacterial lawn and then incubated at 37 °C, overnight. The absence of bacterial growth on the phage-lysate drop indicates that the phage is capable of infecting that strain.

2.1.2. Evaluation of enterobacterial biofilm inhibition

The quantification of phage's biofilm inhibition of non-host bacterial strains was performed following protocol by Knezevic and Petrovic, 2008 [51], with modifications. In 96-well plates, enterobacterial strains - which the phages are not able to infect - were incubated in LB media, at 37 °C for 24 hours. After that, the supernatant was removed, and the wells were washed with a saline solution of 0.9% and left at 55 °C until dried. Thus, 250 µL of methanol was added to the wells and discarded after 15 minutes. The plaque was again kept at 55 °C for complete methanol evaporation. 250 µL of 0.1% violet crystal solution was

added to the wells. After 30 minutes, the solution was discarded, and the wells were washed and left to dry. An alcohol/acetone 4:1 solution was used to dissolve the violet crystals that adhered to the biofilm formed. The absorbance of this mixture was read at the wavelength of 590 nm.

2.2. Phages genomics

The genomes of the phages chosen to compose the cocktail that had not already been sequenced were extracted using the phenol-chloroform procedure (Sambrook and Russel, 2001). Briefly, into 500 µL of the phage's supernatant was added proteinase K (final concentration of 50 µg/mL) and SDS (final concentration of 0.5% (w/v)). The mixture was incubated for one hour at 56 °C. Then, 500 µL of phenol pH 8.0 was added and the tube was subsequently centrifugated at 8,000 44g, for 5 minutes. The aqueous phase was collected and transferred to a new tube. An equal volume of a 1:1 chloroform/phenol solution was added. After further centrifugation, the aqueous phase was recovered, transferred to another tube and an equal volume of chloroform was added. The mixture was centrifuged and the aqueous phase was transferred to a new tube. Ethanol in a 2:1 ratio was added and the solution was stored at -20°C for 12 hours. Finally, the mixture was centrifuged at 15,000 g for 20 minutes. The supernatant was discarded and, after completely drying, the pellet was resuspended in 20 µL of ultrapure water. The genomes were sent to be sequenced by the company Molecular Research DNA (http://www.mrdnalab.com/), using the Illumina MiSeq platform (coverage of 10 million reads, paired-end). The quality of the raw data was evaluated using the FastQC software version 0.1.16 (https://github.com/s-andrews/FastQC) and the genomes were assembled by CLC genomics Workbench software, version 22.0.2. The ORF's annotation was performed by RAST software (Rapid Annotation using Subsystem Technology - http://rast.theseed.org/FIG/rast.cgi) [52]. The search for depolymerase-like enzymes was performed using the tool Phage Depolymerase Finder [53] from the Galaxy Docker Build platform (https://galaxy.bio.di.uminho.pt/), and the genomic alignments were generated by Viptree [54]. The "Variation analysis tool" from the BV-BRC platform (https://www.bv-brc.org/) [55] was used for SNPs analysis.

2.3. Evaluation of the phage cocktail in the reduction of biofilms formed by mixed cultures of Sulfate Reducing Bacteria (SRB)

In an anaerobic chamber (Whitley A95), 90 µL of SRB mixed cultures - obtained from four different oil industry sites (Table 1), and kept biologically active in anaerobic conditions,

were added to 96-well microplates, together with 90 µL of fresh Postgate E medium. Thus, 20 µL of the phage cocktail was added to the wells (final concentration of 10^7 PFU/mL) and kept at 30 °C, for three days. The atmosphere composition in the chamber was 10% H_2; 10% CO_2 and 80% N_2. The total biomass of biofilms was quantified by the crystal violet method, as previously described [51].

Table 1: Summary of the SRB samples origins used for the biofilm inhibition assay in 96-well plates.

Code	Origin
R1	Injection water
R2	Injection water
R3	Production water
R4	Desulfating membrane

2.4. Evaluation of viral stability against adverse environmental conditions

2.4.1. Thermal stability and at different pH values.

The thermal stability of the phages that compose the cocktail was evaluated as described by Jurczak-Kurek, 2016, with modifications [56]. Tubes of 1,5 mL, containing 900 µL of SM buffer and 100 µL of phage's supernatant (final concentration of 10^4 PFU/mL) were kept in triplicate under the following conditions: -20 °C, 25 °C, 37 °C and 55 °C for two hours, and 80 °C and 95 °C for five minutes. To test the phage's stability under different pH values, Jurczak-Kurek, 2016 [56] was also used. 1,5 mL tubes, containing 900 µL of Luria Bertani Broth (LB medium) adjusted to different pH values (2, 4, 7, 10, and 12) and 100 µL of each phage (final concentration of 10^4 PFU/mL) were kept in triplicate at room temperature for 2 hours. After the respective treatments, the quantification of viable viral particles was performed using the double agar layer plating [57]. Briefly, after serial dilution, 100 µL of the phage supernatant was added to 300 µL of previously grown host and mixture with 4 mL of LB top agar (0.7%). The mixture was then poured into a Petri dish containing LB bottom agar (1.5%) and the plates were kept overnight at 37 °C. The phage titer after the treatments was compared to the titer in the control groups (25 °C for thermal assays and pH 7 for pH sensibility). One-way ANOVA was used to compare the average differences between treatments, and Dunnet's posthoc test was used to compare treatments with the control group.

2.4.2. Phage stability in conditions similar to those found in oil-related environments

To measure the phage's stability in high-salinity environments, their supernatant was diluted to a final concentration of 10^7 PFU/mL in filtered seawater. For the treatment tubes, NaCl was added until the concentrations of 5.5% and 7.5% were reached. To evaluate the stability of viral particles in chlorinated saline environments, the phages were diluted to a final concentration of 10^7 PFU/mL in seawater, with adjusted chlorine concentrations of 0.5% and 1%. Phages diluted in seawater were used as a control. Finally, to assess viral stability in the presence of THPS biocide, phages were diluted to a final concentration of 10^7 PFU/mL in LB medium containing THPS 200 ppm. Phages diluted in pure LB were used as a control. Each experimental unit was stored in 15 ml tubes and kept in triplicate at 37°C, without shaking. The final volume was 5 mL. For thermal and pH stability, the viral quantification was performed after 24 hours and 20 days of incubation. For THPS, the viral titer was measured after 1, 7, and 20 days of incubation. Double agar layer plating was used for phage quantification [57].

2.5. Long-term storage analysis

2.5.1. Long-term stability in SM buffer

For the assessment of long-term viral stability in a well-known phage buffer, but at a non-usual temperature, phages were diluted to a final concentration of 10^7 PFU/ml in SM. The final volume was 5 mL. The 15 ml tubes were kept in triplicate at 30°C, without shaking. The evaluation of viral titers was performed on days 1, 120, and 210 of incubation, using the double agar layer method [57].

2.5.2 Long-term stability in LB media enriched with conservative compounds

The long-term stability of a mixture of LB medium + UFV13 phage particles, enriched with different compounds also was tested. The evaluated conditions were: pure LB (control); LB + $CaCl_2$ + gelatin (1g/L); LB + salts (K_2HPO_4, NaH_2PO_4, and $MgSO_4$: 0.25 g/L; gelatin: 1g/L; glycerol: 20 mL/L); LB + glycerol 20%; LB + DMSO 20%; LB + sucrose 0.5M; LB + seawater 37.5 % (gelatin: 1g/L; glycerol: 20 mL/L). For each condition, eighteen 1,5 mL tubes, containing 900 mL of LB media and phage UFV 13 (final concentration of 10^7 PFU/mL) were stored at 37 °C, without agitation. The viral quantification was measured after 0, 15, 30, 60, 90, and 120 days of incubation, using the double agar layer method [57]. For the measurements, three tubes of each condition were used and the others were kept untouched.

2.6. Cocktail Petro01 production

2.6.1. Cocktail production yield on bench scale

Silva et al. 2021 [37] tested the UFV09 virion production in different media and conditions. To evaluate if the results obtained with phage UFV09 would apply to the others, 50 mL tubes containing 7 mL of LB medium and the cocktail's phages in the initial concentrations of 10^3, 10^5, and 10^7 PFU/mL were incubated for 4 hours at 37 °C and 100 rpm. After this time, the phage titer was measured by a double agar layer [57]. The production yield was estimated by dividing the final viral titer by the initial.

2.6.2. Cocktail production yield in 20 L bioreactor

To determine if the phage production in larger volumes would follow the same tendency found in the bench, new experiments were performed using bioreactors (Allbiom - model Allmic Lab – 12 L). 400 mL of the bacterial host (*E. coli* 30 for phages UFV 09, UFV 10 and UFV 13; and *E. cloacae* ATCC 13047 for ENT01) was grown overnight in LB media, at 37 °C, without shaking, until reach the $OD_{600} \cong 1$. The inoculum was added to the bioreactor, containing 3,6 L of LB sterile medium, followed by the phages (initial titer of 10^5 PFU/mL). The agitation was 150 rpm and the temperature was 37 °C. Samples of 10 mL were taken immediately after the beginning of the experiment (T0) and after 4, 5, and 24 hours of batching. The aliquots were filtered and quantified by double agar layer plating [57].

3. Results

3.1. Phage's cocktail formulation

The first assays used to evaluate the phage's potential to compose a polyvalent cocktail were the host range and the ability to decrease the biofilm formation of enterobacterial strains. The phages were tested against four *E. coli* isolates, two *S. marcenscens* isolates, and one isolate of the species *C. freundii*, *P. vulgaris*, *E. cloacae* and *S. liquefaciens.* The results of both experiments are summarized in Table 2.

Table 2: Host range and biofilm inhibition capacity of ten phages tested against ten bacterial isolates prevenient from the LIVM collection.

	E. coli 30	*E. coli 8D*	*E. coli SAN 3*	*E. coli K12 mm93*	*C. freundii ATCC 8090*	*P. vulgaris LIVM 1*	*S. marcenscens ATCC 14756*	*S. marcenscens MIND01*	*E. cloacae ATCC 13047*	*S. liquefaciens 098*
vB_EcoM-UFV09	X*	X	X	X						
vB_EcoM-UFV13	X*		X	X						
Eco1504	X*								B	
Eco05	X*		X	X						
Eco09	X*	B	X	X						
vB_EcoM-UFV10	X*	B		X						
Cit01					X*			B		
Cit03	X			X	X*					
vB_EclM-UFV01			B			B			X*	
vB_SmaP-UFV01	B					B	X	X*		

X*: isolation host;
X: bacterial isolate in which the phage significantly altered the growth curve and had a positive result on the spot test;
B: a significant decrease in biofilm formation driven by a phage that is not able to infect that host.

Phages UFV09, UFV13, Eco05, Eco09, and UFV10 were able to infect different strains of *E. coli* and phage Cit03 was able to infect bacteria of different genera (*E. coli* K12 mm93 and *C. freundii* ATCC 8090. Phages Eco1504, Eco09, UFV10, Cit01, ENT01, and vB_SmaP-UFV01 were able to significantly reduce the biofilm of non-host bacteria, which suggests that the biofilm was affected by some nonspecific phage enzymes. The phages also significantly reduced the biofilm of their host. These data were not shown because crystal violet quantification did not discriminate whether the decline was caused by viral infection-induced cell lysis or by enzymes acting on the bacterial biofilms. None of the tested phages was able to infect or reduce *S. liquefaciens* biofilm.

The phage's propagation capacity and the titles obtained after infection rounds were also evaluated. It became apparent that, despite the phages Eco1504, Eco05, Eco09, Cit01, Cit03, and vB_SmaP-UFV01 exhibiting promising results in terms of host range and biofilm impact, they hardly exceeded titles of 10^6 PFU/mL - 10^7 PFU/mL. The phages UFV09, UFV10, UFV13, and ENT01, on the other hand, reached titers larger than 10^9 PFU/mL, and because of this, were selected to compose the first cocktail formulation, named Petro01.

The impact of Petro01 in the biofilm of different SRB mixed cultures is present in Figure 1. The biofilm concentration decreased significantly in three of the four examined

mixed cultures (Student's t-test, p-value < 0.05). In the case of the sample R1, the presence of phages induced an increase in bacterial biofilm.

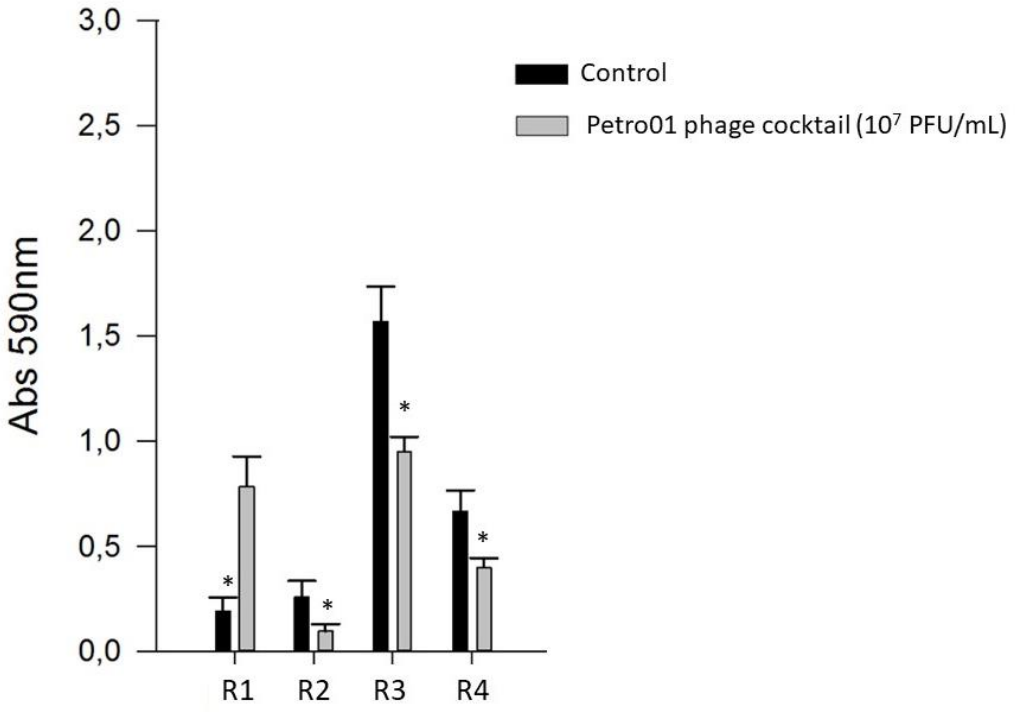

Figure 1: Impact of Petro01 viral cocktail in biofilms of SRB mixed cultures. The black columns represent the biofilm production in wells where the bacterial culture grows without interference (control) and the gray bars represent the biofilm production in the presence of the phage cocktail.

Previous characterization studies demonstrated that phage UFV13 is a member of the genus *Tequatrovirus* [48] while ENT01 belongs to the genus *Karamvirus.* The genomic analysis of phages UFV09 and UFV10 found that both phages have a 165859 bp dsDNA genome, with a G+C content of 35,4 % which encodes 286 ORFs and 11 tRNAs. No lysogeny or pathogenicity genes were found in the genomes of Petro01 phages.

BLASTp analysis showed that the closest phages on the NCBI database were *Escherichia* phage vB_EcoM_11B_SA_NWU (OR062527.1), *Escherichia* phage ECP52 (ON782582.1), *Escherichia* phage vB_EcoM-BECP11 (MW286157.1),*Escherichia* virus CAM-21 (OP611477.1), *Escherichia* phage wV7 (NC_019505.1) *Escherichia* coli O157 typing phage 7 (KP869105.1), *Shigella* phage Sf23 (NC_054941.1), all of them with more than 97% of similarity with UFV09 and UFV10. The phylogenetic analysis confirmed these phages also belong to the genus *Tequatrovirus.* The proteomic tree generated by Viptree

showed that phages UFV09 and UFV10 form a separate clade, close to those formed by *Escherichia coli* phage typing 7 and *Escherichi*a phage wV7 (Figure 2A).

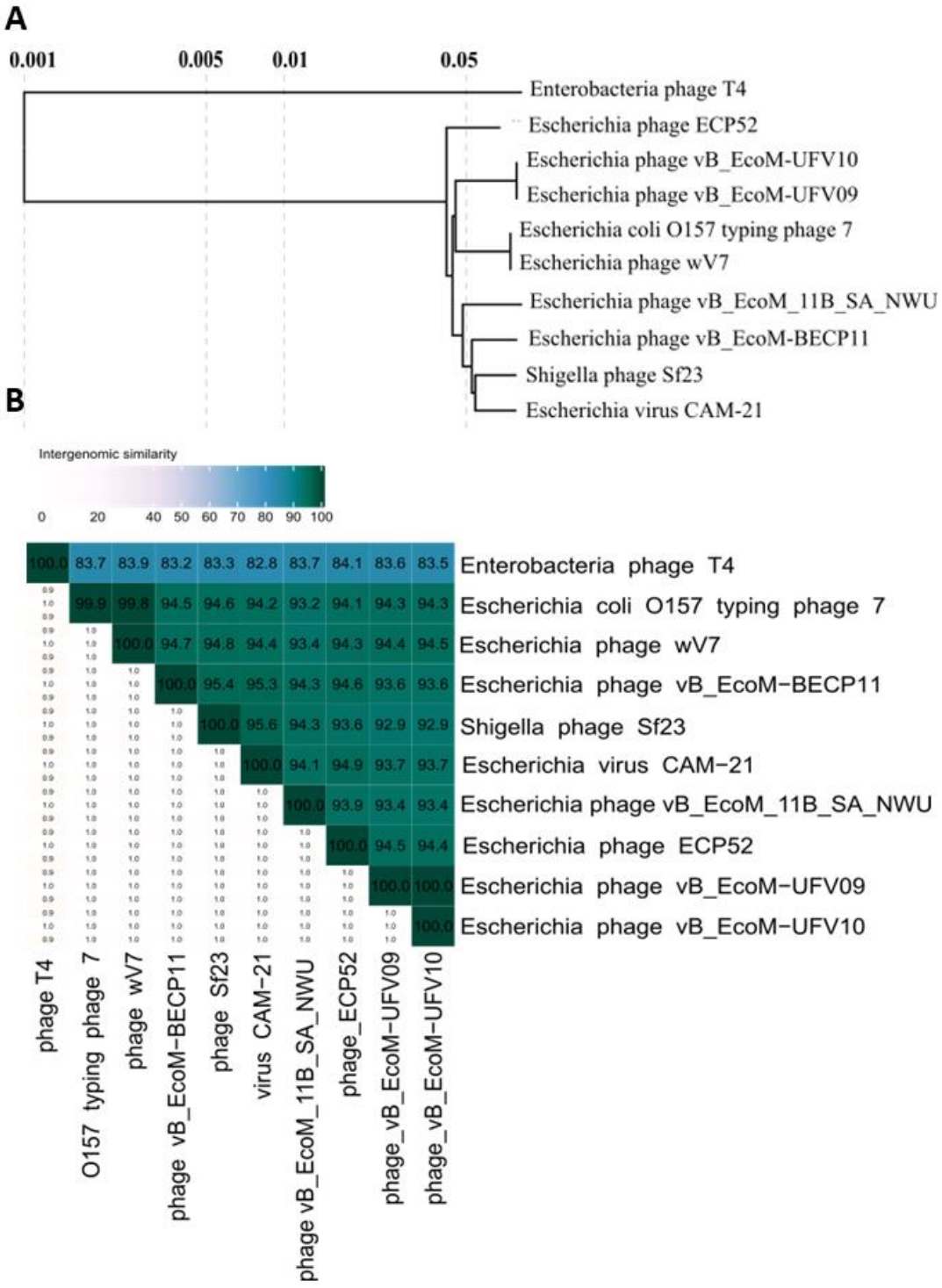

Figure 2: A. Phylogenetic tree created only with genomes that showed more than 97% similarity with UFV09 and UFV10 in BLASTp. **B.** VIRIDIC heatmap showing the intergenomic distance among the related phages. Phages with more than 95% similarity belong to the same species and with more than 70% to the same genus. All phages present more than 70% similarity with T4 phage and are members of the genus *Tequatrovirus*.

VIRIDIC calculates pairwise intergenomic distances and confirms the proximity of *Escherichia coli* phage typing 7 and *Escherichi*a phage wV7 to UFV09 and UFV10 (Figure 2B). According to this calculation, UFV09 and UFV10 share 100% of similarity. The alignment among the phages of cocktail Petro01 and phage T4 is presented in Figure 3.

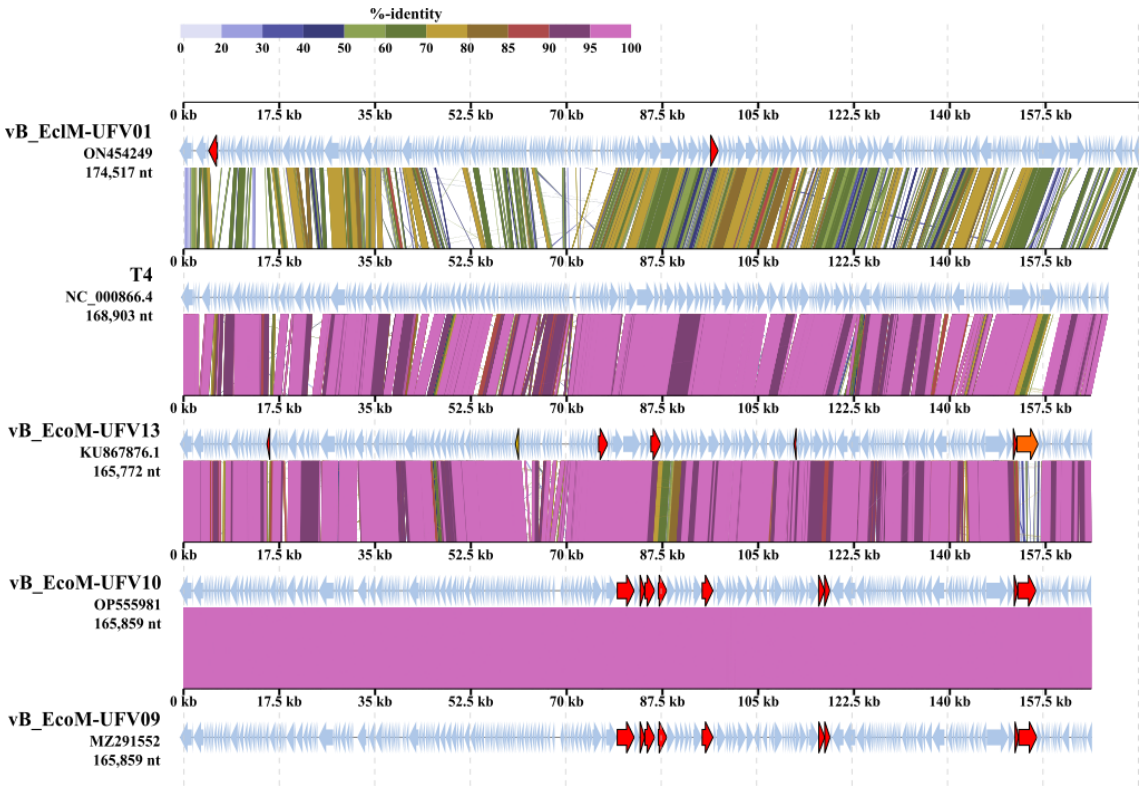

Figure 3: Alignment of phages ENT01, T4, UFV13, UFV09, and UFV10, generated by Viptree. The ORFs colored in red have predicted depolymerase domains (Phage DPO predictor).

The alignment showed the genomic architecture similarities among the phages and reinforced the high identity between UFV09 and UFV10. A deeper investigation showed that, although both phages shared the same genome length and number of CDSs, phage UFV10 possess a sequence repetition of 99 nt located in the NAD--protein ADP-ribosyltransferase modA (gp 20) that is not present in UFV09. On the other hand, UFV09 possess a repetition of 99 nt on Phage long tail fiber (gp 256) that is not present in UFV10. These were the only differences identified between the genomes.

The search for depolymerase domains in phages UFV09 and UFV10 genomes revealed that these domains were present in 9 structural genes. Figure 2 displays their location (red arrows), and Table 3 details them.

Table 3: Open reading frames (ORFs) containing depolymerase domains in UFV09 and UFV10 genomes.

DPO ORF	Position (nt)	Function
gp 161	79535-82633	baseplate wedge initiator
gp 163	83694-84560	baseplate wedge tail fiber connector
gp 164	84560-86365	hypothetical protein (baseplate wedge protein)
gp 166	87021-88571	straight tail fiber
gp 173	94982-96961	tail sheath
gp 202	116178-117272	baseplate tail tube cap
gp 203	117272-118237	tail assembly protein
gp 258	151867-152523	tail connector protein
gp 259	151532-155858	hypothetical protein

3.2. Evaluation of viral stability against different environmental conditions

Figure 4 displays the stability thermal range of Petro01 phages. The findings show that phages UFV09, UFV10, UFV13, and ENT01 maintained their titers after being exposed to temperatures of -20 ℃, 37 ℃, and 55 ℃, whereas temperatures of 80 ℃ significantly reduced phage titers and no viable phage particles were detected at 95 ℃. Phage UFV09 also showed a subtle but significant reduction in title at 37 and 55 ℃. While ENT01 showed a loss of title after being incubated at 55 ℃.

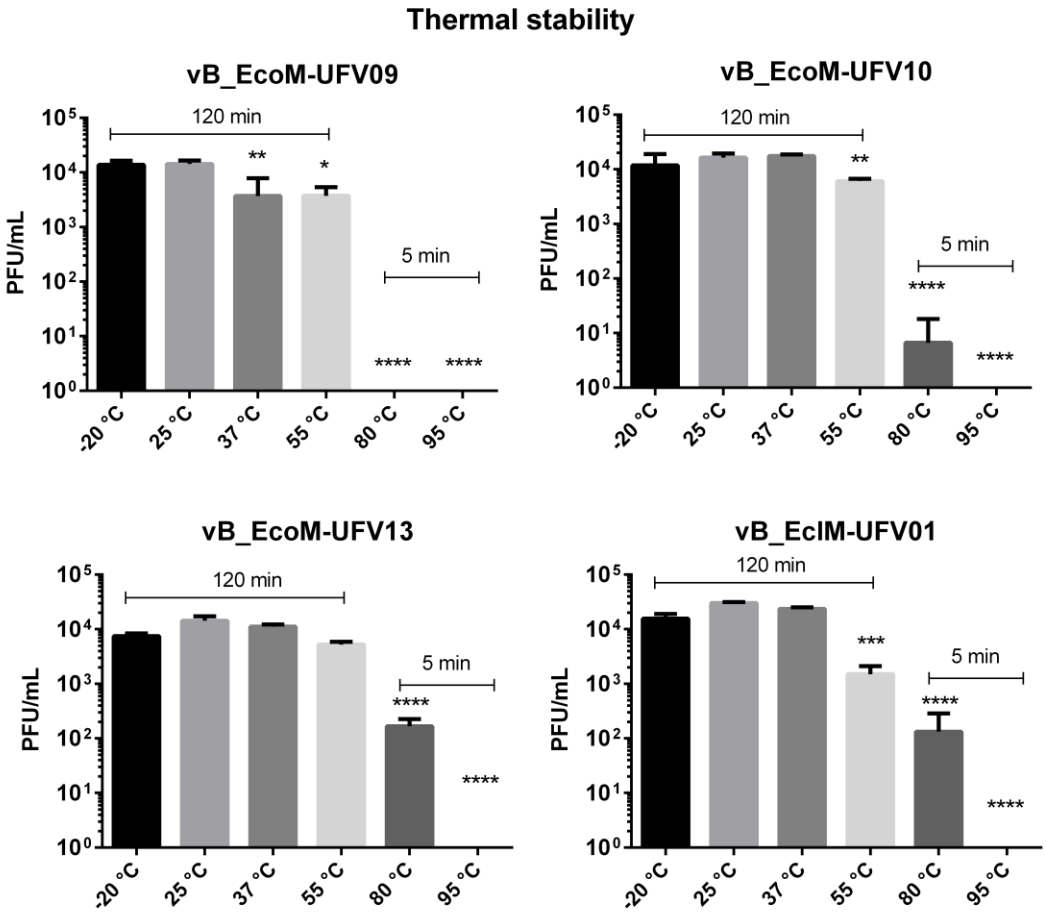

Figure 4: Phages thermal stability. Conditions with asterisks present significant differences (p-value ≤ 0.05) in the phage titer.

Viral stability in the presence of different pH values is illustrated in Figure 5. In general, the only treatment completely incompatible with phage survivability was pH 2, once two hours of incubation at this temperature was sufficient for a complete absence of plaquing forming units (PFU). pH 4 and 12 also appear to slightly affect viral stability, as three out of the four tested phages showed significant decreases in viral titers, with phage UFV09 showing the greatest decline.

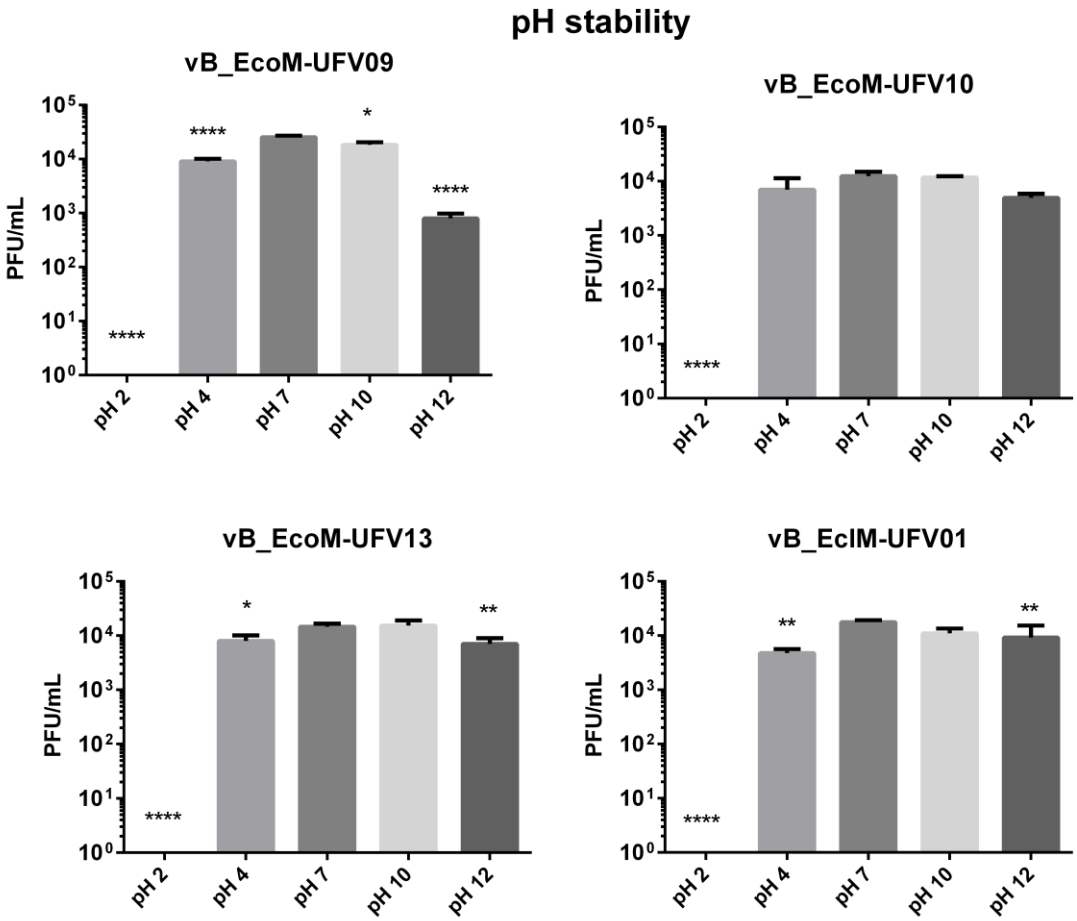

Figure 5: Viral stability in different pH values. Conditions with asterisks present significant differences (p-value ≤ 0.05) in the phage titer.

Phage UFV10 was the most stable when compared to the other phages which compose the cocktail, once no significant titer variation was shown at the tested pHs, except for pH 2. The findings show that virus particles are rather stable in intermediate pH values, but may exhibit discrete titer losses at boundary pH values, such as pH 4 and pH 12.

Regarding the assessment of long-term viral stability in environmental conditions similar to those found in oil extraction lines and wastewater, the first examined condition was the viral titer maintenance in high salinity settings. Figure 6 summarizes the results.

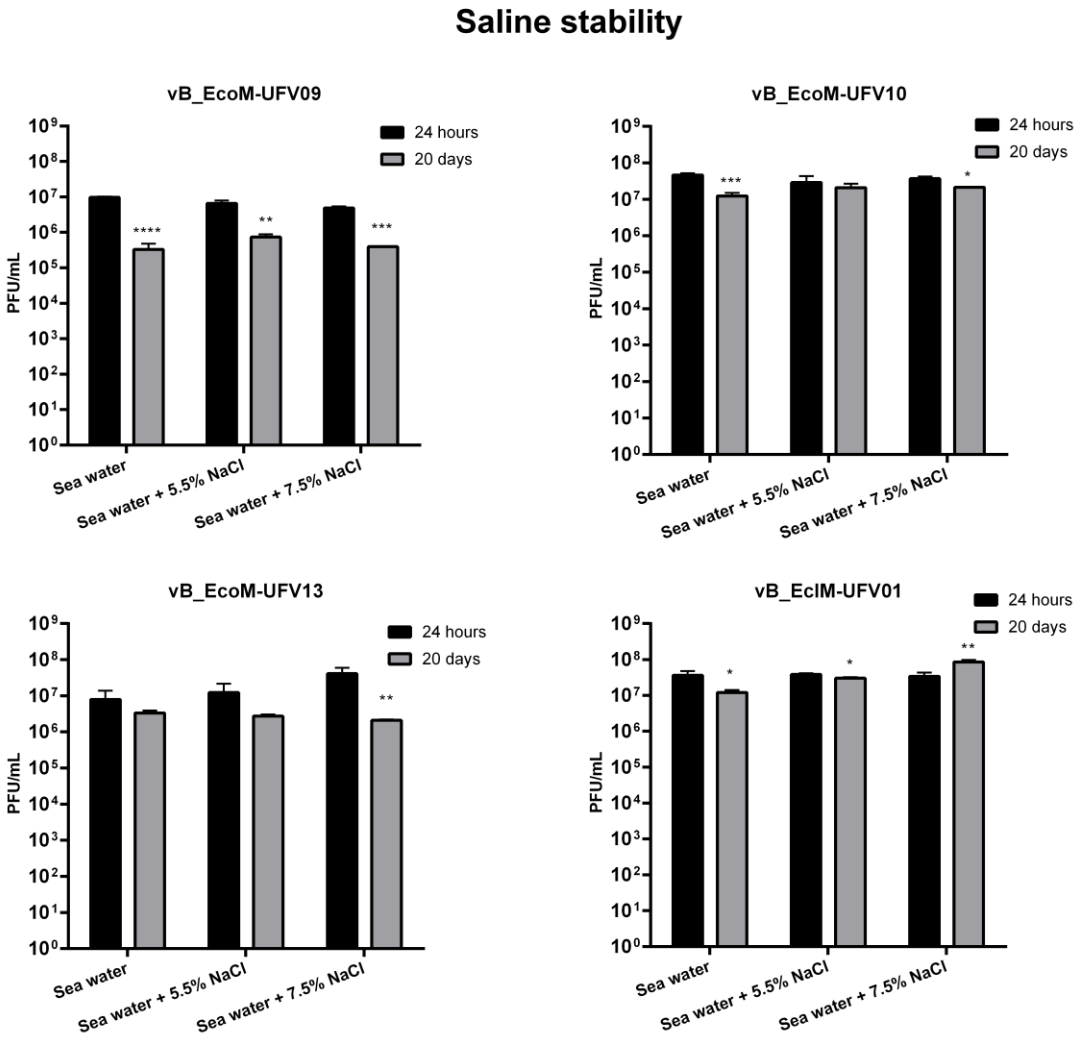

Figure 6: Viral stability in seawater, seawater 5.5% NaCl, and seawater 7.5% NaCl after 24 hours (black columns) and 20 days (grey columns). Incubation at 37 °C. The asterisks represent the significance of the titer decrease compared to the first day of the experiment. (p-value < 0.05).

As observed in Figure 6, the tested *NaCl* concentrations appear to have little effect on viral stability. The differences in virus titer between days 1 and 20 are most likely due to incubation duration and temperature rather than salt concentration (as will be explored later).

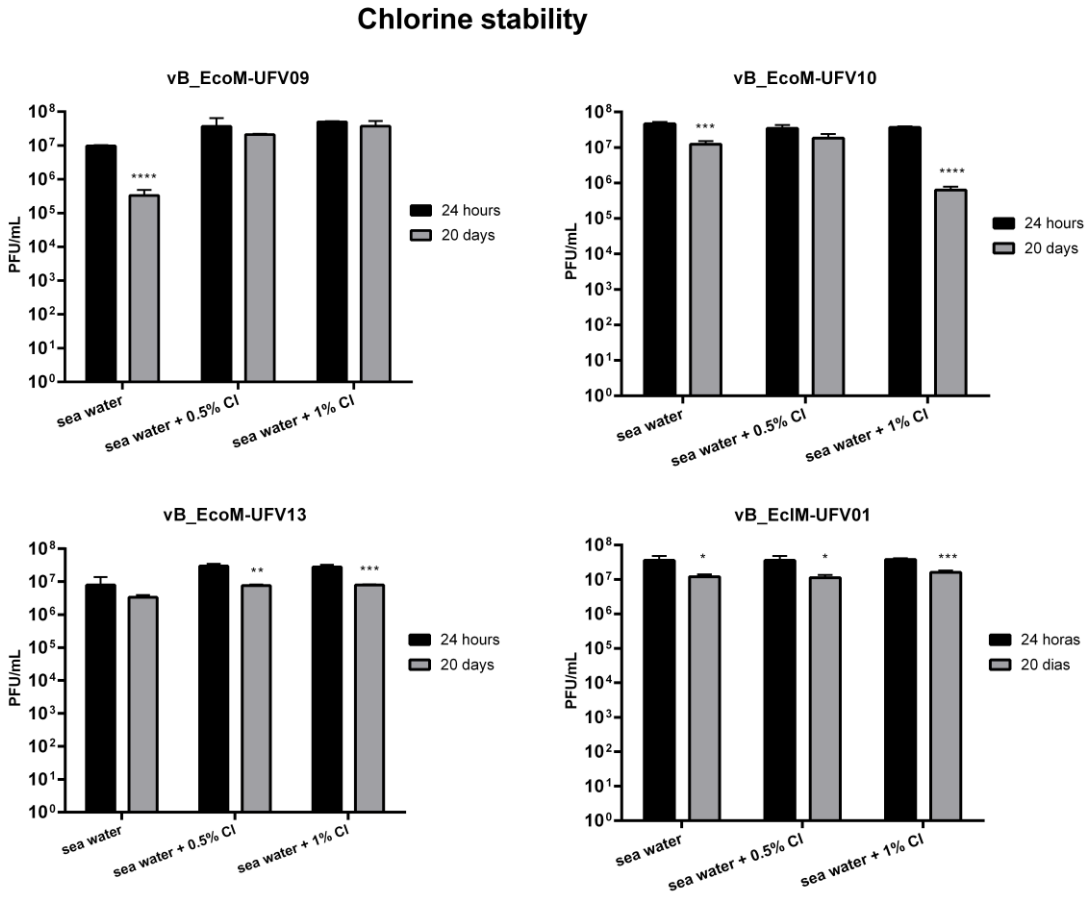

Figure 7: Viral stability after incubation in seawater, seawater 0.5% Cl and seawater 1% Cl after 24 hours (black columns) and 20 days (gray columns) of incubation at 37 °C. The asterisks represent the significance of the titer decrease compared to the first day of the experiment. (p-value < 0.05).

In the same way, as shown in Figure 7, concentrations of 0.5% *Cl* and 1% *Cl* appeared to not affect phages UFV13 and ENT01. The titer of these phages decreased just slightly, which was most likely due to the incubation period at 37 °C. Phage vB_EcoM-UFV10, on the other hand, appears to be affected by *Cl* content, once its titer decreased by 2 logs when incubated in seawater with 1% *Cl.*

The stability of the viral particles in the presence of the biocide THPS (Figure 8) at a concentration of 200 ppm was evaluated.

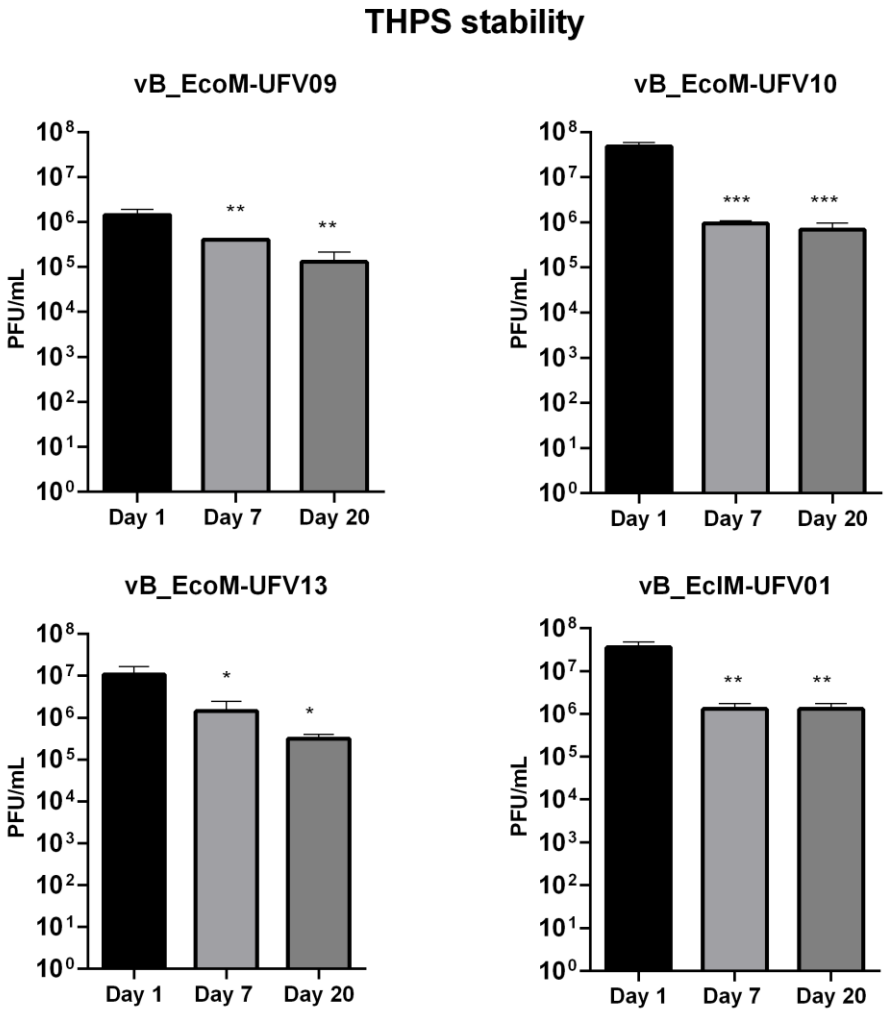

Figure 8: Viral stability after incubation in medium containing THPS after 24 hours (black columns), 7 days (light gray columns), and 20 days (dark gray columns) of incubation at 37 °C. The asterisks represent the significance of the titer decrease compared to the first day of the experiment. (p-value < 0.05).

All phages showed a significant drop in titer after 7 days of incubation (average of 1.5 logs), and this drop gradually continued until day 20 in the case of phages UFV13 and UFV09 and remained stable in the case of phages UFV10 and ENT01. Even with the decreasing viability trend, none of the phages lost more than 2 logs in viral quantification, and all remained with titers above 10^5 PFU/mL.

Finally, to assess the influence of incubation time on viral viability, phages were incubated at 30 °C, in SM buffer for 210 days (Figure 9).

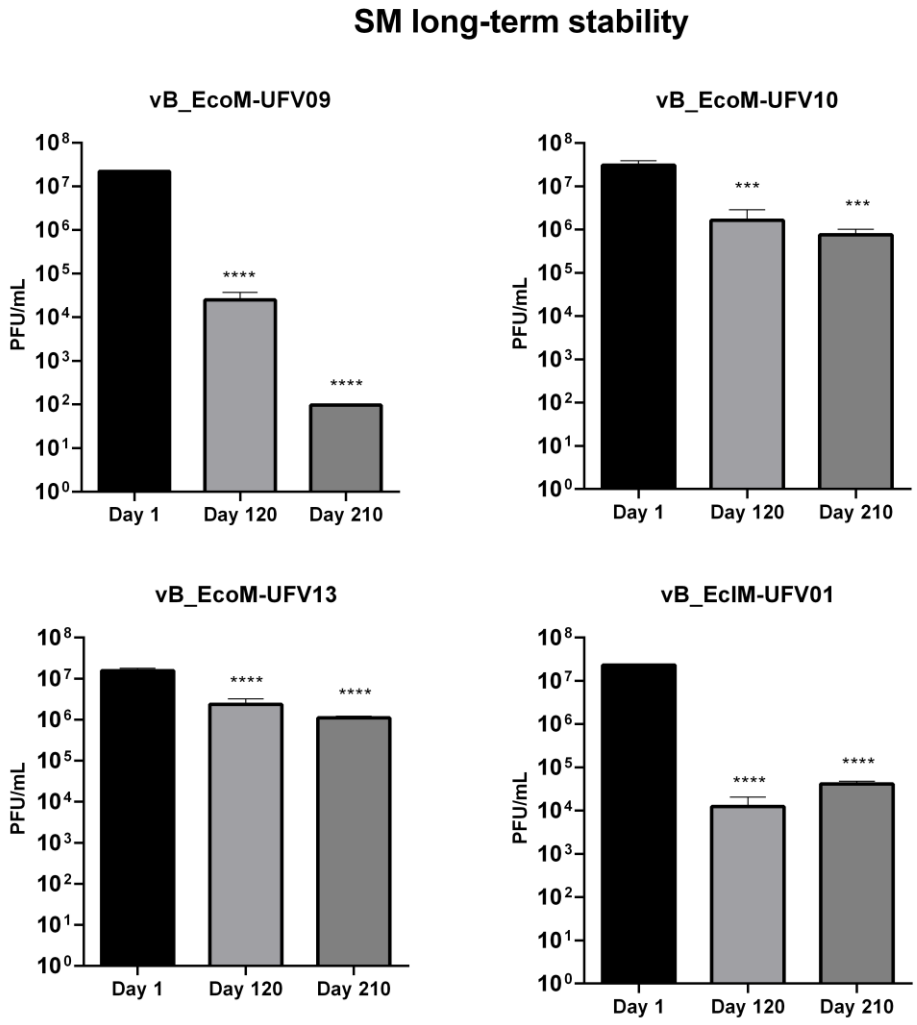

Figure 9: Viral stability after incubation in SM buffer after 24 hours (black columns), 120 days (light gray columns), and 210 days (dark gray columns) of incubation at 30 °C. The asterisks represent the significance of the titer decrease compared to the first day of the experiment. (p-value < 0.05).

In general, all the tested phages showed a considerable decrease in titer over the first 120 days of incubation. During the whole period of 210 days, phages UFV13 and UFV10 showed a decline of around 1.5 logs (a drastic decrease in the first 120 days, followed by another modest decrease until the last quantification). Phage ENT01 dropped three logs in the first 120 days of the experiment, then recovered slightly until day 210. Again, phage UFV09 was the most sensitive, its titer decreased by 3 logs in the first 120 days, then more 2 until day 210, lasting just 10^2 PFU/mL phages at the end of the experiment.

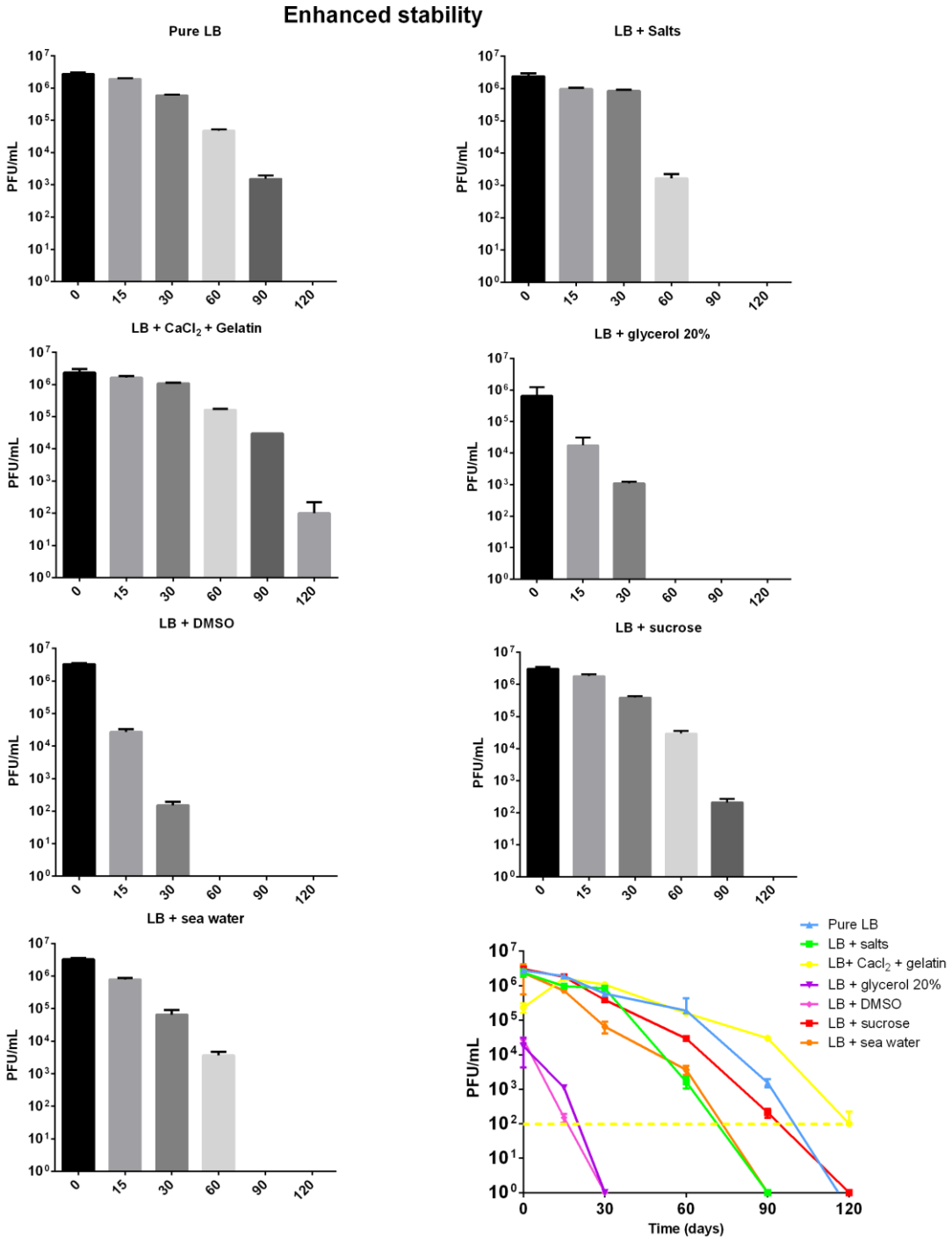

Figure 10: Phage UFV13 stability in LB medium enhanced with different conservative components.

To evaluate the conservative impact of different components in Phage UFV13 stability is illustrated in Figure 10. The tubes containing glycerol 20%, DMSO 20%, salts, and seawater presented an absence of phage particles after the first 60 and 90 days of the experiment, respectively. Tubes containing only pure LB and LB + sucrose had a similar behavior, having the phage titer zeroed only in the last measurement. The addition of $CaCl_2$

and gelatin was the only condition where the presence of stabilizers increased the phage UFV13 shelf life.

3.5. Yield assay of viral production on a bench scale and in bioreactors – LB Medium.

To evaluate the rate of viral propagation on a bench scale, and to analyze whether the cultivation conditions found by Silva *et al.,* 2021 [37] for phage vB_EcoM-UFV09 would extend to the other phages, assays with three initial titles were performed. Phages were incubated for 4 hours at 37 °C and 100 rpm and titrated at the end of this process (Figure 11).

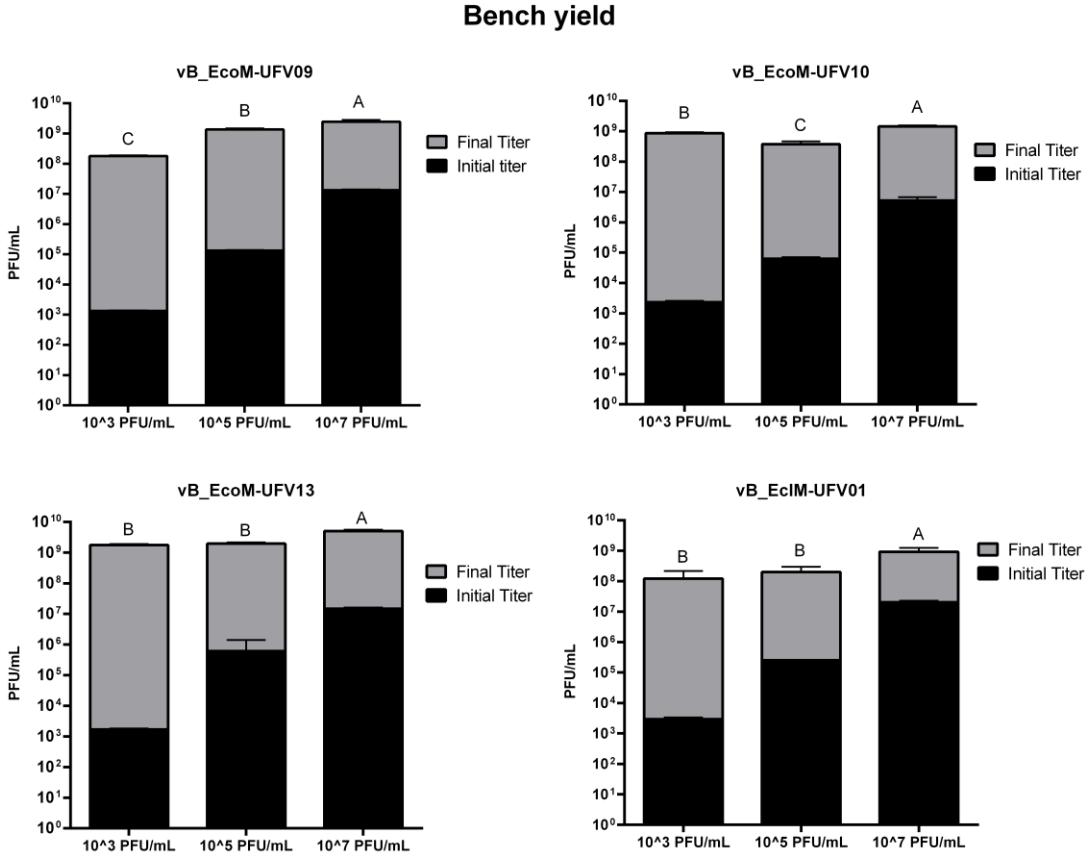

Figure 11: Bench-scale production of new viral particles. Phages were incubated for 4 hours at 37 °C and 100 rpm of agitation. Columns that have the same letter are statistically similar (one-way Anova and Tukey test, p-value < 0.05)

The findings were consistent with those of Silva *et al.* 2021 [47], indicating that a higher initial title (10^7) creates a statistically higher final title than the others. Furthermore, it denotes a balance between virus-host populations when the viral population reaches a titer between 10^9 and 10^{10} (that is, even with the greatest titer, the maximum amount of virus did not surpass 10^{10}).

Regarding the production gradient, the most viral particles were produced in the experiments that began with the lowest viral concentration (10^3) and, while the final titers were slightly lower than those obtained in the experiments that began with 10^7 UFP/mL, we believe that with a longer incubation time, these values would be statistically similar.

Using the bench values as a reference, the phage production capacity in bioreactors was analyzed (Figure 9), using the initial viral concentration of 10^5 PFU/mL, an intermediary titer.

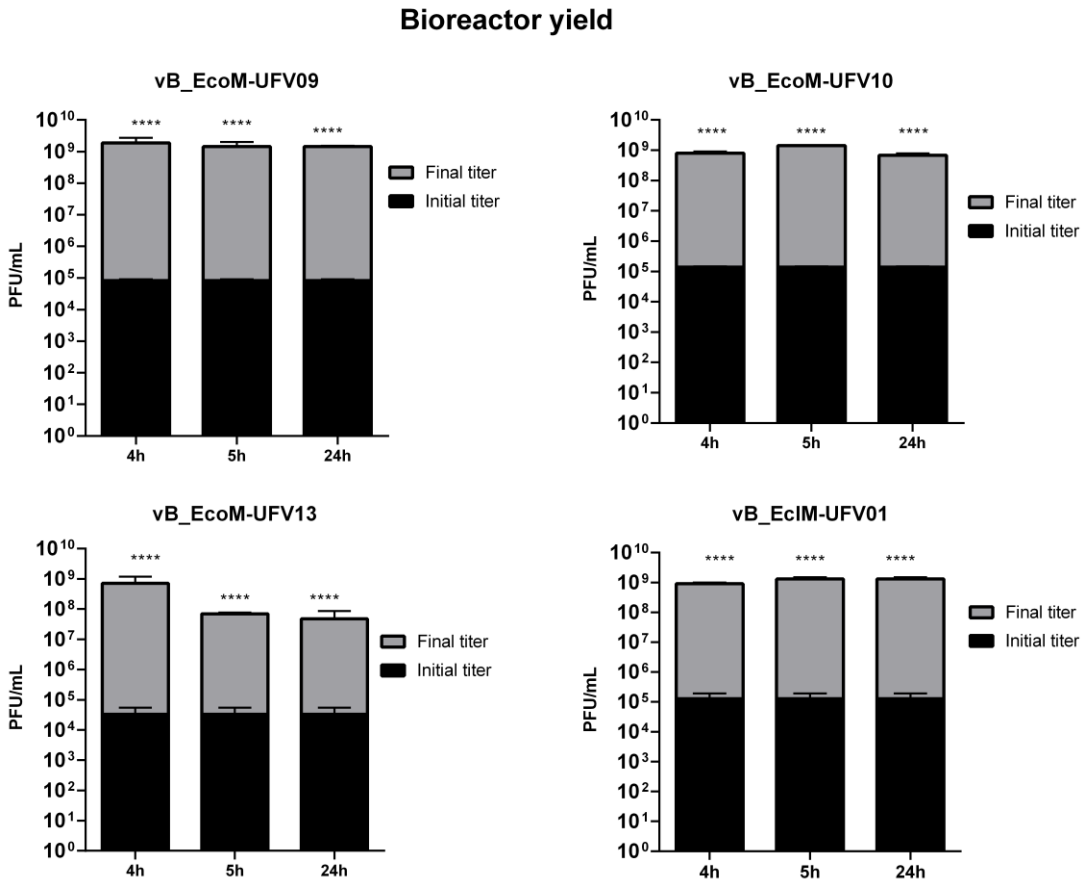

Figure 12: Yield of production of new viral particles in bioreactors. Phages were incubated for 4 hours at 37 °C and 100 rpm of agitation. Three incubation times were evaluated. The final titer after the production time was homogeneous and significantly higher than the initial title. (Student's t-test, p-value <0.05)

The results indicate that the yield of viral production obtained in the bench is very similar to that obtained in a bioreactor, increasing the amount of initial virus by up to 10,000 times and reaching a final titer of 10^9 PFU/mL. The average titer obtained at the end of the experimentation also was very similar between the phages, and no statistical difference between the phage titer with 5 or 24 hours of incubation.

4. Discussion

Phages, viruses that infect bacteria, were recognized for their potential in treating bacterial infections in the early twentieth century. Recently, there has been a resurgence of interest in phage therapy due to the increase in antimicrobial resistance. While human applications are mostly clinical trials, phage therapy shows promise in veterinary diseases and combating biofilms. Biofilms are bacterial arrangements, problematic in various settings and which protect the bacterial cells from antimicrobial agents. Phage enzymes, such as depolymerases and lysins, can target and disrupt biofilms. Phages can also be used as whole particles to combat biofilms, offering cost-effective and efficient solutions. Sulfate Reducing Bacteria (SRB) are anaerobic microorganisms that produce hydrogen sulfide (H2S) and cause damage in the oil industry. Current methods of controlling SRB growth, such as biocides, have limitations and microbial resistance. Bacteriophages, producing enzymes like depolymerases and lysins, offer a potential solution by targeting SRB biofilms. However, the diversity of SRB makes it impractical to isolate specific phages for each strain. Formulating nonspecific phage cocktails and optimizing large-scale production is crucial for effective SRB control in the industry. The aim of this work is the elaboration of a phage cocktail, composed of phages isolated from enterobacterial hosts, but able to reduce SRB biofilms. The development of a phage-based product for future use in oil-related environments led to the execution of unusual experiments such as phage stability in chlorinate and high salinity concentrations, long-term storage conditions, and the evaluation of compounds that could maintain the viral titer in non-refrigerated environments.

For this, the first step to selecting the phages which could be able to compose the cocktail was based on the experiments of host range; inhibition of biofilm production in non-host enterobacteria, and ease of reaching high post-propagation titers. Phages UFV09, UFV13, Eco05, Eco09, and UFV10 were able to infect different strains of *E. coli*, and Cit03 was able to infect isolates of different genera. Phages Eco1504, Eco09, UFV10, Cit01, ENT01, and vB_SmaP-UFV01 were able to significantly reduce the biofilm of non-host bacteria. The low titer rates after liquid propagations led to the inconsideration of phages Eco1504, Eco05, Eco09, Cit01, Cit03, and vB_SmaP-UFV01 as good candidates for the cocktail composition. As a result, UFV09, UFV10, UFV13, and ENT01 were chosen for the following stage, the biofilm inhibition of SRB cultures prevenient from oil-related environments. The cocktail, named Petro01, was able to reduce the biofilm of three of the four SRB mixed cultures, under the tested conditions. These findings suggested that the

cocktail formulated by the phages UFV09, UFV10, UFV13, and ENT01 had a promising potential for regulating SRB biofilms, and that should proceed to the next level of testing, the genomic safety.

Phage UFV13 was described by Duarte *et al*., 2018. The phage genome possesses a genome of 165772 bp, a G+C content of 34.8%, and is a member of the genus *Tequatrovirus.* The author searched for phage enzymes, such as the virion-associated peptidoglycan hydrolases (VAPGHs) genes in the UFV13 genome and found that five ORFs (31, 153, 160, 188, and 246) encode for N-acetylmuramoyl-L-alanine amidases, one (gp 124) encodes for a peptidase (IP3), and other (gp 245) encodes an enzyme that acts on the peptidoglycan chain. Phage ENT01 has a linear double-stranded DNA genome, with 174,517 base pairs (bp) and 287 open reading frames (ORFs), and a G+C content of 39,7%. Phylogenetics similarities showed that ENT01 is a member of the genus Karamvirus. The search for putative depolymerase domains showed that the head outer capsid protein (gp 7) and the fibritin neck whisker (gp 170) are predicted to have this function. For both cases, no lysogeny-associated proteins or virulence genes were predicted. To complete the genomic safety evaluation of the phages that compose the cocktail, the genome of phages UFV09 and UFV10 was sequenced and analyzed. The results found that both phages have a dsDNA genome of 165859 bp, with a G+C content of 35,4 % which encodes 286 ORFs and 11 tRNAs. The phylogenetic analysis allowed the classification of these phages as members of the genus *Tequatrovirus*. Also, no lysogeny or pathogenicity genes were found. Tequatroviruses are well-known virulent phages. Before the binomial system of nomenclature for bacterial viruses was implemented, the karamviruses were classified as tequatroviruses, and like them, do not possess lysogeny genes. The search for putative depolymerase domains in the UFV09 genome predicted 9 ORFs (Table 3). The presence of domains related to different phage enzymes in the cocktail Petro01 is a highly beneficial trait. The alignment (Figure 3) emphasizes their similarities and shows the presence of predicted depolymerase domains among them. Some of these genes, inclusive, are present both for UFV10 and UFV13. Although the action mechanisms of the phage enzymes are being extensively investigated, their interactions are so complex and can alter biofilms in so many different ways that much remains to be learned [17]. Because of this, the way the cocktail can decrease a biofilm of SRB is not totally understood but is probably related to biofilm sugar degradation by the action of phage depolymerases.

The phylogenetic analysis also revealed the high similarity between phages UFV09 and UFV10. The identical genome length, number of ORFs, and absence of low-similarities

regions, as indicated in the alignment (Figure 3), led to a Single Nucleotide Polymorphism (SNPs) analysis. The findings showed that just one point mutation distinguishes one phage from another. The alteration of a C to an A resulted in a missense variation at the phage's DNA helicase (gp 48). However, this single alteration, in this gene location, does not explain the biological differences found between UFV09 and UFV10, and further investigations need to be done to confirm this data.

The analysis of thermal and different pH stability was performed using the phages that presented positive results in the previous steps. The thermal results (Figure 4) showed that all phages maintained their titles after treatment at -20 °C, indicating a good resistance to negative temperatures and an excellent perspective of stability and storage under these conditions. On the other hand, they showed a significant titer drop in temperatures of 80 °C and 95 °C, which indicates the incompatibility of these temperatures with maintaining viral stability, even with a short exposure time. In this field, phages UFV13 and ENT01, even with the significant titer decreasing, Phage UFV09 also showed a slight but significant decrease in titer at temperatures of 37 °C and 55 °C and phage ENT01 showed a drop in titer when incubated at 55 °C. The phage instability at temperatures above 60 °C is frequently described and associated with protein denaturation and tequatroviruses can normally withstand temperatures ranging from 60 to 70 °C. The capacity of some viral isolates to remain stable at higher temperatures is normally associated with mutations in structural proteins, that can strengthen protein interactions and thus increase heat resistance[58,59]. The stability in different pH values showed that pH 2 was incompatible with phage stability and pH 12 could slightly decrease the phage title. These findings are correlated with what is described in the literature, once extreme pH values can alter the chemical bonds between proteins and consequently change their shape and function [60,61].

To keep discussing the phage stability in the other conditions evaluated in this study is important to emphasize some particular traits that drove the development of this work. Phage cocktails are typically developed to treat specific conditions, such as individual patients or even animals suffering from bacterial infections, and even in institutes where phages are widely used as a treatment methodology, they are typically produced on demand, on a small bioprocessing scale. In these locations, phages are often kept under well-known storage settings, such as PEG purification, followed by resuspension in SM buffer and storage at 4°C, or even more advanced procedures, such as affinity column purification. Our cocktail was created with a completely different goal in mind. Oil facilities are massive structures with

hundreds of meters in length and thousands of m3 storage tanks. It was expected that our phage cocktail would be utilized in these tanks, prompting us to investigate a mixture of diverse conditions in which our cocktail must be stable, such as chlorine, stability in the presence of seawater, high salinity concentrations, and the presence of THPS. Low pH concentrations are also a normal situation in oil-related tanks and pipelines. Given the enormous size of the tanks, we will need to manufacture a big volume of phage cocktails, which will not necessarily be stored in cool rooms or go through purification stages. In fact, the only downstream procedures we intended to perform were the filtration steps. Hence, we needed, for example, to evaluate phage stability at 37 °C, a temperature easily achieved in tropical storage sheds, and investigate the inclusion of stabilizing components aiming to boost phage stability in not-typical phage storage conditions.

As a result, as illustrated by Figures 6, 7, and 8, high-saline concentrations (5.5% and 7.5%), seawater with chlorine (concentrations of 0.5% and 1%), and the presence of the biocide THPS (200 ppm) appear to not affect viral stability, at least for the first 24 hours. The small, but still significant, titer decrease after 20 days of experimentation is probably due to a long time of incubation in a supernatant without any form of conserving, at 37 °C, instead of the presence of salt, chlorine, or THPS.

The addition of phage-conservative components to evaluate the better post-propagation storage supernatant composition (Figure 10) revealed that, under the evaluated conditions, just the tubes boosted with $CaCl_2$ increased the phage UFV13 shelf life. This was the only combination where infective phages were recovered with 120 days of experimentation, even in a concentration of 5 logs smaller. The addition of 20% glycerol, 20% DMSO, salts, and seawater appears to have a negative effect, with total phage particle loss occurring after 60 and 90 days of experimentation, much earlier than in tubes containing just LB. Sucrose, on the other hand, seems to have had a neutral influence, exhibiting a similar titer loss pattern to those observed in pure LB. It’s worth noting that the preservative components chosen in this work were previously mentioned in the literature, in studies that also attempted to increase the shelf life of phages. However, in those cases, the conservatives were combined with refrigerated (sometimes even negative) storage temperatures[60,62–65]. The use of higher temperatures than the standard 4 degrees could explain the low conservative efficiency of the components tested under our incubation conditions. As shown in Figure 9, the better supernatant for phage long-term stabilization was the well-known SM buffer, even though, in this study, the temperature of incubation was 30 °C. These findings lead to

important considerations. Resuspending phages in SM buffer can increase the lifetime and maintain the titer of a phage-based product longer. But in this case, in addition to the standard downstream filtration steps, additional steps of concentration with PEG, centrifugation and subsequent resuspension would be required, which would make the viral large-scale production process more onerous, time-consuming, and expensive.

Finally, the last step to consolidate the Petro01 cocktail as a good candidate for the development of a phage-based product was the evaluation of viral production on a bench scale and in bioreactors. The findings revealed that the yield did not change with the increase in the production scale. The phages propagated homogeneously and in a short period of production (4 hours). The intermediate title (10^5) was defined as the standard for the other batches since a smaller phage concentration and volume is required (compared to the initial title of 10^7) and a shorter production time (compared to the initial title of 10^3) for an average production of 10^9 PFU/mL.

5. Conclusions

In this study, ten phages were tested to identify those with the best properties for composing a cocktail suitable for oil-related environments. The phages UFV09, UFV10, UFV13, and ENT01 were selected to form the Petro01 cocktail. Phylogenetic analysis revealed that the *Escherichia* phages UFV09, UFV10, and UFV13 belong to the genus *Tequatrovirus*, and the Enterobacter phage ENT01 is member of the genus *Karamvirus*. None of their genomes exhibited pathogenic or lysogeny genes, and UFV09 and UFV10 were predicted to encode depolymerases in nine genes. Phages UFV09 and UFV10 also showed to be polymorphics. The long-term stability of these phages was evaluated at temperatures of 30 and 37 °C, as well as in high-salinity and high-chlorine environments, SM buffer, and LB medium enriched with preservatives. The results showed overall good stability, although the long-term titer maintenance in non-refrigerate temperatures is an aspect that requires refinement. The bench ad in bioreactor propagation rate of the phages belonging to Petro01evidenciates their similar propagation profiles. Our data indicate that a four-hour batch process is sufficient to achieve an average phage production of 10^9 PFU/mL. These encouraging findings highlight the significant biotechnological potential of Petro01, suggesting its ability to withstand environmental challenges in oil facilities and potentially reduce sulfate-reducing bacteria biofilms.

6. Data availability

Accession numbers: *Escherichia* phage vB_EcoM-UFV09 (MZ291552.2); Escherichia phage vB_EcoM-UFV10 (OP555981.1); *Escherichia* phage vB_EcoM-UFV13 (KU867876); *Enterobacter* phage vB_EclM-UFV01 (ON454249)

7. Bibliography

1. Comeau, A.M.; Hatfull, G.F.; Krisch, H.M.; Lindell, D.; Mann, N.H.; Prangishvili, D. Exploring the prokaryotic virosphere. *Res. Microbiol.* **2008**, *159*, 306–313, doi:10.1016/j.resmic.2008.05.001.
2. Keen, E.C. Phage therapy : concept to cure. *Front. Microbiol.* **2012**, *3*, 238, doi:10.3389/fmicb.2012.00238.
3. Fruciano, E.; Bourne, S. Phage as an antimicrobial agent: d'Herelle's heretical theories and their role in the decline of phage prophylaxis in the West. *Can. J. Infect. Dis. Med. Microbiol.* **2007**, *18*, 19–26.
4. Golkar, Z.; Bagasra, O.; Gene Pace, D. Bacteriophage therapy: A potential solution for the antibiotic resistance crisis. *J. Infect. Dev. Ctries.* **2014**, *8*, 129–136, doi:10.3855/jidc.3573.
5. Pires, D.P.; Costa, A.R.; Pinto, G.; Meneses, L.; Azeredo, J. Current challenges and future opportunities of phage therapy. *FEMS Microbiol. Rev.* **2020**, *44*, 684–700, doi:10.1093/femsre/fuaa017.
6. Petrov, V.M.; Ratnayaka, S.; Nolan, J.M.; Miller, E.S.; Karam, J.D. Genomes of the T4-related bacteriophages as windows on microbial genome evolution. *Virol. J.* **2010**, *7*, 292, doi:10.1186/1743-422X-7-292.
7. Salmond, G.P.C.; Fineran, P.C. A century of the phage: Past, present and future. *Nat. Rev. Microbiol.* **2015**, *13*, 777–786, doi:10.1038/nrmicro3564.
8. Ventola, C.L. The Antibiotic Resistance Crisis. *P&T* **2015**, *40*, 278–283, doi:10.5796/electrochemistry.82.749.
9. Andersson, D.I.; Hughes, D. Antibiotic resistance and its cost: Is it possible to reverse resistance? *Nat. Rev. Microbiol.* **2010**, *8*, 260–271, doi:10.1038/nrmicro2319.
10. Brives, C.; Pourraz, J. Phage therapy as a potential solution in the fight against AMR: obstacles and possible futures. *Palgrave Commun.* **2020**, *6*, 1–11, doi:10.1057/s41599-020-0478-4.
11. Verbeken, G.; Pirnay, J.P. European regulatory aspects of phage therapy: magistral phage preparations. *Curr. Opin. Virol.* **2022**, *52*, 24–29, doi:10.1016/j.coviro.2021.11.005.
12. Jault, P.; Leclerc, T.; Jennes, S.; Pirnay, J.P.; Que, Y.A.; Resch, G.; Rousseau, A.F.; Ravat, F.; Carsin, H.; Le Floch, R.; et al. Efficacy and tolerability of a cocktail of bacteriophages to treat burn wounds infected by Pseudomonas aeruginosa (PhagoBurn): a randomised, controlled, double-blind phase 1/2 trial. *Lancet Infect. Dis.* **2019**, *19*, 35–45, doi:10.1016/S1473-3099(18)30482-1.

13. Onsea, J.; Uyttebroek, S.; Chen, B.; Wagemans, J.; Lood, C.; Van Gerven, L.; Spriet, I.; Devolder, D.; Debaveye, Y.; Depypere, M.; et al. Bacteriophage therapy for difficult-to-treat infections: The implementation of a multidisciplinary phage task force (the phageforce study protocol). *Viruses* **2021**, *13*, doi:10.3390/v13081543.

14. Gambino, M.; Brøndsted, L. Looking into the future of phage-based control of zoonotic pathogens in food and animal production. *Curr. Opin. Biotechnol.* **2021**, *68*, 96–103, doi:10.1016/j.copbio.2020.10.003.

15. Kumar, C.G.; Anand, S.K. Significance of microbial biofilms in food industry : a review. *Int. J. Food Microbiol.* **1998**, *42*, 9–27.

16. Harper, D.R.; Parracho, H.M.R.T.; Walker, J.; Sharp, R.; Hughes, G.; Werthé, M. Bacteriophages and Biofilms. **2014**, 270–284, doi:10.3390/antibiotics3030270.

17. Visnapuu, A.; Der Gucht, M.; Wagemans, J.; Lavigne, R. Deconstructing the Phage–Bacterial Biofilm Interaction as a Basis to Establish New Antibiofilm Strategies. *Viruses* **2022**, *14*, doi:10.3390/v14051057.

18. Flemming, H.C.; Wingender, J.; Szewzyk, U.; Steinberg, P.; Rice, S.A.; Kjelleberg, S. Biofilms: An emergent form of bacterial life. *Nat. Rev. Microbiol.* **2016**, *14*, 563–575, doi:10.1038/nrmicro.2016.94.

19. Costerton, J.W.; Cheng, K.J.; Geesey, G.G.; Ladd, T.I.; Nickel, J.C.; Dasgupta, M.; Marrie, T.J. Bacterial biofilms in nature and disease. *Annu. Rev. Microbiol.* **1987**, *41*, 435–464.

20. López, D.; Vlamakis, H.; Kolter, R. Biofilms. *Cold spings* **2010**, 1–12.

21. Høiby, N.; Ciofu, O.; Johansen, H.K.; Song, Z.J.; Moser, C.; Jensen, P.Ø.; Molin, S.; Givskov, M.; Tolker-Nielsen, T.; Bjarnsholt, T. The clinical impact of bacterial biofilms. *Int. J. Oral Sci.* **2011**, *3*, 55–65, doi:10.4248/IJOS11026.

22. Fernandes, S.; São-José, C. Enzymes and mechanisms employed by tailed bacteriophages to breach the bacterial cell barriers. *Viruses* **2018**, *10*, 1–22, doi:10.3390/v10080396.

23. Shymialevich, D.; Wójcicki, M.; Wardaszka, A.; Świder, O.; Sokołowska, B.; Błażejak, S. Application of Lytic Bacteriophages and Their Enzymes to Reduce Saprophytic Bacteria Isolated from Minimally Processed Plant-Based Food Products-In Vitro Studies. *Viruses* **2022**, *15*, doi:10.3390/v15010009.

24. Maciejewska, B.; Olszak, T.; Drulis-Kawa, Z. Applications of bacteriophages versus phage enzymes to combat and cure bacterial infections: an ambitious and also a realistic application? *Appl. Microbiol. Biotechnol.* **2018**, *102*, 2563–2581, doi:10.1007/s00253-018-8811-1.

25. Chan, B.K.; Abedon, S.T. Bacteriophages and their Enzymes in Biofilm Control. *Curr. Pharm. Des.* **2015**, *21*, 85–99.

26. Pires, D.P.; Oliveira, H.; Melo, L.D.R.; Sillankorva, S.; Azeredo, J. Bacteriophage-encoded depolymerases : their diversity and biotechnological applications. *Appl. Microbiol. Biotechnol.* **2016**, *100*, 2141–2151, doi:10.1007/s00253-015-7247-0.

27. Carlos, S. Engineering of Phage-Derived Lytic Enzymes : Improving Their Potential as Antimicrobials. **2018**, doi:10.3390/antibiotics7020029.

28. Rabus, R.; Venceslau, S.S.; Wöhlbrand, L.; Voordouw, G.; Wall, J.D.; Pereira, I.A.C. A Post-Genomic View of the Ecophysiology, Catabolism and Biotechnological Relevance of Sulphate-Reducing Prokaryotes. *Adv. Microb. Physiol.* **2015**, *66*, 55–321, doi:10.1016/bs.ampbs.2015.05.002.

29. Song, J.; Hwang, J.; Kang, I.; Cho, J.C. A sulfate-reducing bacterial genus, Desulfosediminicola gen. nov., comprising two novel species cultivated from tidal-flat sediments. *Sci. Rep.* **2021**, *11*, 1–13, doi:10.1038/s41598-021-99469-5.

30. Waite, D.W.; Chuvochina, M.; Pelikan, C.; Parks, D.H.; Yilmaz, P.; Wagner, M.; Loy, A.; Naganuma, T.; Nakai, R.; Whitman, W.B.; et al. Proposal to reclassify the proteobacterial classes deltaproteobacteria and oligoflexia, and the phylum thermodesulfobacteria into four phyla reflecting major functional capabilities. *Int. J. Syst. Evol. Microbiol.* **2020**, *70*, 5972–6016, doi:10.1099/ijsem.0.004213.

31. Barton, L.L.; Fauque, G.D. Biochemistry, Physiology and Biotechnology of Sulfate-Reducing Bacteria. In *Advances in Applied Microbiology*; Elsevier Inc.: Amsterdam, The Netherlands, 2009; Vol. 68, pp. 41–98 ISBN 9780123748034.

32. Gieg, L.M.; Jack, T.R.; Foght, J.M. Biological souring and mitigation in oil reservoirs. *Appl. Microbiol. Biotechnol.* **2011**, *92*, 263–282, doi:10.1007/s00253-011-3542-6.

33. Gieg, L.M.; Davidova, I.A.; Duncan, K.E.; Suflita, J.M. Methanogenesis, sulfate reduction and crude oil biodegradation in hot Alaskan oilfields. *Environ. Microbiol.* **2010**, *12*, 3074–3086, doi:10.1111/j.1462-2920.2010.02282.x.

34. Reiffenstein, R.J.; Hulbert, W.C.; Roth, S.H. Toxicology of hydrogen sulfide. *Annu. Rev. Pharmacol. Toxicol.* **1992**, *32*, 109–134, doi:10.1146/annurev.pa.32.040192.000545.

35. Tang, K.; Baskaran, V.; Nemati, M. Bacteria of the sulphur cycle: An overview of microbiology, biokinetics and their role in petroleum and mining industries. *Biochem. Eng. J.* **2009**, *44*, 73–94, doi:10.1016/j.bej.2008.12.011.

36. Fraise, A.P. Susceptibility of antibiotic-resistant cocci to biocides. *J. Appl. Micriobiology Symp. Suppl.* **2002**, *92*, 158–162.

37. Okoro, C.C. The Biocidal Efficacy of Tetrakis-hydroxymethyl Phosphonium Sulfate (THPS) Based Biocides on Oil Pipeline PigRuns Liquid Biofilms The Biocidal Efficacy of Tetrakis-hydroxymethyl Phosphonium Sulfate (THPS) Based Biocides on Oil Pipeline PigRuns Liquid . **2015**, *6466*, doi:10.1080/10916466.2015.1062781.

38. Gu, D.X.Y.L.T. A synergistic D -tyrosine and tetrakis hydroxymethyl phosphonium sulfate biocide combination for the mitigation of an SRB biofilm. **2012**, 3067–3074, doi:10.1007/s11274-012-1116-0.

39. Stewart, P.S.; Costerton, J.W. Antibiotic resistance of bacteria in biofilms. *Lancet* **2001**, *358*, 135–138.

40. Berry, D.; Widder, S. Deciphering microbial interactions and detecting keystone species with co-occurrence networks. *Front. Microbiol.* **2014**, *5*, 1–14, doi:10.3389/fmicb.2014.00219.

41. Tudela, H.; Claus, S.P.; Saleh, M. Next Generation Microbiome Research: Identification of Keystone Species in the Metabolic Regulation of Host-Gut Microbiota Interplay. *Front. Cell Dev. Biol.* **2021**, *9*, doi:10.3389/fcell.2021.719072.

42. Chan, B.K.; Abedon, S.T.; Loc-carrillo, C. Phage cocktails and the future of phage therapy. *Futur. Med.* **2013**, *8*, 769–783.

43. Knecht, L.E.; Veljkovic, M.; Fieseler, L. Diversity and Function of Phage Encoded Depolymerases. *Front. Microbiol.* **2020**, *10*, 2949, doi:10.3389/fmicb.2019.02949.

44. Mohaghegh, A.; Ananda, M.; Bhattacharjee, S.; Goel, R. Biofilm control with natural and genetically-modified phages. *World J. Microbiol. Biotechnol.* **2016**, *34*, 67, doi:10.1007/s11274-016-2009-4.

45. Agboluaje, M.; Sauvageau, D. Bacteriophage Production in Bioreactors. In *Bacteriophage Therapy: From Lab to Clinical Practice*; Azeredo, J., Sillankorva, S., Eds.; Human Press: Totowa, NJ, USA, 2018; Vol. 1693, pp. 173–193 ISBN 9781493973958.

46. Jurač, K.; Nabergoj, D.; Podgornik, A. Bacteriophage production processes. *Appl. Microbiol. Biotechnol.* **2019**, *103*, 685–694, doi:10.1007/s00253-018-9527-y.

47. Silva, J.; Dias, R.; Junior, I.; Silva, M.; Carmo, A.; Sousa, M.; Silva, C.; Paula, S. De A Rapid Method for Performing a Multivariate Optimization of Phage Production Using the RCCD Approach. *Pathogens* **2021**, *10*, 1–19, doi:https://doi.org/10.3390/pathogens10091100.

48. Duarte, V.S.; Dias, R.S.; Kropinski, A.M.; Xavier, A. da S.; Ferro, C.G.; Vidigal, P.M.P.; Silva, C.C. da; Paula, S.O. de A T4virus prevents biofilm formation by Trueperella pyogenes. *Vet. Microbiol.* **2018**, *218*, 45–51, doi:10.1016/j.vetmic.2018.03.025.

49. Vieira, M.S.; Duarte da Silva, J.; Ferro, C.G.; Cunha, P.C.; Vidigal, P.M.P.; Canêdo da Silva, C.; Oliveira de Paula, S.; Dias, R.S. A highly specific Serratia-infecting T7-like phage inhibits biofilm formation in two different genera of the Enterobacteriaceae family. *Res. Microbiol.* **2021**, *172*, doi:10.1016/j.resmic.2021.103869.

50. Mirzaei, M.K.; Nilsson, A.S. Isolation of phages for phage therapy: A comparison of spot tests and efficiency of plating analyses for determination of host range and efficacy. *PLoS One* **2015**, *10*, 1–13, doi:10.1371/journal.pone.0118557.

51. Knezevic, P.; Petrovic, O. A colorimetric microtiter plate method for assessment of phage effect on Pseudomonas aeruginosa biofilm. *J. Microbiol. Methods* **2008**, *74*, 114–118, doi:10.1016/j.mimet.2008.03.005.

52. Aziz, R.K.; Bartels, D.; Best, A.; DeJongh, M.; Disz, T.; Edwards, R.A.; Formsma, K.; Gerdes, S.; Glass, E.M.; Kubal, M.; et al. The RAST Server: Rapid annotations using subsystems technology. *BMC Genomics* **2008**, *9*, 1–15, doi:10.1186/1471-2164-9-75.

53. Vieira, M.F.; Duarte, J.; Domingues, R.; Oliveira, H.; Dias, O. PhageDPO: Phage Depolymerase Finder. *bioRxiv* **2023**, 2023.02.24.529883.

54. Nishimura, Y.; Yoshida, T.; Kuronishi, M.; Uehara, H.; Ogata, H.; Goto, S. ViPTree: The viral proteomic tree server. *Bioinformatics* **2017**, *33*, 2379–2380, doi:10.1093/bioinformatics/btx157.

55. Olson, R.D.; Assaf, R.; Brettin, T.; Conrad, N.; Cucinell, C.; Davis, J.J.; Dempsey, D.M.; Dickerman, A.; Dietrich, E.M.; Kenyon, R.W.; et al. Introducing the Bacterial and Viral Bioinformatics Resource Center (BV-BRC): a resource combining PATRIC, IRD and ViPR. *Nucleic Acids Res.* **2023**, *51*, D678–D689, doi:10.1093/nar/gkac1003.

56. Jurczak-Kurek, A.; Gasior, T.; Nejman-Faleńczyk, B.; Bloch, S.; Dydecka, A.; Topka, G.; Necel, A.; Jakubowska-Deredas, M.; Narajczyk, M.; Richert, M.; et al. Biodiversity of bacteriophages: Morphological and biological properties of a large group of phages isolated from urban sewage. *Sci. Rep.* **2016**, *6*, 1–17, doi:10.1038/srep34338.

57. Kropinski, A.M.; Mazzocco, A.; Waddell, T.E.; Lingohr, E.; Johnson, R.P. Enumeration of bacteriophages by double agar overlay plaque assay. In *Bacteriophages, Methods in molecular biology (Clifton, N.J.)*; Human Press, 2009; Vol. 501, pp. 69–76 ISBN 9781603271646.

58. Litt, P.K.; Jaroni, D. Isolation and Physiomorphological Characterization of Escherichia coli O157:H7-Infecting Bacteriophages Recovered from Beef Cattle Operations. *Int. J. Microbiol.* **2017**, *2017*, doi:10.1155/2017/7013236.

59. Taj, M.K.; Ling, J.X.; Bing, L.L.; Qi, Z.; Taj, I.; Hassani, T.M.; Samreen, Z.; Yunlin, W. Effect of dilution, temperature and pH on the lysis activity of t4 phage against E.coli BL21. *J. Anim. Plant Sci.* **2014**, *24*, 1252–1255.

60. Jończyk-matysiak, E.; Łodej, N.; Kula, D.; Owczarek, B.; Orwat, F.; Międzybrodzki, R.; Neuberg, J.; Bagińska, N.; Weber-dąbrowska, B.; Górski, A. Factors determining phage stability/activity: challenges in practical phage application Ewa. *Expert Rev. Anti. Infect. Ther.* **2019**, *0*, 1, doi:10.1080/14787210.2019.1646126.

61. Lopes, J.L.S.; Yoneda, J.S.; Martins, J.M.; DeMarco, R.; Jameson, D.M.; Castro, A.M.; Bossolan, N.R.S.; Wallace, B.A.; Araujo, A.P.U. Environmental factors modulating the stability and enzymatic activity of the petrotoga mobilis esterase (PmEst). *PLoS One* **2016**, *11*, 1–16, doi:10.1371/journal.pone.0158146.

62. Malik, D.J.; Sokolov, I.J.; Vinner, G.K.; Mancuso, F.; Cinquerrui, S.; Vladisavljevic, G.T.; Clokie, M.R.J.; Garton, N.J.; Stapley, A.G.F.; Kirpichnikova, A. Formulation, stabilisation and encapsulation of bacteriophage for phage therapy. *Adv. Colloid Interface Sci.* **2017**, *249*, 100–133, doi:10.1016/j.cis.2017.05.014.

63. Puapermpoonsiri, U.; Ford, S.J.; van der Walle, C.F. Stabilization of bacteriophage during freeze drying. *Int. J. Pharm.* **2010**, *389*, 168–175, doi:10.1016/j.ijpharm.2010.01.034.

64. Duyvejonck, H.; Merabishvili, M.; Vaneechoutte, M.; de Soir, S.; Wright, R.; Friman, V.P.; Verbeken, G.; De Vos, D.; Pirnay, J.P.; Van Mechelen, E.; et al. Evaluation of the stability of bacteriophages in different solutions suitable for the production of magistral preparations in Belgium. *Viruses* **2021**, *13*, 1–11, doi:10.3390/v13050865.

65. Rosner, D.; Clark, J. Formulations for bacteriophage therapy and the potential uses of immobilization. *Pharmaceuticals* **2021**, *14*, doi:10.3390/ph14040359.

Chapter 3: Isolation and Characterization of the *Acadevirus* Members BigMira and MidiMira Infecting a Highly Pathogenic *Proteus mirabilis* Strain

Jéssica Duarte da Silva [1], Lene Bens [2], Adriele J. do Carmo Santos [1], Rob Lavigne [2], José Soares [1], Luís D. R. Melo [3,4], Marta Vallino [5], Roberto Sousa Dias [6], Zuzanna Drulis-Kawa [7], Sérgio Oliveira de Paula [16] and Jeroen Wagemans [2,*].

[1] Laboratory of Molecular Immunovirology, Department of Microbiology, Federal University of Viçosa, Viçosa 36570-900, MG, Brazil;

[2] Laboratory of Gene Technology, Department of Biosystems, Division of Animal and Human Health Engineering, KU Leuven, 3000 Leuven, Belgium;

[3] Centre of Biological Engineering, University of Minho, 4710-057 Braga, Portugal;

[4] LABBELS – Associate Laboratory, 4710-057, Braga, Guimarães, Portugal

[5] Institute for Sustainable Plant Protection, National Research Council of Italy, 10135 Torino, Italy; [6] Department of General Biology, Federal University of Viçosa, Viçosa 36570-900, MG, Brazil;

[7] Department of Pathogen Biology and Immunology, University of Wroclaw, 50-335 Wroclaw, Poland;

*****Correspondence: jeroen.wagemans@kuleuven.be

Abstract: *Proteus mirabilis* is an opportunistic pathogen and is responsible for more than 40% of all cases of catheter-associated urinary tract infections (CAUTIs). Healthcare-associated infections have been aggravated by the constant emergence of antibiotic-resistant bacterial strains. Because of this, the use of phages to combat bacterial infections gained renewed interest. In this study, we describe the biological and genomic features of two *P. mirabilis* phages, named BigMira and MidiMira. These phages belong to the *Acadevirus* genus (family *Autographiviridae*). BigMira and MidiMira are highly similar, differing only in four missense mutations in their phage tail fiber. These mutations are sufficient to impact the phages' depolymerase activity. Subsequently, the comparative genomic analysis of ten clinical *P. mirabilis* strains revealed differences in their antibiotic resistance profiles and lipopolysaccharide locus, with the latter potentially explaining the host range data of the phages. The massive presence of antimicrobial resistance genes, especially in the phages' isolation strain *P. mirabilis* MCS, highlights the challenges in treating infections caused by multidrug-resistant bacteria. The findings reinforce BigMira and MidiMira phages as candidates for phage therapy purposes.

Keywords: Podoviruses. *Acadevirus.* Depolymerases. CAUTI. *Proteus mirabilis*

1. Introduction

Proteus mirabilis is a Gram-negative opportunistic pathogen, well known as one of the major causes of catheter-associated urinary tract infections (CAUTIs), and a common cause of secondary bloodstream and healthcare-related infections [1–3]. *P. mirabilis* is also routinely isolated from extra-intestinal infections, such as wounds; eye, nose, and skin meningoencephalitis; and osteomyelitis [4–6]. The pathogenicity of this bacterium is associated with its remarkable swarming capacity, combined with the production of adhesive virulence factors, pili, and fimbriae, resulting in the formation of robust translucent biofilms in catheter devices (which can cause encrustations and even block the flow of urine). Moreover, *P. mirabilis* produces ureases that hydrolyze urea into ammonia and carbon dioxide, a process that favors the development of infection-induced stones [1,6,7]. More and more *P. mirabilis* strains resistant to antibiotics commonly used to treat urinary tract infections, such as fluoroquinolones, aminoglycosides, and even extended-spectrum β-lactamases, are being isolated, thereby raising concerns about infections caused by this organism [3–7].

The use of phages, viruses that infect bacteria, to combat bacterial infections has been widely explored since their discovery at the beginning of the 20th century [8,9]. This strategy, called phage therapy, began with great success but lost its appeal due to inconsistencies in treatments (mainly related to the lack of knowledge about viral infectious mechanisms) and with the establishment of antibiotics as a cheap and effective treatment [9–11]. However, the evolutionary pressure of antibiotics, combined with their overuse, has resulted in an alarming rise of antibiotic-resistant strains, which have become a worldwide source of concern and are leading to an antimicrobial resistance (AMR) crisis [12–14]. The COVID-19 pandemic has elevated this problem to a new level, as evidenced by the last reports of the US Center for Disease Control and Prevention (CDC) and the Pan American Health Organization (PAHO) [14,15,16]. These reports found an alarming rise in the incidence of Gram-negative AMR bacteria, including carbapenem-resistant *Acinetobacter*, extended-spectrum beta-lactamase (ESBL)-producing Enterobacterales, and carbapenem-resistant Enterobacterales, and describe a high level of antibiotic prescription to patients with COVID-19, despite the relatively low proportion of patients who actually developed secondary bacterial infections. The latter is thought to be primarily responsible for an increase of 15% in mortality and resistant hospital-onset infections in 2020 [14,16–18]. Agencies such as the World Health Organization (WHO) invest significant resources in initiatives that aim to bring solutions to the antimicrobial

resistance crisis [13,17], and phage therapy is considered again an alternative for the treatment of bacterial infections.

The use of lytic phages to treat bacterial infections has various advantages, including host specificity, low toxicity, fast isolation of specific phages, potentially low production costs, and the irremediable death of the host at the end of the infection cycle [19–21]. Despite this, the general narrow host range and the possible emergence of resistance to phages by the bacterial population are challenges to be overcome. A well-known approach to addressing these problems is the use of phage cocktails, which can infect multiple bacterial strains and decrease the development of resistance mechanisms [22–24].

Although countries like Belgium, Georgia, Poland, and Russia already have specific regulations for phage therapy, and others like the United Kingdom, France, and the United States are moving in this direction, the lack of laws that regulate the use of phages around the world is also a factor that hinders the wide spread of this approach, especially when the objective is recurrent use and not a therapy of last resort [25–27]. For this reason, the global phage scientific community is committed to the establishment of high-quality clinical trials, such as PhagoBurn, or multidisciplinary approaches, such as the PHAGEFORCE study, to create solid and accurate data about the safety and efficacy of phage therapy [28–30]. Systematic reviews are additionally being developed in order to organize and assign statistical significance to previous non-standardized clinical studies and case reports that have been published [31,32]. Because of this, new studies demonstrating the efficacy of phage therapy, the isolation and characterization of novel phages, and, consequently, the advancement of knowledge of these viruses are essential steps for phage therapy to be considered as a safe and beneficial approach for treating bacterial infections.

This work aimed to characterize biologically and genomically the *Proteus* phages BigMira-UFV01 and MidiMira-UFV02, isolated against the super-resistant clinical strain *Proteus mirabilis* MCS, and to assess their potential as phage therapy agents.

2. Materials and Methods

2.1. Phage Isolation, Propagation, and Purification

Phages BigMira-UFV01 and MidiMira-UFV02 (called BigMira and MidiMira) were isolated from aqueous samples from a swine farmer located in the city of Viçosa (Minas Gerais, Brazil) using a protocol adapted from Van Twest and Kropinski (2009) [33]. Briefly,

the liquid sample was repeatedly centrifuged at 10,000 g for 15 min, until no visible particles remained in the supernatant, and then filtered through 0.45 µm and 0.22 µm filters. Then, 10 mL of the filtered supernatant was added to the same volume of 2X lysogeny broth (LB) medium. Isolation host *P. mirabilis* MCS, isolated from a chronic wound of a diabetic patient, was grown to the exponential growth phase and added to the mixture (100 µL), followed by overnight incubation at 37 °C, while shaking (100 rpm). After the incubation, a double agar overlay assay was performed [33]. The lysis plaques resulting from this process that showed a distinct morphology were picked from the agar and propagated independently in LB medium containing the host. This process was repeated at least five times. When phages were considered pure, they were concentrated and purified by PEG precipitation [34]. Hence, 20 mL of a solution of 25% (*p*/*v*) PEG8000 was added to 30 mL of the previously filtered and pure phage supernatant, reaching a final concentration of 10% PEG. The mixture was kept at 4 °C overnight, under agitation of 100 rpm, and then centrifuged at 12,000 g for 30 min. The supernatant was discarded, and the pellet was resuspended in 400 µL of phage buffer.

2.2. Biological Features

2.2.1. Lysis Plaque Measurements

The diameters of fifteen lysis plaques resulting from the BigMira infections and fifteen lysis plaques resulting from the MidiMira infections were measured using the software ImageJ (https://imagej.net/ij/ (accessed on 21/08/2023)) [35].

2.2.2. Transmission Electron Microscopy (TEM)

TEM micrographs were obtained following the protocol described by Vallino et al. (2021) [36]. Briefly, 10 µL of purified phage stock (about 10^9 PFU/mL) was dropped onto a carbon/Formvar-coated grid and set aside for three minutes. Uranyl acetate (0.5% *w*/*v*) was used for negative staining. Observations and image acquisition were performed using an 80 kV CM 10 electron microscope (Philips, Eindhoven, The Netherlands).

2.2.3. Host Range

The host range of BigMira and MidiMira was determined both by spot and killing assays. Briefly, a panel of clinical *P. mirabilis* strains (Table 1) was incubated overnight in LB medium, without agitation, at 37 °C. An aliquot of 700 µL of grown bacteria was mixed with 5 mL of LB top agar (0.7%) and poured into a Petri dish containing LB bottom agar (1.5%). After solidification, 5 µL of the phage stock (about $5x10^6$ PFU/mL) was dropped on the

bacterial lawn. The absence of bacterial growth where the phage suspensions were dropped confirmed that the bacterial strain was a phage host. By way of comparison, the *Proteus* phage vB_PmiP_Pm5460 [37] was also tested against the clinical *P. mirabilis* panel. The phage-killing curves were constructed by taking consecutive OD_{600} absorbance measurements every 15 min, for 24 h. Briefly, 10 µL of BigMira and MidiMira (final concentration of 10^8 PFU/mL) was added to 190 µL of freshly grown *P. mirabilis* strains (OD_{600} of 0.1) in a 96-well plate. The experiment was performed in triplicate and repeated in three biological replicates. The bacterial growth curves (with and without phages) were compared to identify differences between the growth curves.

Table 1. Host range and *Proteus mirabilis* clinical strains. The phages BigMira and MidiMira were only able to infect their isolation host strain *P. mirabilis MCS*. +: infection, -: no infection.

Host Strain	BigMira	MidiMira
Proteus mirabilis 074	-	-
Proteus mirabilis 082	-	-
Proteus mirabilis 114	-	-
Proteus mirabilis 129	-	-
Proteus mirabilis 159	-	-
Proteus mirabilis 163	-	-
Proteus mirabilis 195	-	-
Proteus mirabilis 204	-	-
Proteus mirabilis 218	-	-
Proteus mirabilis MCS	+	+
Proteus mirabilis 5460	-	-

2.2.4. One-Step Growth Curve

A one-step growth curve was performed to determine the infection behavior (latency time and burst size) of BigMira and MidiMira. Phages were added to 4 mL of the host *P. mirabilis* MCS, in the early exponential phase (OD_{600} = 0.4; about 10^8 CFU/mL) at a final concentration of 10^3 PFU/mL, to obtain a multiplicity of infection (MOI) of 0.00001. A first sample (100 µL) was collected to determine the titer of phages at the beginning of the experiment. The phage/host mixture was incubated for five minutes, at 37 °C and then centrifuged for eight minutes at 6000 g. The supernatant was discarded together with the unabsorbed phages, after which the pellet was gently washed and resuspended in 5 mL of LB. Samples were collected in intervals of 5 or 10 min over one hour, and the phage titer was immediately quantified by double-layer agar assay. The experiment was performed in three biological replicates. The burst size was calculated as follows: burst size = average of first phage peak (PFU/mL)/average of the initial phage titer.

2.2.5. Phage Stability

The stability of the BigMira and MidiMira phages was measured under different conditions. For thermal stability, five temperatures were evaluated (−80, −20, 4, 37, and 55 °C). The phages (final concentration of 10^8 PFU/mL) were diluted in phage buffer (10 mM Tris.HCl; 10 mM $MgSO_4$; 150 mM NaCl; pH 7.5) and kept for 48 h at the tested temperatures. For pH stability, several pH values were tested (3, 4, 6, 7, 9, 11, 12, and 13). The phages were diluted in pH buffer (150 mM KCl; 10 mM KH_2PO_4; 10 mM Na citrate; 10 mM H_3BO_3), with adjusted pH values, and kept in triplicate for 48 h at 25 °C. To evaluate the phages' stability in an environment similar to a real UTI, the phages (final concentration of 10^8 PFU/mL) were incubated at 37 °C in voided and sterile (filtered in 0.22 µm) urine. The phages were titered after 24 and 48 h, using a spot assay. The phages' propagation capacity was also tested in this condition. The phages (final concentration of 10^4 PFU/mL) and their host *P. mirabilis* MCS (final concentration of 10^8 CFU/mL) were kept at 37 °C in voided and sterile urine. The titration was performed using a spot assay after 24 h. The experiments were performed in triplicate and repeated in three biological replicates. An ANOVA two-way analysis was used to compare the average differences among the treatments (*p*-value 0.05).

2.3. Genome Analysis

2.3.1. DNA Extraction and Sequencing

The phages' DNA was extracted using the protocol described by Kot (2018) [38]. Briefly, in a 1.5 mL tube, 90 µL of phage lysate was filtered through a 0.45 µm ultrafiltration spin-column and then mixed with 10 µL of DNase I buffer and 5 U of DNase I. After 30 min of incubation (37 °C), 10 µL of 50 mM EDTA and 10 µL of 1% SDS were added for DNase I inactivation. Then, 5 µL of proteinase K was added, and the mixture was kept at 55 °C for 45 min. The viral DNA was then purified using the DNA Clean and Concentrator kit. The sequencing was performed on an Illumina MiniSeq device (San Diego, CA, USA) (2*150 bp paired reads) with a library generated with the Nextera Flex DNA library kit (Illumina).

2.3.2. Assembly and Annotation

The raw sequences of BigMira and MidiMira were assembled using default parameters of the "Assembly tool" on the Bacterial and Viral Bioinformatics Resource Center (PATRIC) (https://www.bv-brc.org/ (accessed on 21/08/2023)) [39]. The resulting contigs were annotated using the "annotation tool" on PATRIC, following the "Classic RAST pipeline" (Rapid Annotation using Subsystem Technology) (https://rast.nmpdr.org/rast.cgi (accessed on 21/08/2023)) [40], and using the PROKKA database [41]. The ORFs were manually checked, and the consensus CDSs were maintained on the fasta and GenBank files. Host promoters were predicted using Sapphire (https://sapphire.biw.kuleuven.be/ (accessed on 21/08/2023)) [42], and phage promoters were

predicted using Multiple Em for Motif Elicitation (MEME) (https://meme-suite.org/meme/tools/meme (accessed on 21/08/2023)) [43], followed by manual checking. tRNAscan_SE [44] was used to search for tRNAs, and ARNold was used to find terminators for the identification of Rho-independent terminators [45].

2.3.3. Genomic and Phylogenetic Analysis

The Viral Proteomic Tree server (Viptree) (https://www.genome.jp/viptree/ (accessed on 21/08/2023)) [46] was used to identify the proteomic similarity between BigMira and MidiMira and the reference genomes from its database. To identify the similarity of both phages with the National Center for Biotechnology Information (NCBI) database (https://blast.ncbi.nlm.nih.gov/Blast (accessed on 21/08/2023)), a comparative Megablast was performed. The start of the genomes of BigMira and MidiMira and their relatives was chosen using *Proteus* phage vB_PmiP_Pm5460 as a reference. The pairwise intergenomic distances/similarities of the genomes were calculated using VIRIDIC (http://rhea.icbm.uni-oldenburg.de/VIRIDIC/ (accessed on 21/08/2023)) [47] and then aligned using Clinker [48] to generate a gene cluster comparison. The Snippy tool from Galaxy Australia (https://usegalaxy.org.au/ (accessed on 21/08/2023)) was used to calculate putative SNPs between the BigMira and MidiMira genomes.

2.3.4. Putative Depolymerase Enzyme Search and Tertiary Structure Prediction

The search for depolymerase-like enzymes was performed using the tool Phage Depolymerase Finder [49] (Galaxy Version 0.1.0) from the Galaxy Docker Build platform (https://galaxy.bio.di.uminho.pt/ (accessed on 21/08/2023)). The proteins predicted as putative depolymerases were then submitted for sensitive sequence searching based on profile HMMs (HMMER) [50], and homology detection and structure prediction by HMM–HMM comparison (HHPRED) [51] on the MPI bioinformatics toolkit (https://toolkit.tuebingen.mpg.de/ (accessed on 21/08/2023)) [52] for an accurate search for conserved domains. The AlphaFold2 [53] pipeline was used to predict the tertiary structure of the proteins, using version 1.3.0 and the default settings.

2.4. Proteus mirabilis Clinical Strains

2.4.1. Bacterial Strains

Proteus mirabilis MCS was isolated from a pressure ulcer wound of a diabetic female patient in Brazil, who was also suffering from a chronic case of urinary tract infection. The ulcer was located on the sacral region of the patient's back and developed during a long period of hospitalization due to a severe case of COVID-19. The *P. mirabilis* clinical strains were isolated at university hospitals in Leuven (Belgium) from patients of both genders suffering from hidradenitis suppurativa, a skin

disease. *P. mirabilis* SGSC 5460 [37] was also used in this study in the host range assay. The bacterial isolates were grown in LB media at 37 °C.

2.4.2. *Proteus Mirabilis* DNA Extraction and Sequencing

The bacterial genomes were extracted using the DNeasy UltraClean Microbial Kit Handbook (Qiagen), following the protocol instructions. Illumina sequencing was performed as described for the phage genomes.

2.4.3. Genome Assembly and Annotation

The raw sequencing data of the *P. mirabilis* clinical strains were assembled using the default parameters of the "Assembly tool" on PATRIC (https://www.bv-brc.org/ (accessed on 21/08/2023)) [39]. The resulting contigs were annotated using RAST and the PROKKA database.

2.4.4. Bioinformatics Analysis

For the core genome determination, Roary [54] was run. The Core Gene Alignment files were then submitted to RAxML—maximum likelihood-based inference of large phylogenetic trees [55]. Both tools are available on the Galaxy Australia platform (https://usegalaxy.org.au/ (accessed on 21/08/2023)). The core genome alignment visualization was created using Phandango—Interactive visualization of genome phylogenies (https://jameshadfield.github.io/phandango/#/ (accessed on 21/08/2023)) [56]. The lipopolysaccharide (LPS) locus of the *P. mirabilis* clinical strains was predicted by the Subsystem Features Categories on Rast SEED Viewer (https://rast.nmpdr.org/rast.cgi (accessed on 21/08/2023)) [40], using the "Cell Wall and Capsule" category, "Gram-Negative cell wall components" subcategory, and "Lipopolysaccharide assembly" subsystem. The genes related to the LPS locus were then organized in GFF3 files and submitted on the same pipeline previously described. Finally, the analysis tool Resistance Gene Identifier (RGI) on the Comprehensive Antibiotic Resistance Database (CARD) was used to perform in silico detection of antibiotic resistance genes among the isolates used in this study.

3. Results

3.1. Phage Isolation

Two phages were isolated against the host *Proteus mirabilis* MCS, using swine farm samples. Based on the different morphologies of the lysis plaques (Figure 1A,B), the phages were named BigMira-UFV01 (BigMira), which presents bigger lysis plaques (average diameter of 26.85 ± 1.81 mm) surrounded by halos (99.83 ± 6.9 mm), and MidiMira-UFV02 (MidiMira), which possesses smaller (average diameter of 12.66 ± 1.5 mm) but still clear lysis plaques without halos.

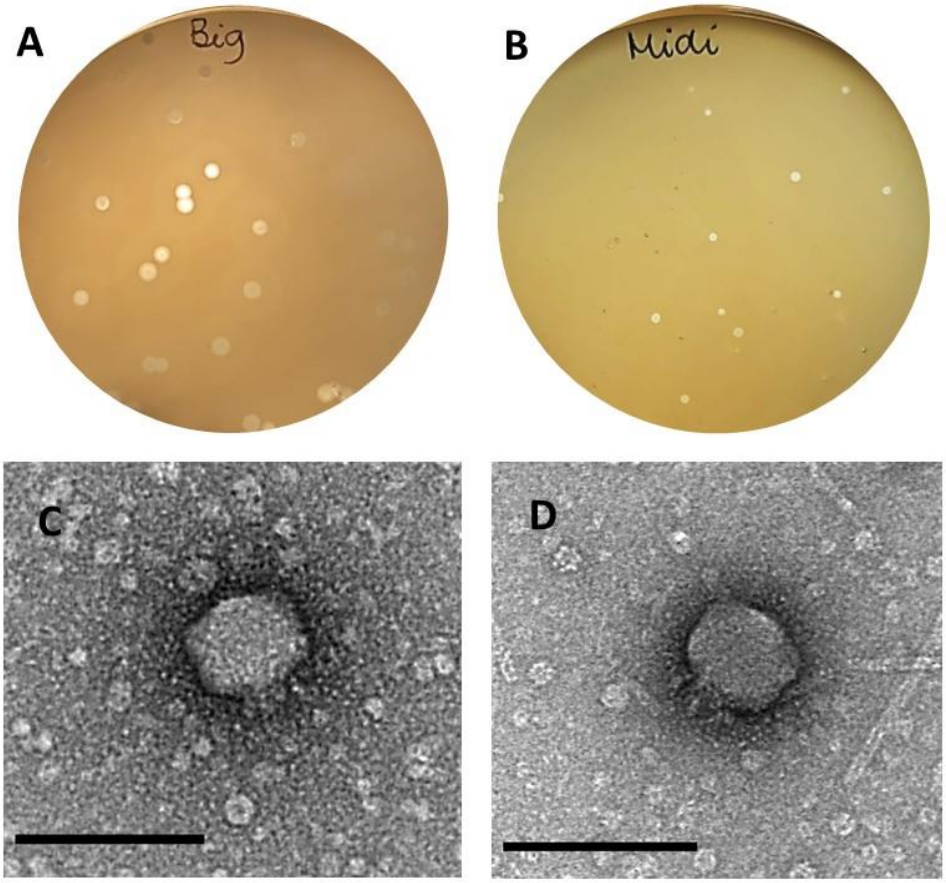

Figure 1. Lysis plaques and TEM morphology. (**A**) BigMira plaque morphology. The larger plaques are surrounded by halos. (**B**) MidiMira plaque morphology. The plaques are smaller compared to BigMira plaques, but still very clear through the plates, without halos, even after several days of incubation. (**C**,**D**) Transmission electronic microscopy (TEM) of BigMira and MidiMira viral particles. Both present the same podovirus morphology; bar = 100 nm.

3.2. Biological Features

The micrographs obtained by TEM showed that both phages BigMira (Figure 1C) and MidiMira (Figure 1D) possess the morphology typical of podoviruses, characterized by an icosahedral capsid and a short tail. Also, as confirmed both by spot and killing assays, BigMira and MidiMira were only able to infect their specific isolation host strain MCS. The results are summarized in Table 1.

A one-step growth curve analysis (Figure 2A and 2D) shows that both BigMira and MidiMira have a latent period of approximately 15 min. The estimated burst size was 13 phage particles per infected cell (p.p/i.c) for BigMira and 39 p.p/i.c for MidiMira.

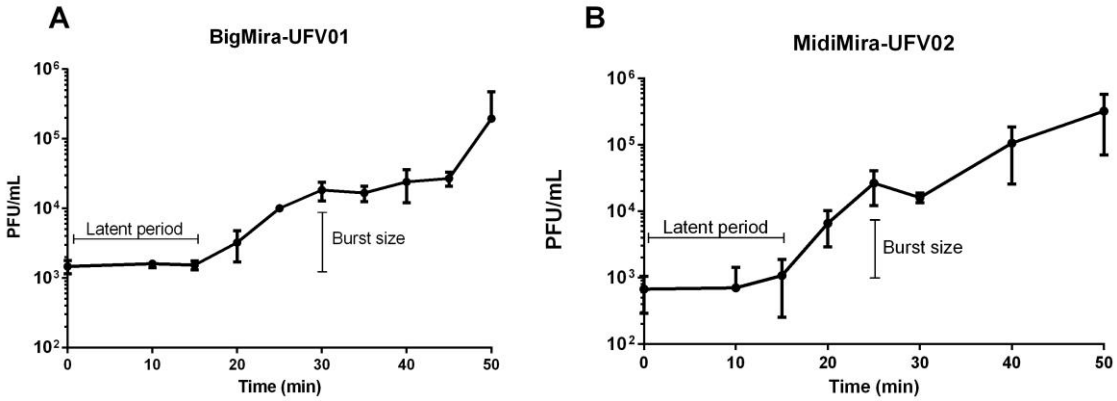

Figure 2. One-step growth curves. The initial phage titer was 10^3 PFU/mL. (**A**) BigMira one-step growth curve. The calculated latent period was 15 min, and the burst size was 13 phage particles per infected cell (p.p/i.c). (**B**) MidiMira one-step growth curve. For this phage, the latent period was also approximately 15 min, and the calculated burst size was 39 phage particles per infected cell (p.p/i.c).

The phages' thermal stability was measured after 24 and 48 h of treatment at temperatures of −80, −20, 4, 37, and 55 °C (Figure 3). For both phages, no viral particles were detected after 24 h incubation at 55 °C. The incubation time (24 or 48 h) at remaining temperatures did not alter the viral stability under the tested conditions. Also, BigMira showed a discrete (one order decrease) yet significant (p-value ≤ 0.05) viral titer alteration at −80, −20, and 4 °C when compared to the 37 °C sample.

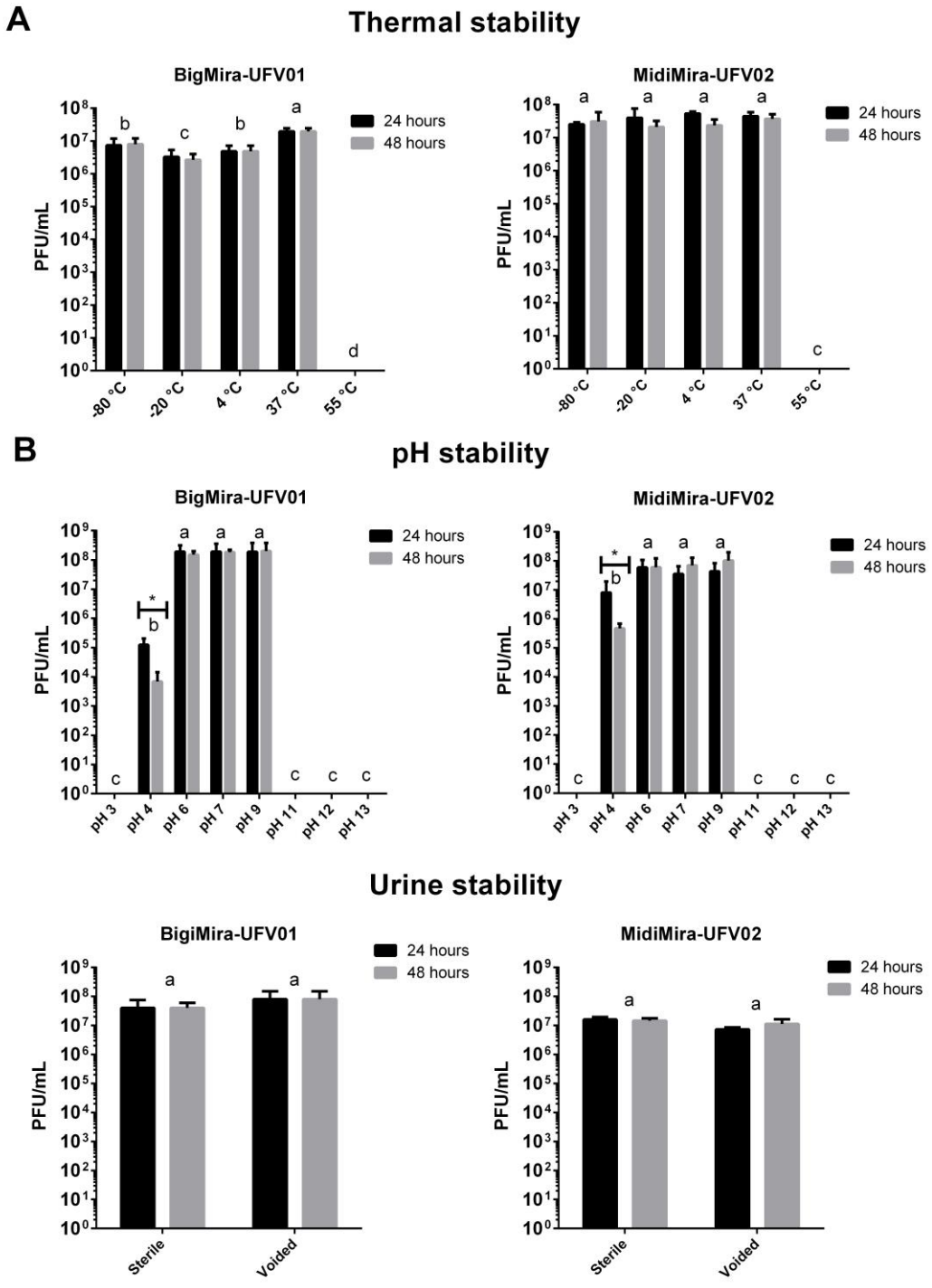

Figure 3. BigMira and MidiMira stability. To perform the statistical analysis, the phage titer was normalized using the Log10 baseline, but the graphics show the original titer (PFU/mL). (**A**) Phages' thermal stability. Conditions with different letters present significant differences (p-value ≤ 0.05) in the phage titer. (**B**) Phages' pH stability. (**C**) Phages' urine stability. Conditions with different letters present significant differences (p-value ≤ 0.05) in the phage titer. The values with asterisks present a significant difference in phage titer based on the incubation time.

The phages' stability at different pH values was measured after 24 and 48 h of incubation. BigMira and MidiMira did not differ from each other in stability. In both cases, no significant variations in viral titer were found when the phages were incubated at a pH of 6, 7, or 9. On the other hand, no viral particles were detected when the phages were kept at pH values of 3, 11, 12, and 13. Furthermore, the only scenario where the incubation time showed a significant difference (*p*-value 0.05) was at pH 4, where fewer phage particles were detected after 48 h of incubation than after 24 h. In terms of stability in urine, the results indicate that the phages maintained their titers even after 48 h of incubation at 37 °C and the fact that the urine was sterile or voided had no effect on the viral stability. The phages were also able to infect their host *P. mirabilis* MCS and propagate normally in urine (Figure S2).

3.3. Genomic Features

The BigMira and MidiMira sequencing results revealed that both phages have a dsDNA genome of 43,026 bp with a GC content of 39.4%. They contain 52 open reading frames (ORFs) and no predicted tRNAs. None of the predicted ORFs encode lysogeny-associated proteins, allowing the classification of these phages as virulent.

A search for related phages using BLASTn showed that BigMira and MidiMira present more than 95% identity with *Proteus* phages PM 116 (NC_047858), PM 93 (NC_027390), PM 85 (NC_027379), and vB_PmiP_Pm5460 (NC_28916). All these phages belong to the same *Acadevirus* genus within the *Molineuxvirinae* subfamily and *Autographiviridae* family. The *Citrobacter* phage vB_CroP_CrRp3 (NC_047920), the next closest neighbor, only showed 75.65% identity and belongs to another genus, *Vectrevirus*. A proteome analysis using the Viptree database confirmed that the *Proteus* phages form a distinct clade (Figure 4A).

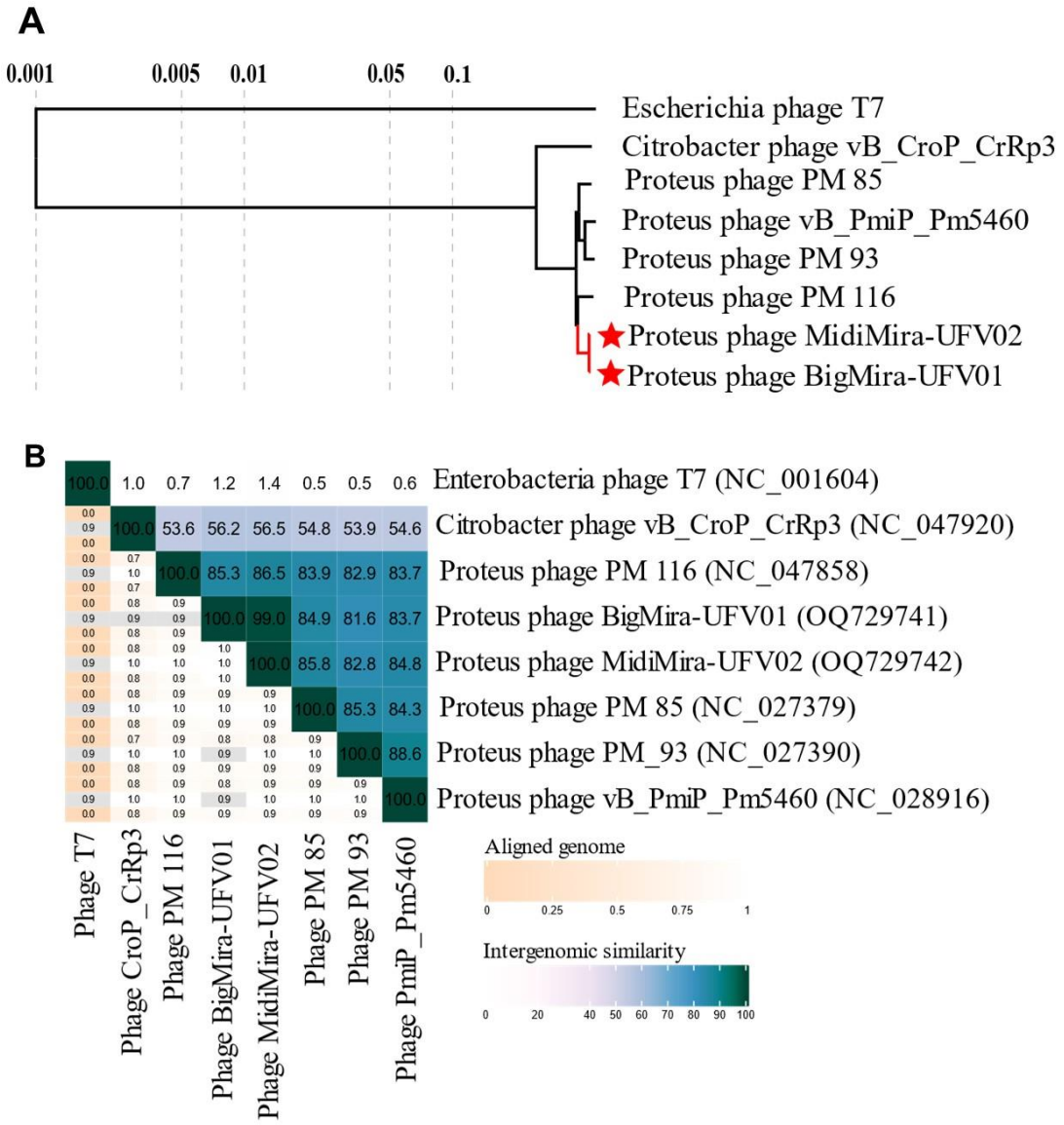

Figure 4. Acadevirus phylogeny. (**A**) Phylogenetic tree created only with the closest genomes ($S_G \geq 0.8$) to BigMira and MidiMira. Acadeviruses form an independent clade. *Citrobacter* phage vB_CroP_CrRp3 was used as a related phage, but from a different genus, and the phage T7 (NC_001604) was used as an outgroup. (**B**) VIRIDIC heatmap showing the intergenomic distance among the related phages. Phages with more than 95% similarity belong to the same species, and with phages more than 70% similarity belong to the same genus.

The intergenomic distance between the related phages calculated by VIRIDIC indicates that BigMira and MidiMira share 99% similarity and belong to the same species. The phages also share more than 70% intergenomic similarity with PM 116, PM 93, PM 85, and Pm5460, indicating that they are members of the same genus, but of a different species (Figure 4C). The main features of the different phages within the genus *Acadevirus* are summarized in Table 2. All of them had been isolated from *Proteus mirabilis* strains and have similar G+C content and genome length. Other biological characteristics, such as their burst

sizes, exhibit higher variances. As shown in Table 1, BigMira and MidiMira were also evaluated for their ability to infect the host strain of *Acadevirus* Pm5460, namely *P. mirabilis* 5460. However, it could not infect this strain. Phage Pm5460, on the other hand, could also not infect *P. mirabilis* MCS, the host strain of BigMira and MidiMira, indicating a narrow host range for these types of viruses, which was also observed for PM 85, PM 93, and PM 116 (Table 2).

Table 2. General features of the *Acadevirus* members, present within the NCBI database.

Proteus Phage	**Host Range (*Proteus* spp.)**	**Burst Size**	**Genome Length (bp)**	**G+C Content (%)**	**Putative CDSs**
PM 85 [57]	3/30	18	43,642	39.3	47
PM 93 [57]	2/30	75	45,169	39.4	48
PM 116 [57]	2/30	70	44,601	39.2	53
Pm 5460 [37]	16/26	46	44,573	39.6	56
BigMira	1/11	13	43,026	39.4	52
MidiMira	1/11	39	43,026	39.4	52

An alignment of BigMira and MidiMira and their relatives (Figure 5B) demonstrates the similarity between their genome architectures. The early gene module, although relatively well conserved within the genus, appears to be unique for *Acadevirus* phages. A BLASTn analysis showed that these early genes, particularly those encoding hypothetical proteins, had no similarity with phages from other genera. The general genome organization of these phages is typical for the *Autographiviridae* family, and except for the last two proteins, the ORFs are highly conserved. Due to the extensive sequence similarity between BigMira and MidiMira, only the BigMira genomic map is depicted in Figure 5A.

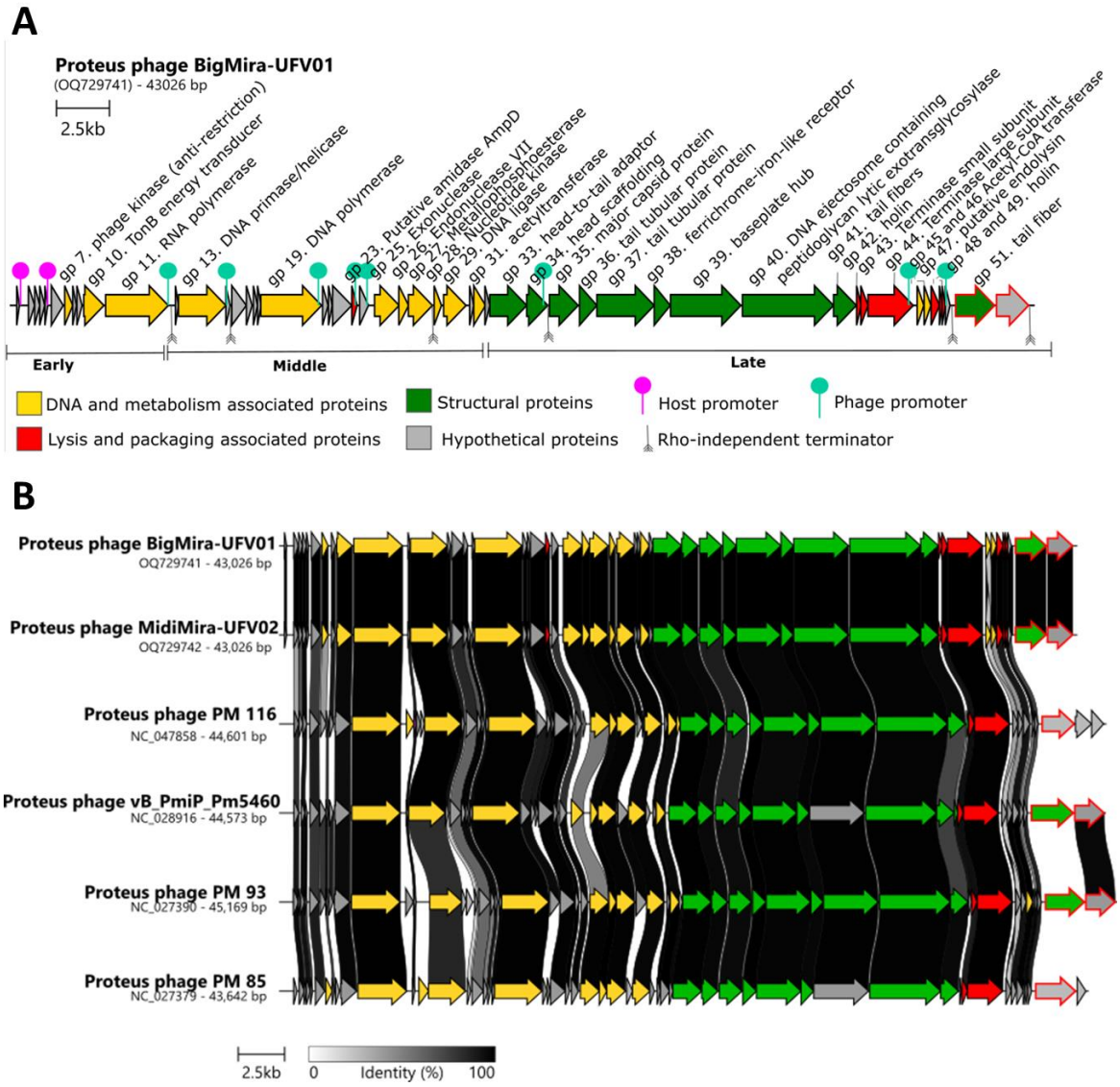

Figure 5. Genomic map of *Proteus* phage BigMira-UFV01 and alignment of the phages belonging to the genus *Acadevirus*. (**A**) Genomic map of *Proteus* phage BigMira. Each arrow represents an ORF, colored according to the encoded protein function: yellow—proteins associated with DNA and metabolism; green—structural proteins; red—lysis and package proteins; gray—hypothetical proteins. The ORFs contoured in red have predicted depolymerase domains. The pink pins illustrate the host-associated promoters and the green ones illustrate specific phage promoters. The Rho-independent terminators are represented by gray arrows. (**B**) Alignment of phage genomes that compose the genus *Acadevirus*. The genomes were opened using the *Proteus* phage vB_PmiP_Pm5460 as a reference. The background is colored according to the identity percentage: the blacker, the greater the identity between the ORFs. Sequences without connections do not share similarities. For the arrow colors, see the legend of Figure 5A.

3.4. Putative Depolymerase-Encoding Domain Prediction

A search for proteins with biotechnological potential revealed that all the published *Acadevirus* phages contain putative depolymerase domains. Their genes are located in the

least conserved region of the *Acadevirus* genomes. In the case of *Proteus* phages PM 116 and PM 85, only the phage tail fiber is predicted to possess depolymerase activity. For BigMira, MidiMira, Pm5460, and PM 93, the predicted domains can be found in two proteins, the phage tail fiber (gp51) and the hypothetical protein located immediately downstream (gp52). A promoter prediction shows that the promoters on the BigMira/MidiMira genomes are located at the same sites as those in *Proteus* phage vB_PmiP_Pm5460 and that in both cases, the expression of the proteins with depolymerase domains is controlled by an individual promoter. The Rho-independent terminators are also located in the same regions.

Given the high similarity between the viral genomes (same length, ORFs, and organization), but a different plaque morphology, a single-nucleotide polymorphism (SNP) analysis was performed to search for mutations that could explain the differences between the phages. The results are summarized in Table 3.

Table 3. Single nucleotide polymorphisms (SNPs) identified between the phages BigMira and MidiMira leading to non-synonymous mutations**.**

BigMira-UFV01			**MidiMira-UFV02**			**Nucleotide Position**	**Altered Protein**
Nucleo-tide	**Amino Acid**	**Classification**	**Nucleo-tide**	**Amino Acid**	**Classification**		
A	Y (Tyrosine)	Hydrophobic aromatic	G	C (Cysteine)	Hydrophilic uncharged	40,548	Phage tail fiber (gp51)
G	G (Glycine)	Hydrophobic aliphatic	A	S (Serine)	Hydrophilic uncharged	41,135	
G	D (Aspartic acid)	Hydrophilic Acidic	A	N (Aspara-gine)	Hydrophilic uncharged	41,141	
C	F (Phenyl-alanine)	Hydrophobic aromatic	A	L (Leucine)	Hydrophobic aliphatic	41,275	

Only four SNPs leading to a non-synonymous mutation in the protein were observed, all present in the same gene, encoding the phage tail fiber Gp51, one of the predicted proteins containing a depolymerase domain (Table 3). Figure 6 displays a tertiary structure prediction of the BigMira and MidiMira phage tail fiber Gp51. The colored areas show the sites where the amino acids were changed. The substitution of a tyrosine (BigMira) for a cysteine (MidiMira) in the central monomer's beta-helical region is colored in blue. The substitution of a glycine for a serine and an aspartic acid for an asparagine happened just with six nucleotides of difference and are colored in pink and red, respectively. Finally, the replacement of phenylalanine for leucine is colored yellow. These substitutions are located on the C-terminal region of the protein. AlphaFold2 did not support the prediction of a protein trimer, often

found on phage tail fibers. Hence, the prediction of the modified regions in a model closer to the phage physiological reality was not possible.

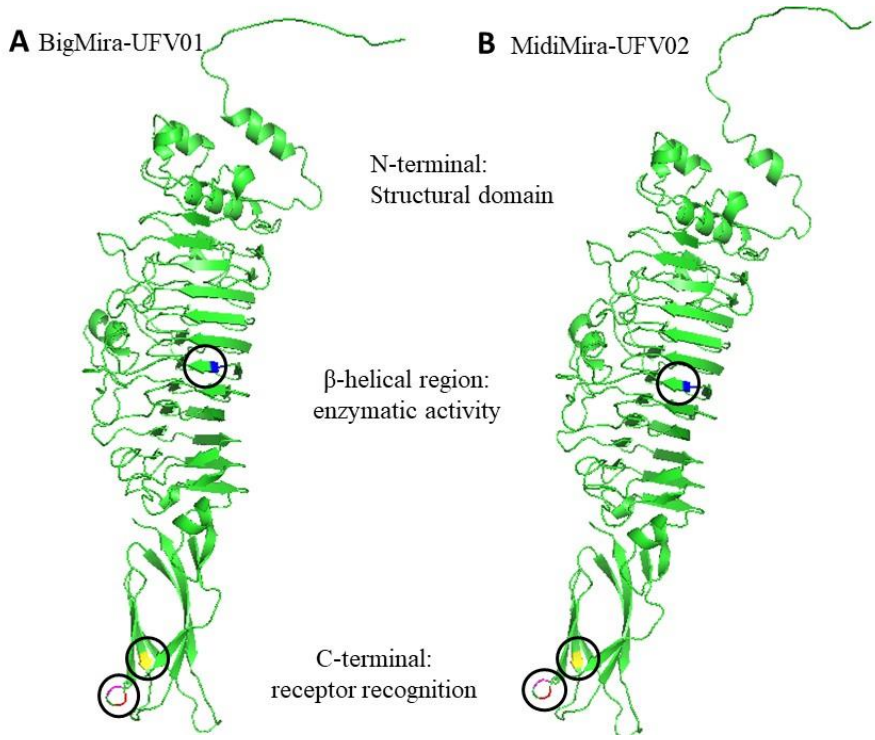

Figure 6. Phage tail fiber (gp 51) — monomer prediction**.** (**A**) BigMira-UFV01 and (**B**) MidiMira-UFV02 three-dimensional illustration of the phage tail fiber Gp52. The colored areas indicate the sites of amino acid substitution. Blue: tyrosine to cysteine (substitution A-G; nucleotide (nt) 40,548). Pink: glycine to serine (G-A; nt 41,135). Red: aspartic acid to asparagine (G-A; nt 41,141). Yellow: phenylalanine to leucine (C-A; nt 41,275).

BLASTp, HHPRED, and HMMER were used to search for conserved domains or distant homologies that could assign a function to the hypothetical protein Gp52. While no similarities were found using BLASTp or HMMER, the HHPRED results (more than 50 hits with high similarity) indicated that the protein may be classified as a tail spike with a hydrolase or lyase activity. AlphaFold2 was used to predict the 3D structure of a Gp52 monomer (Figure S1A) and trimer (Figure S1B). However, due to the lack of similarity of this protein with other proteins in the AlphaFold database, although the prediction suggested a common depolymerase RBP structure, the resulting prediction had low quality and failed to present the correct folding of several regions of the protein, including its catalytic site.

3.5. Proteus Mirabilis Clinical Strain Genomic Analysis

The pan-genome analysis of all used *P. mirabilis* clinical strains is shown in Figure 7A. The genome profile of the phages' host *P. mirabilis* MCS is most similar to that of the Belgian strain *P. mirabilis* 082. Next, we investigated the LPS locus, since LPS is most likely

the primary receptor of the acadeviruses' receptor-binding protein (RBP), with its enzymatic activity enabling the start of the infection process. Interestingly, when only considering the LPS locus (Figure 7B), *P. mirabilis* MCS does not cluster with other clinical isolates, demonstrating that the LPS composition of this strain is unique and may be significantly different from the others, thereby potentially explaining the observed narrow host range.

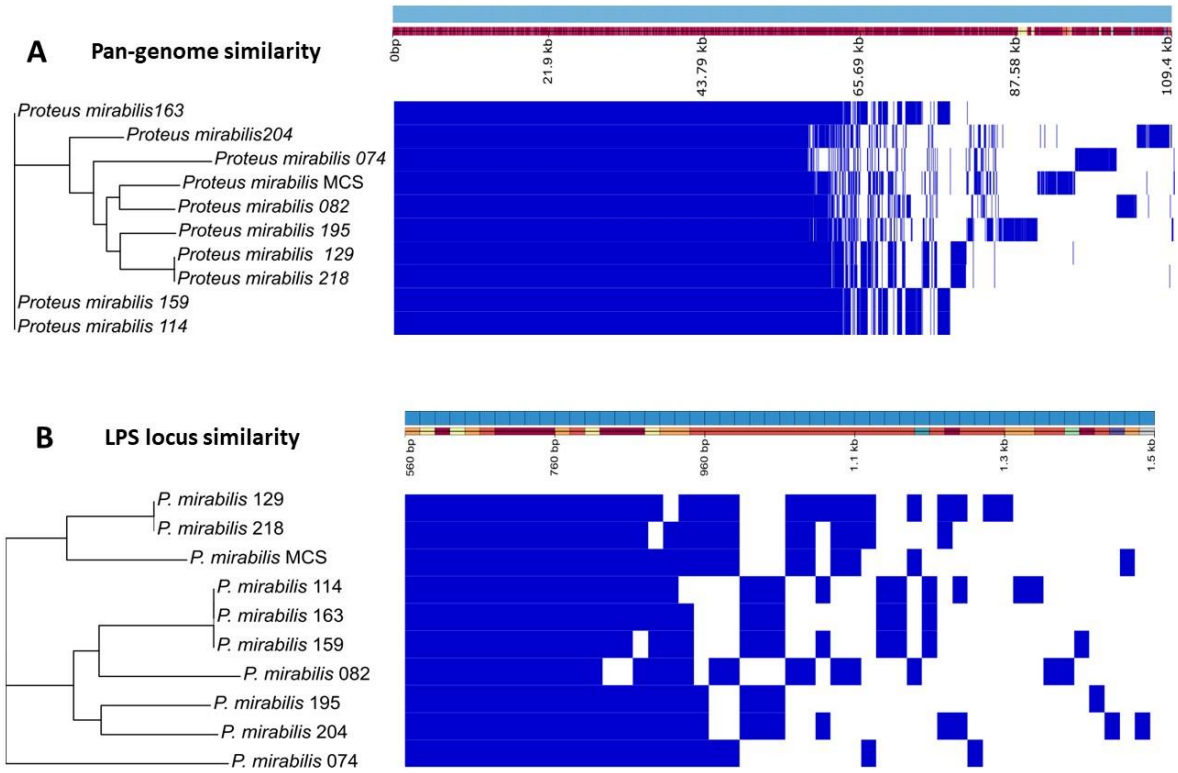

Figure 7. Pan-genome and LPS locus similarity of the *P. mirabilis* clinical strains.

Still aiming to explore the differences and similarities among the clinical strains of *P. mirabilis*, the antibiotic resistance genes of each isolate were identified (Table 4). The genes *kpnH*, *gyrB*, *rsmA*, *catA4*, and *crp* are considered core genes that are found in all isolates, except for *crp*, which is missing in *P. mirabilis* 218. *kpnH*, *rsmA*, and *crp* are related to multidrug efflux pumps, while *gyrB* is important for the quinolone resistance mechanism and *catA4* is important for chloramphenicol resistance. The strains *P. mirabilis* 074, *P. mirabilis* 082, *P. mirabilis* 129, and *P. mirabilis* 218 possess just the genes *qnrD1*, *tetQ*, and $bla_{\text{TEM-2}}$ in addition to the core ones, respectively. *P. mirabilis* 114, *P. mirabilis* 159, and *P. mirabilis* 163 present the same resistance profile and share the genes *vat* and *dfrA1*. Beyond the previous genes, *P. mirabilis* 195 also possesses the genes *aadA* and *catII*.

Table 4. Antimicrobial resistance (AMR) gene profile of the clinical *P. mirabilis* isolates.

Bacterial Strain	Number of AMR Genes	Gene Name	Antimicrobial Class
P. mirabilis MCS	12	*sulI*	sulfonamides
		catA2	chloramphenicol
		vat	streptogramins
		dfrA1	diaminopyramidines
		qacEdelta1	antiseptics
		tetQ	tetracyclines
		tetA	
		bla$_{\text{OXA-9}}$	β-lactams
		bla$_{\text{CTX-M-2}}$	
		aac(6')-Iq	aminoglycosides
		aac(6')-Ib'	
		aadA	
P. mirabilis 204	8	*sulI*	sulfonamides
		tetA	tetracyclines
		bla$_{\text{TEM-135}}$	β-lactams
		aadA	aminoglycosides
		aadA2	
		aph(3')-Ia	
		aph(6)-Id	
		aph(3'')-Ib	
P. mirabilis 195	4	*catII*	chloramphenicol
		vat	streptogramins
		dfrA1	diaminopyramidines
		aadA	aminoglycosides
P. mirabilis 114	2	*vat*	streptogramins
P. mirabilis 159		*dfrA1*	diaminopyramidines
P. mirabilis 163			
P. mirabilis 074	1	*qnrD1*	fluoroquinolones
P. mirabilis 082	1	*tetQ*	tetracyclines
P. mirabilis 129	1	*bla*$_{\text{TEM-2}}$	β-lactams
P. mirabilis 218	1	*bla*$_{\text{TEM-2}}$	β-lactams
Core genes: *crp*, *kpnH*, *gyrB*, *rsmA*, and *catA4*			multidrug efflux pump, quinolones, chloramphenicol

The strain *P. mirabilis* 204 possesses more than eight genes on top of the core resistome that confer resistance against four different classes of antibiotics: aminoglycosides—*aadA*, *aadA2*, *aph(3')-Ia*, *aph(6)-Id aph(3")-lb*; tetracyclines—*tetA*; β-lactams—$bla_{\text{TEM-135}}$; and sulfonamides—*sulI*, presenting a high antimicrobial resistance profile.

The most remarkable antimicrobial resistance profile among the evaluated isolates was found for *P. mirabilis* MCS, the host strain of BigMira and MidiMira, with 17 resistance genes being identified. Five are considered core genes, and the others confer resistance to eight distinct classes of antibiotics: tetracyclines—*tetA*, *tetQ*; aminoglycosides—*aac(6')-Iq*, *aac(6')-Ib'*, *aadA*; diaminopyramidines—*dfrA1*; β-lactams—$bla_{\text{OXA-9}}$, $bla_{\text{CTX-M-2}}$; streptogramins—*vat*; chloramphenicol—*catA2*; sulfonamides—*sul1*; and the gene *qacEdeltal* which confers resistance to disinfecting agents and antiseptics, such as ethidium bromide.

4. Discussion

Catheter-associated urinary tract infections (CAUTIs) are a common and serious healthcare-associated issue. Among the microorganisms that cause CAUTIs, *Proteus mirabilis* is one of the major pathogens, responsible for up to 40% of all cases [2,6,7,37]. *P. mirabilis* is known for its ability to form crystalline biofilms in catheter devices, leading to encrustations and blockage of the flow of urine, and for producing ureases that can promote the formation of stones in the urinary tract, cystitis, pyelonephritis, and difficult-to-treat infections [1,6,58,59]. The emergence of *P. mirabilis* strains resistant to different antibiotic classes worsens the problems caused by this organism. Unfortunately, the acquisition of antibiotic resistance genes has not only occurred with *P. mirabilis*, and over the years, this problem has become more unmanageable. The enormous number of hospitalizations and antibiotics ingested during the COVID-19 pandemic accelerated this problem, especially for Gram-negative bacteria [14,15,16,18].

This study describes the isolation and characterization of two *P. mirabilis* phages, named BigMira and MidiMira. The phages were isolated from swine farm samples, and their plaque morphology was the main criterion used to separate them. TEM revealed that both phages present a podovirus morphology, and phylogenetic analysis confirmed that they belong to the family *Autographiviridae* and the genus *Acadevirus*. Only four other phage genomes of this genus are available on NCBI: PM116, PM85, PM93 [57], and vB_PmiP_Pm5460 [37]. These genomes are also the only ones found in the taxonomic

browser of the International Committee on Taxonomy of Viruses and in the Viptree reference genome database, implying that few phages from this genus have been isolated thus far and that *Acadevirus* is a small group with highly conserved characteristics. Until 2019, *Acadevirus* members were classified as T7-like phages. After that, the family *Autographiviridae* became an independent family, containing 9 subfamilies and 52 genera, including *Acadevirus*. The genus is named after the district of Academgorodok, part of the Russian city of Novosibirsk, from which the type species *Proteus* phage PM85 was isolated [60]. However, despite the low nucleotide similarity between acadeviruses and the more prevalent teseptimaviruses (Figure 4C), they share a similar gene architecture and a distinct separation between early, middle, and late genes [61].

Morozova et al. tested 37 hosts and described the *Proteus* phages PM 85, PM 93, and PM 116 as having a narrow host range, once they were able to infect just 1–3 *P. mirabilis* strains [57]. On the other hand, Melo et al. described *Proteus* phage Pm5460 as capable of infecting almost 62% of the tested 24 *Proteus* spp. strains [37]. Although BigMira and MidiMira appear to have a narrow host range (only infecting the isolation host) (Table 1), they were tested against a smaller host strain collection compared to their relatives and were not tested against hosts from other species of the same origin as strain MCS (Table 2). Thus, further investigation is required before the phage's narrow host range can be confirmed. The one-step growth curve revealed that the *Acadevirus* phages have a latent period that ranges from 7 to 15 min and an average burst size of 43.5 phage particles per infected cell (p.p/i.c) (Table 2) [37,57]. It is important to point out that the burst size can be calculated in different ways, but we chose to use the same formula as the previous studies to enable comparison.

BigMira and MidiMira also showed similar results on the stability tests. Both phages were not able to endure a temperature of 55 °C but were stable in the other tested temperatures. Regarding pH stability, the phages do not withstand pH 3, 11, 12, and 13. pH 4 seems to be the threshold for these phages since they slowly lost stability over the 48 h of the experiment. This was the only condition where the incubation time interfered with viral stability. Even though these are the first data on *Acadevirus* stability (the previous studies did not include these trials), the findings are comparable to those obtained for other podoviruses. In general, these phages are resistant to low temperatures (including long-term storage at −80 and −20 °C) and are stable at neutral and mildly basic or acidic pHs. Temperatures above 55 °C or pH values below 4 and above 10 usually render these virus particles inactive [62–65]. Both phages also proved to be stable in environments that mimic the conditions of urinary

tract infections, and their titers remained unaltered even when incubated in voided and sterile urine for 48 h at 37 °C. They also maintained their ability to infect and propagate in their host unaltered under these conditions. The fact that the phages BigMira and MidiMira maintained their titers under different thermal, pH, and urine conditions reinforces that they can be kept for up to 48 h in non-refrigerated situations and further strengthens their candidacy as phage therapy agents.

The genomic features of BigMira and MidiMira also resemble those described for other phages of the genus *Acadevirus* (Table 2). The genome size of 43,026 bp, the G+C content of 39.4%, and the 52 predicted coding sequences (CDSs) are consistent with the genus averages of 44,006 bp, 39.38% GC content, and 51.3 ORFs, respectively [37,57]. The differences in the number of CDSs for each phage can be attributable primarily to small hypothetical proteins found in different regions of the genome. These proteins affect genomic alignment and appear to be poorly conserved since they have a low rate of similarity with other proteins found in databases such as NCBI. The active search to assign functions to these hypothetical proteins in programs such as HHPred and HMMR also ends up leading to poorly conserved domains and functions that do not fit bacteriophages. Therefore, the “hypothetical protein” annotation, with no function attribution, was maintained.

A feature observed in all the acadeviruses described until now is the presence of a translucent halo around the lysis plaques resulting from their infective process [37,57]. This halo is characteristic of the presence of depolymerase-type enzymes in the phage tail fibers [66]. The prediction of putative depolymerases (DPOs) indicated that in the case of BigMira and MidiMira, two ORFs have depolymerase-like domains, the phage tail fiber Gp51 and hypothetical protein Gp52. As shown in Figure 5, these genes are found in the least conserved region of the genome of the acadeviruses; some phages present just one putative depolymerase, and the others possess two [37,57]. Latka et al. described the architecture of depolymerase-containing receptor-binding proteins (RBPs) [67]. These proteins are usually annotated as tail fibers, tail spikes, or hypothetical proteins on NCBI [67,68]. According to these authors, phages like the podovirus G7C present two RBPs and a structural organization where a longer RBP is directly connected to the phage particle by its N-terminal anchor domain, and the second and smaller one is attached to the first RBP and does not interact with the phage particle, forming an anchor-branched complex. Based on the structural and sequence similarities, this is probably the arrangement found on the acadeviruses with two putative depolymerase enzymes [67]. In the case of BigMira and MidiMira, the phage tail

fiber Gp51 is the RBP that directly connects to the phage particle and anchors the hypothetical protein Gp52. The *Acadevirus* members with just one putative depolymerase enzyme presumably present the T7/K1F organization, the simplest one, where the phage tail fiber directly connects to the phage particle. Once the depolymerase halo is present in both acadeviruses having a single or double RBP organization, the phage tail fibers are most likely the proteins where the depolymerase enzyme actively cleaves the LPS. The second RBP, the hypothetical protein (Gp52), probably has a different enzymatic specificity. HHPred predicted this second protein as a phage tail spike that functions as a lyase/hydrolase, but HMMR prediction failed. The tertiary structure prediction also obtained low folding reliability in several regions, leading to the conclusion that this protein may have a structure uncommonly found in the available databases.

However, although the depolymerase halo is a characteristic of *Acadevirus*, phage MidiMira does not have it. This was one of the reasons why BigMira and MidiMira phages were considered distinct until the sequencing result was obtained. As these phages not only look similar, but also share the same genome size, the same G+C content, the same number of ORFs, and more than 99% sequence identity, only an SNP analysis was able to differentiate them and indicate their differences. The results showed that only four missense point mutations distinguish one phage from the other (Table 3), all occurring in the phage tail fiber Gp51. As previously discussed, this protein was predicted as having a depolymerase activity, being potentially responsible for the cleavage of LPS in the host cell wall [66,69]. These mutations not only led to a change of amino acids but also changed their interactions, since the characteristic of the amino acids generated by the mutated triplet of nucleotides is different from the original one [70], thereby potentially explaining the difference in halo formation.

Figure 6 illustrates the monomeric structure of the tail fiber Gp51 of BigMira and MidiMira. It was not possible to identify conformational alterations just by observing the predicted models, but three of the four mutations happened on the C-terminal region of the protein. They occur in a region related to the receptor recognition and/or protein trimerization of the phage tail fiber [67,69]. The substitution between amino acids with the most distinct characteristics happened in the beta-catalytic region of the enzyme. Tyrosine is a hydrophobic aromatic amino acid that can be involved in stacking and hydrogen bonding interactions. Cysteine is an uncharged hydrophilic amino acid, capable of forming disulfide bonds with other cysteines present in the protein. In fact, disulfide bonds between cysteine residues are

one of the forces that drive and stabilize proteins folding into a tertiary structure. The fact that tyrosine is a hydrophobic amino acid and cysteine is hydrophilic can lead to discrete differences in the folding of this protein, since hydrophobic groups tend to face the internal side of the protein and hydrophilic ones tend to be located on its surface. Thus, this minor alteration, strengthened by the other amino acid alterations, resulted in a change in the phage tail fiber structure and impacted its enzymatic function [70]. Mutations in the catalytic domain of an enzyme may potentially alter or inactivate the enzymatic catalytic pocket, which is a three-dimensional region, usually with a specific conformation, that contains the amino acid residues and substrates necessary for catalyzing a reaction. In the case of phage RBPs, alterations in the catalytic pocket might result in a switch of receptors, which usually incorporates extra point mutations in the C-terminal domain but still allows the phage to infect the same host [71,72].

The clinical strains of *P. mirabilis* were sequenced to find evidence that explains why BigMira and MidiMira could only infect their isolation host. Figure 7A illustrates their pan-genome composition, and Figure 7B displays the similarity between the genes just related to the LPS locus. The separation of the isolation strain *P. mirabilis* MCS into a single clade is an indication that its LPS is different from that of the other evaluated strains. Although this difference may seem discrete, phage depolymerases are extremely specific [67,69]. The pan-genome analysis indicated that the closest isolate to *P. mirabilis* MCS is *P. mirabilis* 082; however, the analysis of the LPS locus showed that they are quite different in this regard.

Finally, the prediction of antibiotic resistance genes within the genomes of the clinical isolates of *P. mirabilis* provided interesting insights for this study. *P. mirabilis* is described as naturally resistant to polymyxins and tetracyclines and susceptible to β-lactams, chloramphenicol, fluoroquinolones, and aminoglycosides [4,73,74]. Besides that, over time, more and more *P. mirabilis* strains harboring other AMR genes were isolated, such as those containing *bla*$_{\text{TEM}}$ genes, which confer resistance to the first generation of beta-lactams (such penicillin), the mutated variant of *gyrB*, which confers resistance to fluoroquinolones, and the *aac*s and *aph*s genes, which confer resistance to aminoglycosides [4,73,74]. In fact, *bla*$_{\text{TEM}}$ genes were found in three out of the ten *P. mirabilis* strains evaluated in this study. Three out of ten was also the number of strains containing aminoglycoside resistance genes, although in this case, they were present in up to five different variants, in the strains with the largest AMR gene profile (*P. mirabilis* MCS, 204, and 195). *gyrB* was considered a core gene for the isolates in this study, as it was present in all of them. However, besides the presence of the

previous genes being alarming, the genes *bla*$_{CTX}$ (which confers resistance to an extended spectrum of beta-lactamases (ESBLs)) and *bla*$_{OXA}$ (which confer resistance to carbapenems) potentially impact public health and are considered by the World Health Organization (WHO) as causing increasing concern; the antibiotics these genes confer resistance to are used for difficult-to-treat infections and the increase in bacterial strains resistant to them means a significant reduction in therapeutic alternatives [16,18]. Variants of both genes are present in *P. mirabilis* MCS, together with genes that confer resistance to sulfonamides, chloramphenicol, streptogramins, diaminopyramidines, antiseptics, tetracyclines (two), and aminoglycosides (three), besides the core genes (five), totaling seventeen AMR genes in a single bacterial isolate. As all the strains evaluated in this study originated from clinical settings, the presence of resistance genes beyond those classically described for the species is not uncommon. Even so, the resistance profile found in *P. mirabilis* MCS proved to be much more worrying than expected. This isolate not only has a large number of resistance genes, but they also confer resistance to a large range of antibiotic groups. This finding indicates that antibiotic treatment of this bacterial strain is complex and that an infection induced by it has a high potential for becoming difficult to treat. Thus, whether used in tandem with antibiotics or as part of a specific phage cocktail, the BigMira and MidiMira phages would be valuable tools for combating infections caused by the isolate *Proteus mirabilis* MCS or closely related isolates.

5. Conclusions

The use of phages to treat bacterial infections has resurfaced as an attractive alternative, and in fact, some studies already demonstrate the effectiveness of using phage cocktails to control *P. mirabilis* infections [7,37,75,76]. Phages BigMira-UFV01 and MidiMira-UFV02 belong to the genus *Acadevirus* and have characteristics that classify them as excellent candidates for phage therapy, such as the absence of lysogeny genes, good stability, and the presence of enzymes of high biotechnological interest. Although these phages produce different plaques, only four missense point mutations differentiate one from the other. The fact that these phages were isolated against a very pathogenic strain of *P. mirabilis* shows how relevant phage therapy is and how phages have the potential to become an adjunct treatment for difficult-to-treat infections.

6. Data Availability Statement

NCBI Accession numbers: *Proteus* phage BigMira-UFV01: OQ729741; *Proteus* phage MidiMira-UFV02; OQ729742; *P. mirabilis* clinical strains: BioProject ID: PRJNA979110.

7. Supplementary material

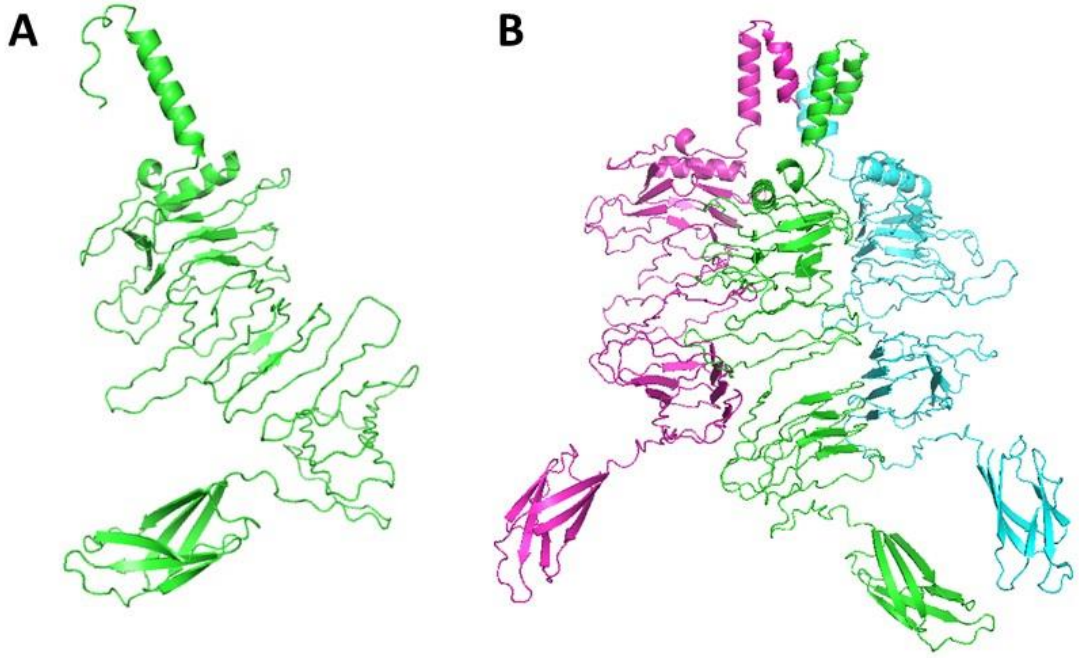

Figure S1: 3D prediction of Gp 52, a hypothetical protein. A. Monomer folding prediction. B. Trimer prediction.

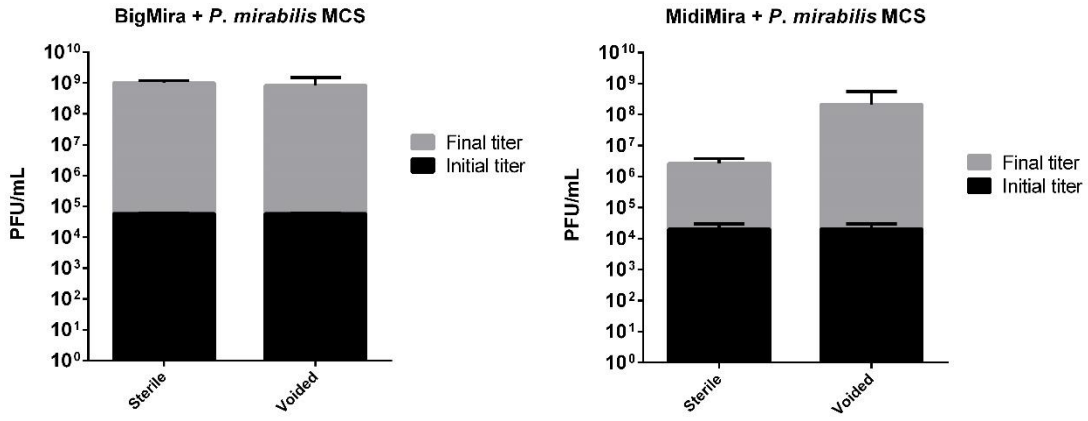

Figure S2: Phages BigMira and MidiMira propagation rate in sterile and voided urine after 24 hours of incubation.

8. References

1. Yuan: F.; Huang, Z.; Yang, T.; Wang, G.; Li, P.; Yang, B.; Li, J. Pathogenesis of Proteus mirabilis in Catheter-Associated Urinary Tract Infections. *Urol. Int.* **2021**, *105*, 354–361. https://doi.org/10.1159/000514097.
2. Werneburg, G.T. Catheter-Associated Urinary Tract Infections: Current Challenges and Future Prospects. *Res. Rep. Urol.* **2022**, *14*, 109–133. https://doi.org/10.2147/RRU.S273663.
3. Nicolle, L.E. Catheter associated urinary tract infections. *Antimicrob. Resist. Infect. Control* **2014**, *3*, 23. https://doi.org/10.1186/2047-2994-3-23.
4. Girlich, D.; Bonnin, R.A.; Dortet, L.; Naas, T. Genetics of Acquired Antibiotic Resistance Genes in Proteus spp. *Front. Microbiol.* **2020**, *11*, 256. https://doi.org/10.3389/fmicb.2020.00256.
5. Li, Z.; Peng, C.; Zhang, G.; Shen, Y.; Zhang, Y.; Liu, C.; Liu, M.; Wang, F. Prevalence and characteristics of multidrug-resistant Proteus mirabilis from broiler farms in Shandong Province, China. *Poult. Sci.* **2022**, *101*, 101710. https://doi.org/10.1016/j.psj.2022.101710.
6. Armbruster, C.E.; Mobley, H.L.T.; Pearson, M.M. Pathogenesis of Proteus mirabilis Infection. *EcoSal Plus* **2018**, *8*, 10-1128. https://doi.org/10.1128/ecosalplus.esp-0009-2017.
7. Mirzaei, A.; Wagemans, J.; Nasr Esfahani, B.; Lavigne, R.; Moghim, S. A Phage Cocktail To Control Surface Colonization by Proteus mirabilis in Catheter-Associated Urinary Tract Infections. *Microbiol. Spectr.* **2022**, *10*, e0209222. https://doi.org/10.1128/spectrum.02092-22.
8. Fruciano, E.; Bourne, S. Phage as an antimicrobial agent: d'Herelle's heretical theories and their role in the decline of phage prophylaxis in the West. *Can. J. Infect. Dis. Med. Microbiol.* **2007**, *18*, 19–26.
9. Skurnik, M.; Strauch, E. Phage therapy: Facts and fiction. *Int. J. Med Microbiol.* **2006**, *296*, 5–14. https://doi.org/10.1016/j.ijmm.2005.09.002.
10. Doss, J.; Culbertson, K.; Hahn, D.; Camacho, J.; Barekzi, N. A review of phage therapy against bacterial pathogens of aquatic and terrestrial organisms. *Viruses* **2017**, *9*, 50. https://doi.org/10.3390/v9030050.
11. Weber-d, B.; Majewska, J.; Borysowski, J.; Krystyna, D. Phage Therapy: Combating Infections with Potential for Evolving from Merely a Treatment for Complications to Targeting Diseases. *Front. Microbiol.* **2016**, *7*, 1515. https://doi.org/10.3389/fmicb.2016.01515.
12. Ventola, C.L. The Antibiotic Resistance Crisis. *Pharm. Ther.* **2015**, *40*, 278–283. https://doi.org/10.5796/electrochemistry.82.749.

13. Razzaque, M.S. Commentary: Microbial Resistance Movements: An Overview of Global Public Health Threats Posed by Antimicrobial Resistance, and How Best to Counter. *Front. Public Health* **2021**, *8*, 10–13. https://doi.org/10.3389/fpubh.2020.629120.

14. Centers for Disease Control and Prevention COVID-19 U.S. *Impact on Antimicrobial Resistance*; Department of Health and Human Services, CDC: Atlanta, GA, USA, 2022; pp. 1–44.

15. CDC COVID-19: US. *Impact on Antimicrobial Resistance*; Special Report 2022; U.S. Department of Health and Human Services, CDC: Atlanta, GA, USA, 2022.

16. Pan American Health Organization. Antimicrobial Resistance, Fueled by the COVID-19 Pandemic; Pan American Health Organization: Washington, DC, USA, 2022; pp. 1–14.

17. Cahan, E. As Superbugs Flourish, Bacteriophage Therapy Recaptures Researchers' Interest. *J. Am. Med. Assoc.* **2023**, *329*, 781–784.

18. Langford, B.J.; Soucy, J.P.R.; Leung, V.; So, M.; Kwan, A.T.H.; Portnoff, J.S.; Bertagnolio, S.; Raybardhan, S.; MacFadden, D.R.; Daneman, N. Antibiotic resistance associated with the COVID-19 pandemic: A systematic review and meta-analysis. *Clin. Microbiol. Infect.* **2023**, *29*, 302–309. https://doi.org/10.1016/j.cmi.2022.12.006.

19. Loc-Carrillo, C.; Abedon, S.T. Pros and cons of phage therapy. *Bacteriophage* **2011**, *1*, 111–114. https://doi.org/10.4161/bact.1.2.14590.

20. Ferry, T.; Kolenda, C.; Briot, T.; Souche, A.; Lustig, S.; Josse, J.; Batailler, C.; Pirot, F.; Medina, M.; Leboucher, G.; et al. Past and future of phage therapy and phage-derived proteins in patients with bone and joint infection. *Viruses* **2021**, *13*, 2414. https://doi.org/10.3390/v13122414.

21. Lin, D.M.; Koskella, B.; Lin, H.C. Phage therapy: An alternative to antibiotics in the age of multi-drug resistance. *World J. Gastrointest. Pharmacol. Ther.* **2017**, *8*, 162. https://doi.org/10.4292/wjgpt.v8.i3.162.

22. Pires, D.P.; Costa, A.R.; Pinto, G.; Meneses, L.; Azeredo, J. Current challenges and future opportunities of phage therapy. *FEMS Microbiol. Rev.* **2020**, *44*, 684–700. https://doi.org/10.1093/femsre/fuaa017.

23. Hatfull, G.F.; Dedrick, R.M.; Schooley, R.T. Phage Therapy for Antibiotic-Resistant Bacterial Infections. *Annu. Rev. Med.* **2022**, *73*, 197–211. https://doi.org/10.1146/annurev-med-080219-122208.

24. Manohar, P.; Tamhankar, A.J.; Lundborg, C.S.; Nachimuthu, R. Therapeutic characterization and efficacy of bacteriophage cocktails infecting Escherichia coli, klebsiella pneumoniae, and enterobacter species. *Front. Microbiol.* **2019**, *10*, 574. https://doi.org/10.3389/fmicb.2019.00574.

25. Vázquez, R.; Díez-Martínez, R.; Domingo-Calap, P.; García, P.; Gutiérrez, D.; Muniesa, M.; Ruiz-Ruigómez, M.; Sanjuán, R.; Tomás, M.; Tormo-Mas, M.Á.; et al. Essential Topics for the Regulatory Consideration of Phages as Clinically Valuable Therapeutic

Agents: A Perspective from Spain. *Microorganisms* **2022**, *10*, 717. https://doi.org/10.3390/microorganisms10040717.

26. Naureen, Z.; Malacarne, D.; Anpilogov, K.; Dautaj, A.; Camilleri, G.; Cecchin, S.; Bressan, S.; Casadei, A.; Albion, E.; Sorrentino, E.; et al. Comparison between American and European legislation in the therapeutical and alimentary bacteriophage usage. *Acta Biomed.* **2020**, *91*, e2020023. https://doi.org/10.23750/abm.v91i13-S.10815.

27. Verbeken, G.; Pirnay, J.P. European regulatory aspects of phage therapy: Magistral phage preparations. *Curr. Opin. Virol.* **2022**, *52*, 24–29. https://doi.org/10.1016/j.coviro.2021.11.005.

28. Jault, P.; Leclerc, T.; Jennes, S.; Pirnay, J.P.; Que, Y.A.; Resch, G.; Rousseau, A.F.; Ravat, F.; Carsin, H.; Le Floch, R.; et al. Efficacy and tolerability of a cocktail of bacteriophages to treat burn wounds infected by Pseudomonas aeruginosa (PhagoBurn): A randomised, controlled, double-blind phase 1/2 trial. *Lancet Infect. Dis.* **2018**, *19*, 35–45. https://doi.org/10.1016/S1473-3099(18)30482-1.

29. Onsea, J.; Uyttebroek, S.; Chen, B.; Wagemans, J.; Lood, C.; Van Gerven, L.; Spriet, I.; Devolder, D.; Debaveye, Y.; Depypere, M.; et al. Bacteriophage therapy for difficult-to-treat infections: The implementation of a multidisciplinary phage task force (the phageforce study protocol). *Viruses* **2021**, *13*, 1543. https://doi.org/10.3390/v13081543.

30. Onsea, J.; Soentjens, P.; Djebara, S.; Merabishvili, M.; Depypere, M.; Spriet, I.; De Munter, P.; Debaveye, Y.; Nijs, S.; Vanderschot, P.; et al. Bacteriophage application for difficult-to-treat musculoskeletal infections: Development of a standardized multidisciplinary treatment protocol. *Viruses* **2019**, *11*, 891. https://doi.org/10.3390/v11100891.

31. Uyttebroek, S.; Chen, B.; Onsea, J.; Ruythooren, F.; Debaveye, Y.; Devolder, D.; Spriet, I.; Depypere, M.; Wagemans, J.; Lavigne, R.; et al. Safety and efficacy of phage therapy in difficult-to-treat infections: A systematic review. *Lancet Infect. Dis.* **2022**, *22*, e208–e220. https://doi.org/10.1016/S1473-3099(21)00612-5.

32. Liu, D.; Van Belleghem, J.D.; de Vries, C.R.; Burgener, E.; Chen, Q.; Manasherob, R.; Aronson, J.R.; Amanatullah, D.F.; Tamma, P.D.; Suh, G.A. The safety and toxicity of phage therapy: A review of animal and clinical studies. *Viruses* **2021**, *13*, 1268. https://doi.org/10.3390/v13071268.

33. Twest, R.; Kropinski, A.M. *Bacteriophages: Methods and Protocols, Volume 1*; Clokie, M.R.J., Kropinski, A.M., Eds.; Humana Press: Leicester, UK, 2009; ISBN 9781588296825.

34. Yamamoto, K.R.; Alberts, B.M.; Benzinger, R.; Lawhorne, L.; Treiber, G. Rapid bacteriophage sedimentation in the presence of polyethylene glycol and its application to large-scale virus purification. *Virology* **1970**, *40*, 734–744. https://doi.org/10.1016/0042-6822(70)90218-7.

35. Schneider, C.A.; Rasband, W.S.; Eliceiri, K.W. Image to ImageJ: 25 years of image analysis. Nature methods. *Nat. Methods* **2012**, *9*, 671–675.

36. Vallino, M.; Rossi, M.; Ottati, S.; Martino, G.; Galetto, L.; Marzachì, C.; Abbà, S. Bacteriophage-host association in the phytoplasma insect vector euscelidius variegatus. *Pathogens* **2021**, *10*, 612. https://doi.org/10.3390/pathogens10050612.

37. Melo, L.D.R.; Veiga, P.; Cerca, N.; Kropinski, A.M.; Almeida, C.; Azeredo, J.; Sillankorva, S. Development of a phage cocktail to control Proteus mirabilis catheter-associated urinary tract infections. *Front. Microbiol.* **2016**, *7*, 1024. https://doi.org/10.3389/fmicb.2016.01024.

38. Kot, W. Genome Sequencing of dsDNA-Containing Bacteriophages Directly from a Single Plaque. In *Bacteriophages: Methods and Protocols, Volume 3*; Al, M.R.J.C. et, Ed.; Springer Science: Berlin/Heidelberg, Germany; Business Media: Petaling Jaya, Malaysia, 2018; Volume 1681, pp. 179–184, ISBN 9781493973439.

39. Olson, R.D.; Assaf, R.; Brettin, T.; Conrad, N.; Cucinell, C.; Davis, J.J.; Dempsey, D.M.; Dickerman, A.; Dietrich, E.M.; Kenyon, R.W.; et al. Introducing the Bacterial and Viral Bioinformatics Resource Center (BV-BRC): A resource combining PATRIC, IRD and ViPR. *Nucleic Acids Res.* **2023**, *51*, D678–D689. https://doi.org/10.1093/nar/gkac1003.

40. Aziz, R.K.; Bartels, D.; Best, A.; DeJongh, M.; Disz, T.; Edwards, R.A.; Formsma, K.; Gerdes, S.; Glass, E.M.; Kubal, M.; et al. The RAST Server: Rapid annotations using subsystems technology. *BMC Genom.* **2008**, *9*, 75. https://doi.org/10.1186/1471-2164-9-75.

41. Seemann, T. Prokka: Rapid prokaryotic genome annotation. *Bioinformatics* **2014**, *30*, 2068–2069. https://doi.org/10.1093/bioinformatics/btu153.

42. Coppens, L.; Lavigne, R. SAPPHIRE: A neural network based classifier for σ70 promoter prediction in Pseudomonas. *BMC Bioinform.* **2020**, *21*, 415. https://doi.org/10.1186/s12859-020-03730-z.

43. Bailey, T.L.; Johnson, J.; Grant, C.E.; Noble, W.S. The MEME Suite. *Nucleic Acids Res.* **2015**, *43*, W39–W49. https://doi.org/10.1093/nar/gkv416.

44. Chan, P.P.; Lowe, T.M. tRNAscan-SE: Searching for tRNA genes in genomic sequences. *Methods Mol. Biol.* **2019**, *1962*, 1–14. https://doi.org/10.1007/978-1-4939-9173-0.

45. Naville, M.; Ghuillot-Gaudeffroy, A.; Marchais, A.; Gautheret, D. ARNold: A web tool for the prediction of rho-independent transcription terminators. *RNA Biol.* **2011**, *8*, 11–13. https://doi.org/10.4161/rna.8.1.13346.

46. Nishimura, Y.; Yoshida, T.; Kuronishi, M.; Uehara, H.; Ogata, H.; Goto, S. ViPTree: The viral proteomic tree server. *Bioinformatics* **2017**, *33*, 2379–2380. https://doi.org/10.1093/bioinformatics/btx157.

47. Moraru, C.; Varsani, A.; Kropinski, A.M. VIRIDIC—A novel tool to calculate the intergenomic similarities of prokaryote-infecting viruses. *Viruses* **2020**, *12*, 1268. https://doi.org/10.3390/v12111268.

48. Gilchrist, C.L.M.; Chooi, Y.H. Clinker & clustermap.js: Automatic generation of gene cluster comparison figures. *Bioinformatics* **2021**, *37*, 2473–2475. https://doi.org/10.1093/bioinformatics/btab007.

49. Vieira, M.F.; Duarte, J.; Domingues, R.; Oliveira, H.; Dias, O. PhageDPO: Phage Depolymerase Finder. *bioRxiv* **2023**, 2023.02.24.529883.

50. Finn, R.D.; Clements, J.; Eddy, S.R. HMMER web server: Interactive sequence similarity searching. *Nucleic Acids Res.* **2011**, *39*, 29–37. https://doi.org/10.1093/nar/gkr367.

51. Söding, J.; Biegert, A.; Lupas, A.N. The HHpred interactive server for protein homology detection and structure prediction. *Nucleic Acids Res.* **2005**, *33*, 244–248. https://doi.org/10.1093/nar/gki408.

52. Alva, V.; Nam, S.Z.; Soding, J.; Lupas, A.N. The MPI bioinformatics Toolkit as an integrative platform for advanced protein sequence and structure analysis. *Nucleic Acids Res.* **2016**, *44*, W410–W415. https://doi.org/10.1093/nar/gkw348.

53. Jumper, J.; Evans, R.; Pritzel, A.; Green, T.; Figurnov, M.; Ronneberger, O.; Tunyasuvunakool, K.; Bates, R.; Žídek, A.; Potapenko, A.; et al. Highly accurate protein structure prediction with AlphaFold. *Nature* **2021**, *596*, 583–589. https://doi.org/10.1038/s41586-021-03819-2.

54. Page, A.J.; Cummins, C.A.; Hunt, M.; Wong, V.K.; Reuter, S.; Holden, M.T.G.; Fookes, M.; Falush, D.; Keane, J.A.; Parkhill, J. Roary: Rapid large-scale prokaryote pan genome analysis. *Bioinformatics* **2015**, *31*, 3691–3693. https://doi.org/10.1093/bioinformatics/btv421.

55. Stamatakis, A. RAxML version 8: A tool for phylogenetic analysis and post-analysis of large phylogenies. *Bioinformatics* **2014**, *30*, 1312–1313. https://doi.org/10.1093/bioinformatics/btu033.

56. Hadfield, J.; Croucher, N.J.; Goater, R.J.; Abudahab, K.; Aanensen, D.M.; Harris, S.R. Phandango: An interactive viewer for bacterial population genomics. *Bioinformatics* **2018**, *34*, 292–293. https://doi.org/10.1093/bioinformatics/btx610.

57. Morozova, V.; Kozlova, Y.; Shedko, E.; Babkin, I.; Kurilshikov, A.; Bokovaya, O.; Bardashova, A.; Yunusova, A.; Tikunov, A.; Tupikin, A.; et al. Isolation and characterization of a group of new Proteus bacteriophages. *Arch. Virol.* **2018**, *163*, 2189–2197. https://doi.org/10.1007/s00705-018-3853-3.

58. Hung, E.; Darouiche, R.; Trautner, B. Proteus bacteriuria is associated with significant morbidity in spinal cord injury. *Spinal Cord. NIH Public Access* **2008**, *23*, 616–620. https://doi.org/10.1038/sj.sc.3102004.Proteus.

59. Wasfi, R.; Hamed, S.M.; Amer, M.A.; Fahmy, L.I. Proteus mirabilis Biofilm: Development and Therapeutic Strategies. *Front. Cell. Infect. Microbiol.* **2020**, *10*, 414. https://doi.org/10.3389/fcimb.2020.00414.

60. Adriaenssens, E.M.; Sullivan, M.B.; Knezevic, P.; van Zyl, L.J.; Sarkar, B.L.; Dutilh, B.E.; Alfenas-Zerbini, P.; Łobocka, M.; Tong, Y.; Brister, J.R.; et al. Taxonomy of prokaryotic viruses: 2018-2019 update from the ICTV Bacterial and Archaeal Viruses Subcommittee. *Arch. Virol.* **2020**, *165*, 1253–1260. https://doi.org/10.1007/s00705-020-04577-8.

61. Chen, Y.; Sun, E.; Song, J.; Yang, L.; Wu, B. Complete Genome Sequence of a Novel T7-Like Bacteriophage from a Pasteurella multocida Capsular Type A Isolate. *Curr. Microbiol.* **2018**, *75*, 574–579. https://doi.org/10.1007/s00284-017-1419-3.

62. Elhalag, K.; Eldin, M.N.; Hussien, A.; Ahmad, A. Potential use of soilborne lytic podoviridae phage as a biocontrol agent against Ralstonia solanacearum. *J. Basic Microbiol.* **2018**, *58*, 658–669. https://doi.org/10.1002/jobm.201800039.

63. Li, F.; Tian, F.; Li, J.; Li, L.; Qiao, H.; Dong, Y.; Ma, F.; Zhu, S.; Tong, Y. Isolation and characterization of a podovirus infecting the opportunist pathogen Vibrio alginolyticus and Vibrio parahaemolyticus. *Virus Res.* **2021**, *302*, 198481. https://doi.org/10.1016/j.virusres.2021.198481.

64. Cole, A.W.; Tran, S.D.; Ellington, A.D. Heat adaptation of phage T7 under an extended genetic code. *Virus Evol.* **2021**, *7*, veab100. https://doi.org/10.1093/ve/veab100.

65. Favor, A.H.; Llanos, C.D.; Youngblut, M.D.; Bardales, J.A. Optimizing bacteriophage engineering through an accelerated evolution platform. *Sci. Rep.* **2020**, *10*, 13981. https://doi.org/10.1038/s41598-020-70841-1.

66. Knecht, L.E.; Veljkovic, M.; Fieseler, L. Diversity and Function of Phage Encoded Depolymerases. *Front. Microbiol.* **2020**, *10*, 2949. https://doi.org/10.3389/fmicb.2019.02949.

67. Latka, A.; Leiman, P.G.; Drulis-Kawa, Z.; Briers, Y. Modeling the Architecture of Depolymerase-Containing Receptor Binding Proteins in Klebsiella Phages. *Front. Microbiol.* **2019**, *10*, 2649. https://doi.org/10.3389/fmicb.2019.02649.

68. Dams, D.; Brøndsted, L.; Drulis-kawa, Z. Engineering of receptor-binding proteins in bacteriophages and phage tail-like bacteriocins. *Biochem. Soc. Trans.* **2019**, *47*, 449–460.

69. Oliveira, H.; Drulis-Kawa, Z.; Azeredo, J. Exploiting phage-derived carbohydrate depolymerases for combating infectious diseases. *Trends Microbiol.* **2022**, *30*, 707–709. https://doi.org/10.1016/j.tim.2022.05.002.

70. Dietzen, D.J. *Amino Acids, Peptides, and Proteins*; Elsevier Inc.: Amsterdam, The Netherlands, 2018; ISBN 9780128160619.

71. Leveson-Gower, R.B.; Mayer, C.; Roelfes, G. The importance of catalytic promiscuity for enzyme design and evolution. *Nat. Rev. Chem.* **2019**, *3*, 687–705. https://doi.org/10.1038/s41570-019-0143-x.

72. Squeglia, F.; Maciejewska, B.; Łątka, A.; Ruggiero, A.; Briers, Y.; Drulis-Kawa, Z.; Berisio, R. Structural and Functional Studies of a Klebsiella Phage Capsule Depolymerase Tailspike: Mechanistic Insights into Capsular Degradation. *Structure* **2020**, *28*, 613–624.e4. https://doi.org/10.1016/j.str.2020.04.015.

73. Alqurashi, E.; Elbanna, K.; Ahmad, I.; Abulreesh, H.H. Antibiotic Resistance in Proteus mirabilis: Mechanism, Status, and Public Health Significance. *J. Pure Appl. Microbiol.* **2022**, *16*, 1550–1561. https://doi.org/10.22207/JPAM.16.3.59.

74. Stock, I. Natural antibiotic susceptibility of Proteus spp., with special reference to P. mirabilis and P. penneri strains. *J. Chemother.* **2003**, *15*, 12–26. https://doi.org/10.1179/joc.2003.15.1.12.

75. Sanchez, B.C.; Heckmann, E.R.; Green, S.I.; Clark, J.R.; Kaplan, H.B.; Ramig, R.F.; Hines-Munson, C.; Skelton, F.; Trautner, B.W.; Maresso, A.W. Development of Phage Cocktails to Treat *E. coli* Catheter-Associated Urinary Tract Infection and Associated Biofilms. *Front. Microbiol.* **2022**, *13*, 796132. https://doi.org/10.3389/fmicb.2022.796132.

76. Terwiliger, A.; Clark, J.; Karris, M.; Hernandez-Santos, H.; Green, S.; Aslam, S.; Maresso, A. Phage Therapy Related Microbial Succession Associated with Successful Clinical Outcome for a Recurrent Urinary Tract Infection. *Viruses* **2021**, *13*, 2049. https://doi.org/10.3390/v13102049.

General conclusions

This work has explored the potential of bacteriophages as bacterial biocontrol agents, and was divided into two distinct application approaches. Chapter 1 described the isolation and the genomic and biological characterization of the *Enterobacter* phage vB_EclM-UFV01 (ENT01). In Chapter 2, this phage, together with the other three tequatroviruses (UFV09, UFV10, and UFV13) were selected to compose a phage cocktail, able to decrease the biofilm of sulfate-reducing bacteria. All the phages selected to compose the cocktail were virulent, with myovirus morphology, and possessed genes encoding depolymerases in their genomes. The long-term stability of this cocktail, named Petro01, was evaluated in conditions found in petroleum-related environments. The addition of components with putative conservative effects, as well as the large-scale production in bioreactors, were also evaluated. The cocktail showed excellent long-term stability in being stored at 37 °C, and it also remained stable at temperatures below 55 °C, pH greater than 4, and in the presence of significant quantities of chlorine and salt, as well as the biocide THPS. Our results reinforced that phages play an important role in disrupting complex bacterial communities, especially their biofilms, even though they do not necessarily infect the target host. Their large-scale production proved not to be a barrier to the creation of phage-based products. Our results showed that after finding good production parameters, the production scale can be increased and the viral yield adjusted until a compatible production rate is obtained. Supplementary, Chapter 3 discussed the use of phages in clinical settings. Although this approach is not new, phage therapy has only recently been reintroduced as a viable treatment option for bacterial infections. We characterized biological and genomically the phages BigMira and MidiMira, that infect the *Proteus mirabilis* MCS. This strain, isolated from a pressure ulcer wound of a diabetic patient, developed after a long period of hospitalization due to a severe case of COVID-19 and showed to be highly pathogenic. Our findings showed the importance of the constant isolation and good characterization of phages, not only evaluating standard stability conditions but also the ones that mimic the real infection environment. Hence, in this work, we also evaluated the phage's stability in filtered and voided urine, as well as their infection capacity in these conditions. We confirmed that phages BigMira and MidiMira are strong candidates for phage therapy, and we offer another well-structured and developed study, which helps in the understanding of the real potential of phages in the treatment of bacterial diseases. This work not only offers a non-traditional use for bacteriophages in the oil industry but also reinforces their importance in the clinical field. Characterization works may appear simple, but they

serve as the foundation for future synthetic biology and genetic engineering research. The horizontal transfer of resistance genes does not only impact hospital and clinical environments, but has been spreading to veterinary, agricultural, industrial, and environmental fields, and the problems caused by microorganisms may gradually become more difficult to combat. At this point, bacteriophages are our allies. Understanding their control strategies over the host, unraveling the function of hypothetical genes, and evaluating them individually as possible agents for controlling bacterial growth in different contexts is a never-ending effort. The use of phages to minimize the impact of sulfate-reducing bacteria in petroleum environments is an important research line of the Laboratory of Molecular Immunovirology (LIVM), and we are unaware of other research groups that use phages in such a context. We believe that our findings can support and guide further studies aiming at the development of phage-based products in industrial, environmental, and clinical fields.